

# **GERMLINE CEY PROTEINS PREVENT PROTEIN AGGREGATION IN THE SOMA OF *C. ELEGANS***

**Inaugural-Dissertation**

**zur Erlangung des Doktorgrades**

**der Mathematisch-Naturwissenschaftlichen Fakultät**

**der Universität zu Köln**



**vorgelegt von**

**Giuseppe Calculli**

**aus Neapel, Italien**

**Köln, 2020**

---

**Berichterstatter:**

**Dr. David Vilchez**

**Prof. Dr. Aleksandra Trifunovic**

**Tag der mündlichen Prüfung: 24.02.2021**

**Jahr der Veröffentlichung: 2021**

**Mathematisch-Naturwissenschaftliche Fakultät der Universität zu Köln**  
**Zustimmung zur Veröffentlichung der Dissertation**  
nach der Promotionsordnung vom 12.3.2020

**Faculty of Mathematics and Natural Sciences - University of Cologne**  
**Approval of publication of the doctoral thesis**  
according to the doctoral regulations effective as of 12<sup>th</sup> March 2020

Name last name	Calculli
Vorname first name	Giuseppe
Betreuerin / Betreuer Supervisor	David Vilchez
Erste/r Gutachter/in first reviewer	Aleksandra Trifunovic
Titel der zur Promotion eingereichten Dissertation / title of the submitted doctoral thesis	
Germline CEY proteins prevent protein aggregation in the soma of <i>C. elegans</i>	

Hiermit bestätige ich, dass mir die oben genannte Dissertation vorgelegen hat und dass ich gegen deren Veröffentlichung nichts einzuwenden habe. / I herewith confirm that the above-mentioned dissertation has been presented to me and that I have no objection to its publication.

Die Dissertation kann veröffentlicht werden / The thesis can be published

- in elektronischer Form auf dem Hochschulserver KUPS und zusätzlicher Abgabe von vier gebundenen Exemplaren bei der Universitäts- und Stadtbibliothek Köln (USB) / in electronic form on the university server KUPS and by additional submission of four bound copies to the University and City Library of Cologne (USB).
- durch privaten Druck und Abgabe von 20 gebundenen Exemplaren bei der USB sowie der Veröffentlichung der Zusammenfassung der Dissertation in deutscher und in englischer Sprache auf dem Hochschulserver KUPS / by private printing and submission of 20 bound copies to the USB and additional publication of the summary of the doctoral thesis in German and English on the university server KUPS.
- als Einzelpublikation in einem Verlag mit ISBN oder ISSN und Abgabe von sechs gebundenen Exemplaren bei der USB sowie der Veröffentlichung der Zusammenfassung der Dissertation in deutscher und in englischer Sprache auf dem Hochschulserver KUPS / as a single publication in a publishing house with ISBN (minimum number of copies 150) and submission of six bound copies to the to the USB and additional publication of the summary of the doctoral thesis in German and English on the university server KUPS.

Hinweis: Die Veröffentlichung muss auf dem Titelblatt oder auf der Rückseite des Titelblatts einen Hinweis enthalten, aus der oder dem hervorgeht, dass es sich um eine von der Mathematisch-Naturwissen-schaftlichen Fakultät der Universität zu Köln angenommene Dissertation handelt; dabei ist das Jahr der Disputation zu nennen. Von der veröffentlichten Fassung der Dissertation ist zusätzlich ein gebundenes Exemplar und eine elektronische Version der veröffentlichten Fassung der Dissertation im Promotionsbüro des Dekanats einzureichen.

Note: The publication must include a statement on the title page or on the back of the title page declaring that the dissertation has been accepted by the Faculty of Mathematics and Natural Sciences of the University of Cologne; the year of the disputation must be stated. In addition, a bound copy and an electronic version of the published version of the doctoral thesis must be submitted to the Dean's office.

5/3/21  
Datum / date

**David  
Vilchez**  
Unterschrift Betreuer/in  
supervisor's signature

Digitally signed by  
David Vilchez  
Date: 2021.05.03  
10:15:49 +02'00'

CECAD  
JOSEPH-STELZMANN STR. 26  
50931, KÖLN  
Institut bzw. Forschungseinrichtung mit  
Anschrift research institution and address

5/3/21  
Datum / date

**Aleksandra  
Trifunovic**  
Unterschrift Erstgutachter/in (sofern  
nicht Betreuende/r)  
first reviewer's signature (if  
different than supervisor)

Digitally signed by  
Aleksandra Trifunovic  
Date: 2021.05.03  
10:47:59 +02'00'

---

# TABLE OF CONTENT

ABBREVIATIONS .....	6
ABSTRACT.....	8
ZUSAMMENFASSUNG.....	9
INTRODUCTION.....	10
1. The ageing process.....	10
2. The proteostasis network.....	10
2.1 CHAPERONES .....	11
2.2 THE UBIQUITIN PROTEASOME SYSTEM .....	12
2.3 THE AUTOPHAGY PATHWAY .....	12
3. AGE-RELATED NEURODEGENERATIVE DISEASES.....	14
3.1 HUNTINGTON´S DISEASE .....	14
3.1 3.2 AMYOTROPHIC LATERAL SCLEROSIS .....	15
4. CELL NON-AUTONOMOUS REGULATION OF PROTEOSTASIS .....	16
4.1 THE HEAT-SHOCK RESPONSE .....	16
4.2 THE UNFOLDED PROTEIN RESPONSE OF THE ENDOPLASMIC RETICULUM .....	17
4.3 THE UNFOLDED PROTEIN RESPONSE OF MITOCHONDRIA .....	18
4.5 CELL NON-AUTONOMOUS REGULATION OF PROTEOSTASIS BY NON-NEURONAL TISSUES .....	19
5. P GRANULES .....	23
5.1 FUNCTION OF P GRANULES .....	24
5.2 GENERATION OF P GRANULES .....	25
5.3 COMPOSITION OF P GRANULES .....	25
5.4 THE GERMLINE HELICASES PROTEIN FAMILY .....	27
5.5 THE PGL PROTEIN FAMILY .....	27
5.6 P GRANULE ASSOCIATION TO MITOCHONDRIA .....	28
5.7 P GRANULE PHASE TRANSITION .....	29
6. THE <i>C. ELEGANS</i> Y-BOX BINDING PROTEIN FAMILY .....	30

---

6.1 FUNCTION OF YBX PROTEINS .....	31
6.2 ROLE OF YBX PROTEINS ON GERM GRANULES .....	33
6.3 FUNCTIONS OF CEY PROTEINS IN THE <i>C. ELEGANS</i> GERMLINE .....	34
OBJECTIVES OF THIS WORK.....	36
RESULTS .....	37
1. DEPLETION OF <i>CEY-2</i> AND <i>CEY-3</i> PROTEINS INDUCES PGL-1 AGGREGATION .....	37
2. DEPLETION OF <i>CEY-2</i> AND <i>CEY-3</i> DOES NOT AFFECT ORGANISMAL LIFESPAN AND FECUNDITY .....	40
3. DEPLETION OF GERMLINE-SPECIFIC CEYS INDUCES PROTEIN AGGREGATION IN THE NERVOUS SYSTEM .....	42
4. DEPLETION OF <i>CEY-1</i> INDUCES PROTEIN AGGREGATION IN THE NERVOUS SYSTEM VIA A CELL NON-AUTONOMOUS MECHANISM .....	44
5. PGL-1 AGGREGATION IN GERMLINE CAUSES DISRUPTION OF SOMATIC PROTEOSTASIS .....	47
6. DEPLETION OF EITHER <i>CEY-2</i> OR <i>CEY-3</i> INDUCES AN OVERALL SOMATIC PROTEOSTASIS DISRUPTION .....	48
7. DEPLETION OF EITHER <i>CEY-2</i> OR <i>CEY-3</i> CAUSES MITOCHONDRIA PERTURBATION IN GERMLINE .....	50
8. DEPLETION OF EITHER <i>CEY-2</i> OR <i>CEY-3</i> INDUCES A CELL NON-AUTONOMOUS DISRUPTION OF MITOCHONDRIA IN THE SOMA .....	53
9. DEPLETION OF EITHER <i>CEY-2</i> OR <i>CEY-3</i> INDUCES UPR <sup>MT</sup> IN THE SOMA VIA A CELL NON-AUTONOMOUS MECHANISM .....	59
10. THE WNT/ELG-20 SIGNALING IS RESPONSIBLE FOR THE CELL NON-AUTONOMOUS COMMUNICATION INDUCED BY CEYS DEPLETION .....	61
DISCUSSION.....	64
CONCLUSION .....	73
FUTURE PERSPECTIVE.....	74
METHODS.....	77

---

REFERENCES .....	85
ACKNOWLEDGEMENTS .....	99
ERKLÄRUNG .....	100

---

## ABBREVIATIONS

ALS	Amyotrophic lateral sclerosis
ATG	Autophagy related gene
CDS	Cold shock domain
CEY	<i>C. elegans</i> Y-box binding protein
CMA	Chaperone-mediated autophagy
CCO-1	Cytochrome C Oxidase CCO-1 protein
eIF4E	Isoform of eukaryotic initiation factor 4E
ER	Endoplasmic reticulum
ETC	Electron transport complex
FA	Fatty acid
FALS	Familial ALS form
FGF	Fibroblast growth factor
FUS	Fused in sarcoma
GDISR	Germline DNA-damage-induced systemic stress resistance
GLH	Germline helicases
GSC	Germline stem cells
HD	Huntington's disease
Hcrt	Hypocretin neurons
HSR	Heat shock response
HSF	Heat shock factor
HTT	Huntingtin
IDR	Intrinsically disordered region

IDP	Intrinsically disordered protein
IGF	Insulin-like growth factor
IIS	Insulin and IGF1-like signaling
MLO	Membrane-less ribonucleoprotein organelle
mRNP	Messenger ribonucleoprotein
mt	Mitochondria
mtDNA	Mitochondrial DNA
MTOC	Microtubule-organizing centre
MTS	Mitochondria targeting sequence
PG	P granule
PGE2	Prostaglandin E2
polyQ	Polyglutamine
qPCR	Quantitative PCR
RBP	RNA binding protein
RNAi	RNA interference
ROS	Reactive oxygen species
SG	Stress granule
TDP43	Transactive response DNA binding protein 43
UPS	Ubiquitin proteasome system
UPR	Unfolded protein response
YBX	Y-box protein

---

## ABSTRACT

Protein aggregation causes intracellular changes in neurons, that elicit signals to modulate proteostasis in the periphery. Beyond the nervous system, a fundamental question is whether other organs also communicate their proteostasis status to distal tissues. Here, we examined whether proteostasis of the germline influences somatic tissues. To this end, we induced aggregation of germline-specific PGL-1 protein in *C. elegans* germline stem cells. Notably, dysfunction of germline proteostasis triggered neuronal aggregation of distinct proteins linked with neurodegenerative diseases such as Huntington's and amyotrophic lateral sclerosis. The cell non-autonomous effects induced by PGL-1 aggregation were not limited to the nervous system, affecting other tissues such as the muscle and intestine. Importantly, PGL-1 aggregation reduced the mitochondrial network of germline cells. In turn, these cells diminished the mitochondrial content, network and proteostasis of mitochondria in somatic tissues through Wnt/mitokine signaling, resulting in the aggregation of disease-related proteins. Thus, the proteostasis status of germline stem cells coordinates mitochondrial networks and protein aggregation through the organism.

---

## ZUSAMMENFASSUNG

Die Proteinaggregation verursacht intrazelluläre Veränderungen in Neuronen, die Signale auslösen, um die Proteostase in der Peripherie zu modulieren. Über das Nervensystem hinaus ist es eine grundlegende Frage, ob andere Organe ihren Proteostasestatus auch distalen Geweben übermitteln. Hier untersuchten wir, ob die Proteostase der Keimbahn das somatische Gewebe beeinflusst. Zu diesem Zweck induzierten wir die Aggregation von keimbahnspezifischem PGL-1-Protein in Keimbahnstammzellen von *C. elegans*. Bemerkenswerterweise löste eine Funktionsstörung der Keimbahnproteostase eine neuronale Aggregation verschiedener Proteine aus, die mit neurodegenerativen Erkrankungen wie Huntington und Amyotropher Lateralsklerose verbunden sind. Die durch die PGL-1-Aggregation induzierten nichtautonomen Effekte der Zellen waren nicht auf das Nervensystem beschränkt, sondern betrafen ebenfalls andere Gewebe wie Muskel und Darm. Wichtig ist, dass die PGL-1-Aggregation das mitochondriale Netzwerk von Keimbahnzellen verringerte. Im Gegenzug verminderten diese Zellen wiederum den Mitochondriengehalt, das Netzwerk und die Proteostase von Mitochondrien in somatischen Geweben durch Wnt/Mitokin-Signalübertragung, was zur Aggregation krankheitsbedingter Proteine führt. Somit koordiniert der Proteostasestatus von Keimbahnstammzellen die mitochondrialen Netzwerke und die Proteinaggregation durch den Organismus.

---

# INTRODUCTION

## 1. The ageing process

Ageing is a time-dependent progressive decline that impairs the integrity of tissues and physiology of living organisms, leading to the onset of age-related diseases and increasing the risk of death. The process of ageing is characterized by nine different hallmarks, which are further categorized in three subgroups: primary hallmarks, antagonistic hallmarks, and integrative hallmarks (*1*).

The primary hallmarks share the characteristic to be always unequivocally negative. Examples of primary hallmarks are DNA damage and telomerase loss. Contrarily, the antagonist hallmarks are not always negative but their effects depend on their intensity. Low intensity levels are beneficial, whereas high intensity is associated with detrimental effects. Examples of antagonist hallmarks are mitochondrial dysfunction and cellular senescence. For instance, low levels of reactive oxygen species (ROS) production mediates cell signaling and survival, while high levels of ROS can cause cell damage. Similarly, senescence can be beneficial at low level and protect from cancer, whereas it causes ageing at high levels. Therefore, the antagonist hallmarks have the physiological function to protect organisms from damage, however when they become chronic subvert their aim and contribute to ageing. Finally, the integrative hallmarks affect tissue homeostasis and function. This subgroup includes stem cell exhaustion and altered intercellular communication.

A certain hierarchy has been supposed to exist between these hallmarks (*1*). The first hallmarks to appear could be the primary hallmarks, which may start the accumulation of cellular damage. Then, the intensity of antagonist hallmarks rises, so that they become progressively negative. Finally, the integrative hallmarks appear when the tissue homeostasis can no longer cope with damages caused by the other hallmarks.

## 2. The proteostasis network

Loss of protein homeostasis (proteostasis) is a primary hallmark of ageing (*1*). The cellular pathways involved in maintaining the integrity of the proteome are collectively referred to as the proteostasis network, which includes processes such as protein synthesis and folding, conformational maintenance and degradation.

---

## 2.1 Chaperones

The translation process generates new polypeptides that exhibit unfolded or non-native structure. The majority of newly synthesized proteins need to be folded in a proper specific state (native state) to be functional (2). Many proteins consist of different domains and need to reach a complex 3D structure; hence the process of folding requires molecular chaperones that assist the folding process to occur efficiently. Chaperones are defined as factors that contribute to the final folding of other proteins without being part of their final structure (2).

However, the folding protein status is only marginally stable and a partial protein population can undergo misfolding events (2, 3). Additional destabilizing factors like mutations and stress events can enhance protein misfolding and cause accumulation of misfolded proteins. In addition, damaged misfolded proteins accumulate also during ageing as a consequence of decreasing capacity to maintain functional proteasome activity and the accumulation of proteotoxic agents such as ROS (1, 3).

Unfolded proteins, including nascent polypeptides, tend to aggregate due to the exposure of hydrophobic amino acid residues and unpaired  $\beta$ - strands, which confer a high degree of interactivity with cellular proteins and membranes. Thus, unfolded proteins can lead to the formation of protein aggregates. Protein aggregates are potentially harmful and therefore their formation is strictly monitored.

Protein aggregates hold dual toxicity; on one hand, protein aggregates are toxic inclusions that can cause cellular damages, for example on lipid membranes, through gain of new functions; on the other hand, proteins accumulate into the aggregates and therefore cannot pursue their biological function, causing loss of function effects. In fact, proteostasis factors, such as chaperones, can also be sequestered into the aggregate, causing a depletion of proteostasis components that can lead to chronic stress responses, proteostasis collapse and cell death. Therefore, misfolded proteins need to be either correctly refolded in a native state by chaperones or eliminated through protein clearance mechanisms. The two main strategies of cellular protein clearance involve either the ubiquitin proteasome system (UPS) or the autophagy pathway (3).

---

## 2.2 The ubiquitin proteasome system

The proteasome is a complex macromolecule responsible for the clearance of proteins that are targeted for degradation. These proteins are first targeted by the ubiquitination machinery and then recognized, unfolded and proteolyzed into small peptides by the proteasome (3).

The proteasome is composed of several subunits, which are organized in two parts: the core (20s) and the cap (19s) particles of the proteasome (**Fig. 1**). The core (20s) particle shows a barrel-like structure, in which 28 subunits are organized in four rings. The two outer rings consist of seven alpha subunits and control the entrance of the substrate into the inner rings. The two inner rings consist of seven beta subunits and display proteolytic activity (caspase-like, trypsin-like and chymotrypsin-like activities) (3). The cap (19s) particle is organized in two substructures: a base that interacts with the 20s particle, and a lid. The lid is adjacent to the base and is responsible for the substrate recognition (3).

Importantly, several studies have reported that proteasome activity declines with ageing. Accordingly, a decline in proteasome efficiency and activity has been observed in many mammalian tissues including cerebral cortex, hippocampus, spinal cord, heart, muscles and liver (3, 4). Proteasome deregulation can occur via different mechanisms. For instance, proteasome subunits expression decreases with ageing (3, 5), whereas proteasome disassembly (6) and proteasome inhibition (7) increase with senescence. Moreover, knockdown of 19s and 20s proteasome subunits shortens lifespan of adult worms, in *C. elegans* (8). Similarly, mutations of the 20s proteasome subunits, that reduces chymotrypsin-like activity, shortens lifespan in mice (9).

## 2.3 The autophagy pathway

Autophagy is an intracellular catabolic process responsible for the elimination of cytosolic fractions, organelles and macromolecules through lysosomes, which are single-membrane vesicles containing catalytic enzymes such as proteases and lipases (3). Depending on the type of cargo, autophagy can be classified in three different modalities: macroautophagy, microautophagy and chaperone-mediated autophagy (3). Macroautophagy relies on the formation of double membrane vesicles called autophagosomes, which transport cytoplasmic regions to lysosomes for degradation. In microautophagy, small cytoplasmic regions, containing the cargo, are directly sequestered by the lysosomes and degraded. Finally, in chaperone-mediated

autophagy (CMA), specific targeted proteins are recognized by chaperones and transported to lysosomes for degradation.

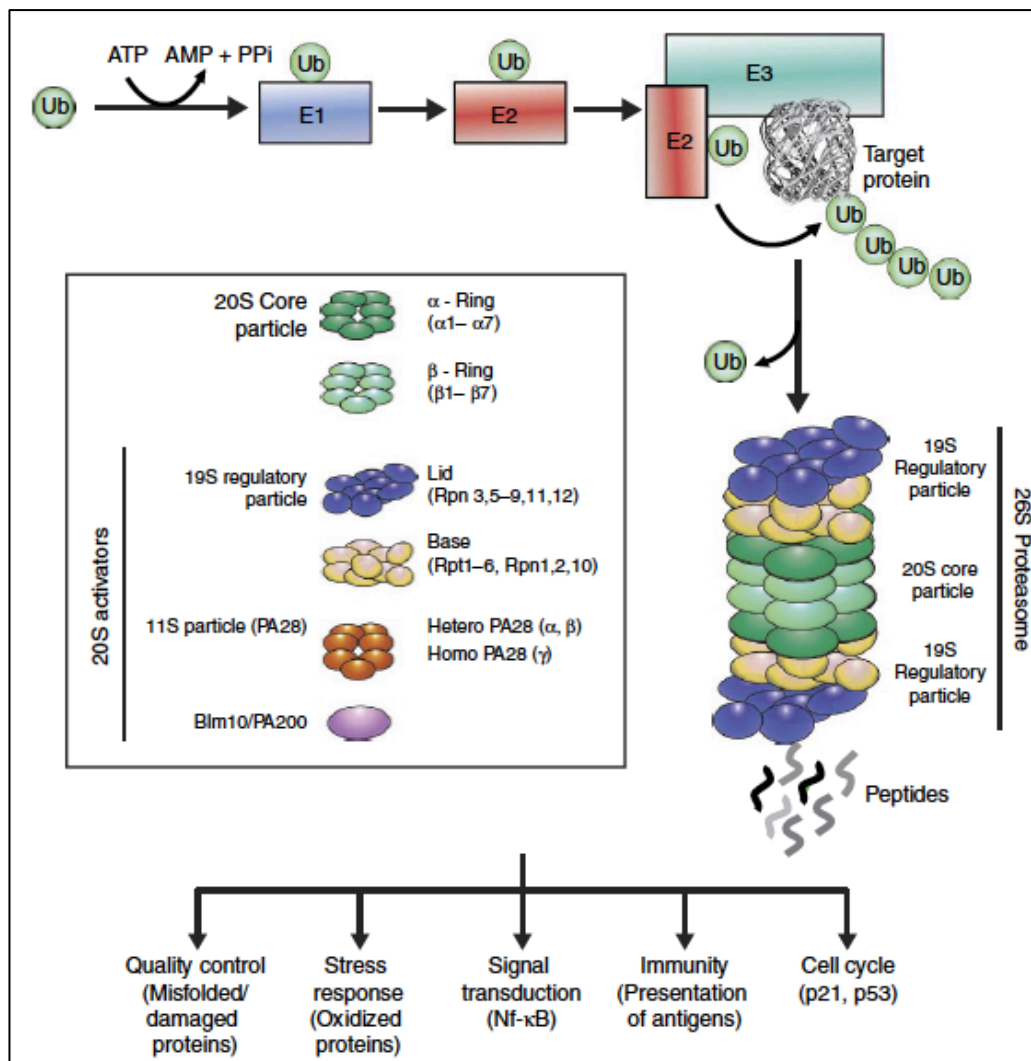


**Fig. 1 The ubiquitin–proteasome system (UPS).** Adapted from Saez et al (2014).

Degradation by the UPS is initiated by the conjugation of ubiquitin, which is achieved through an enzymatic mechanism involving three distinct classes of enzymes. First, the ubiquitin-activating enzyme (E1) activates the carboxyl-terminal glycine residue of ubiquitin, which is next transferred to a cysteine site of a ubiquitin-conjugating enzyme (E2). Finally, a ubiquitin ligase (E3) links ubiquitin from the E2 enzyme to a lysine residue of the target protein. After ubiquitination, the polyubiquitylated protein is recognized and degraded by the proteasome. Active proteasomes are formed by the interaction of proteasomal regulatory particles (19s) with a core particle (20S), which contains the proteolytic active sites. The 19S regulatory protein recognizes the polyubiquitylated substrate, removes the ubiquitin moieties and unfolds the substrate to translocate it into the 20S proteolytic chamber. Finally, the substrate is cleaved into short peptides. The proteasome is involved in a variety of cellular functions, such as quality control of the proteome, stress response or cell cycle regulation.

---

Notably, autophagy is also emerging as a specific mechanism through which misfolded proteins and protein aggregates, such as polyglutamine-expanded proteins, are degraded (10). Unfolded proteins are normally eliminated through the proteasome or CMA, whereas bigger protein aggregates are instead preferentially degraded through the macroautophagy pathway. In particular, the type of autophagy responsible for the selective degradation of protein aggregates is denominated aggrephagy (11). The first phase of this process is the formation of the aggresome, which results from the packaging of several misfolded proteins. This process is carried out by the protein p62, which recognizes and clusters together ubiquitinated proteins. The aggresome is then transported at the MTOC (microtubule-organizing centre), residing near to the centrosome of the cell (12). Subsequently, the aggresome is engulfed by a double autophagic membrane, which forms an autophagosome that is subjected to lysosomal degradation.

Similar to proteasome activity, autophagy efficiency also declines during ageing. For instance, the expression of ATG genes (autophagy-related genes), which regulate the different autophagy steps, decreases with ageing (13), whereas lysosomes become less effective in degrading cargos (14). Accordingly, knockdown of several ATG genes decrease lifespan in *C. elegans* (15). In *Drosophila melanogaster*, Atg1 and Atg8 loss-of-function mutations shorten lifespan (16). Finally, knockout of ATG genes is lethal in mice (17).

### **3. Age-related neurodegenerative diseases**

Defects in proteostasis and subsequent accumulation of abnormal proteins can cause cellular dysfunction and cell death (3). Many age-related neurodegenerative diseases are associated to defective proteostasis and protein aggregates accumulation. Among them, age-related neurodegenerative diseases such as Alzheimer's disease, Parkinson's disease, Huntington's disease (HD) and amyotrophic lateral sclerosis (ALS) (3).

#### **3.1 Huntington's disease**

Huntington's disease is an autosomal dominant disease that affects the striatum area of the brain (18), resulting in progressive cognitive decline and muscle coordination defects (18). HD is caused by mutations (duplication) in the amino-terminal domain of the *Huntingtin* (HTT) gene (18). This region is rich in CGC codons, which codify for a polyglutamine stretch (polyQ). In healthy condition, this area contains less than 40 CGCs, whereas a polyQ stretch with more than

---

40 CGC codons triggers the development of the pathological HD phenotype (18). The pathological polyQ stretch causes defects in HTT protein folding. Misfolded HTT protein tends to aggregate forming protein aggregates and inclusions. These aggregates sequester other proteins, including proteostasis factors such as chaperones and proteasomes components (19). Therefore, HTT inclusions are toxic, leading to proteostasis collapse and neuronal death. Importantly, several studies have reported that both proteasome and autophagy appear to be affected in HD, providing a further link between proteostasis deficits and the disease (3).

### **3.2 Amyotrophic lateral sclerosis**

Amyotrophic lateral sclerosis is a late-onset fatal neurodegenerative disorder characterized by the progressive loss of upper and lower motor neurons at the bulbar or spinal level (20). ALS causes muscular impairment that brings to paralysis and death. Moreover, ALS can be categorized in two different types: the most common (90-95%) sporadic form that has no genetic origins, and the less frequent (5–10%) familial ALS form (FALS), which is inherited genetically (20).

So far, mutations in distinct 19 genes have been associated to FALS. Among them, the genes encoding for transactive response DNA binding protein 43 (TDP43) and fused in sarcoma (FUS) (20). TDP43 and FUS proteins are both RNA binding proteins and are part of the regulation process of gene expression. For instance, they play roles in transcription, RNA splicing, RNA transport, and translation (20). TDP43 and FUS are normally both localized in the nucleus, but can shuttle to the cytoplasm. Mutations in either TDP43 or FUS can cause mislocalization and accumulation of these proteins in the cytosol, where they contribute to the formation of protein aggregates. In particular, both mutant TDP43 and FUS can affect stress granules (SGs) dynamics, inducing the generation of abnormal SGs. These abnormal granules behave as solid aggregates and induce the formation of toxic inclusions that lead to proteostasis collapse and cell death (21).

---

## 4. Cell non-autonomous regulation of proteostasis

Although neurodegenerative diseases caused by misfolded proteins can lead to degeneration of specific cell types, they appear rarely associated only to a single cell type or tissue (22). Contrarily, mechanisms that promote disease progression rely on communication between cells and tissues (23). Moreover, pathways that protect against these diseases and age-associated degeneration can also act cell non-autonomously.

In addition, emerging evidence indicates that proteostasis is strongly regulated through cell non-autonomous mechanisms. A bona-fide example of how proteostasis can be regulated via inter-organ communication is represented by stress response pathways activated upon proteotoxic stress. The role of stress response pathways is preserving the integrity of the proteome under stress conditions. Although stress responses act within the cell exposed to stress, they can also be activated in a cell non-autonomous manner. Therefore, cellular activation of stress pathways enables the stressed tissue to communicate and activate cytoprotective stress responses in different tissues and organs to promote survival of the whole organism (24). To date, inter-organ communication of proteostasis has been essentially attributed to the nervous system. Stress response pathways include heat shock response (HSR) as well as organelle-specific unfolded protein responses (UPRs), such as the endoplasmic reticulum UPR (UPR<sup>ER</sup>) and the mitochondria UPR (UPR<sup>mt</sup>) (22, 24).

### 4.1 The heat-shock response

The HSR is induced as a cell autonomous response to thermal stress or the accumulation of cytosolic misfolded proteins. In eukaryotes, the HSR relies on the induction of the master heat shock regulator HSF1 (heat-shock transcription factor 1) (25). In absence of stress, HSF1 is inactivated through the recruitment of his monomeric form by the heat shock proteins (HSPs) HSP40, HSP70 and HSP90 in a cytoplasmic multi-chaperone complex (25). Heat stress or misfolded cytoplasmic proteins induce the release of HSF1 from this complex so that HSF1 oligomerizes in a trimeric form, which holds DNA-binding activity. Subsequently, HSF1 translocates into the nucleus where it binds the HSE (heat shock element) on the promoter of target genes, inducing the transcription of HSPs (**Fig. 2**) (24, 25).

The HSR can also be induced in cell non-autonomous fashion. In *C. elegans*, the thermal response is sensed by a specialized kind of cells, the two AFD thermosensory neurons and the AIY interneurons (22, 24). These cells influence worm behavior as a consequence of heat

---

stress. On a molecular level, the heat stress induces a *gcy-8* (guanylate cyclase 8)-dependent cascade signaling, which activates the HSR and consequent HSPs expression in non-neuronal tissues such as the gut, muscles and germline (26, 27). Moreover, the signal that mediates this cell non-autonomous communication has been identified as serotonin (27). Accordingly, overexpression of HSF-1 in *C. elegans* neurons is sufficient to increase stress resistance in peripheral tissues, by activating transcription of heat stress genes. Moreover, neural HSF-1 overexpression enhances longevity cell non-autonomously via a signaling mechanism that requires the activity of DAF-16 protein in intestinal cells (28). In addition, neuronal expression of misfolding-prone proteins in *C. elegans* induces HSR in distant tissues.

Importantly, cell non-autonomous activation of HSF1 in distal tissues exists also in mammals. In fact, rats exposed to persistent stress release adrenocorticotropin from the pituitary gland that subsequently activates HSF1 in the adrenal gland, inducing HSP70 expression (29). Interestingly, immunostaining experiments revealed accumulation of proteasomal subunits in the brain of Hsp70-treated mice, which suggests that Hsp70 promotes proteasomal activity, inducing cell non-autonomous mechanisms that extend lifespan in mammals. In addition, neuronal regulation of body temperature influences lifespan in mice. In fact, decreasing body temperature, by overexpressing the uncoupling protein 2 (UCP2) in hypocretin neurons (Hcrt), leads to cell non-autonomous lifespan extension of 12–20% in mice (30).

#### **4.2 The unfolded protein response of the endoplasmic reticulum**

The unfolded protein response of the endoplasmic reticulum (UPR<sup>ER</sup>) represents a further example of stress response that can be activated through either cell autonomous and non-autonomous communication (22, 24).

The UPR<sup>ER</sup> is activated by the accumulation and the recognition of misfolded proteins in the ER lumen. The UPR<sup>ER</sup> can be induced via the activation of three different major stress regulators, IRE1, PERK and ATF6, which are localized in the ER membrane (31). The most-studied is the IRE1 pathway, which is highly conserved between species. Unfolded proteins in the ER membrane trigger IRE1 multimerization in its active catalytic form, cleaving the XBP-1 pre-mRNA into the functional form XBP-1s. XBP-1s protein translocates into the nucleus, where it acts as transcriptional factor and induces the expression of UPR<sup>ER</sup> genes (**Fig. 2**) (31).

The first cell non-autonomous mechanisms of the UPR<sup>ER</sup> were discovered in *C. elegans*. In this nematode, expression of active and spliced form of XBP-1s in neurons triggers XBP-1

---

activation and UPR<sup>ER</sup> response in the intestine (32). The XBP-1s overexpressing neurons release vesicles, though the protein UNC-13, containing potential signals able to communicate the UPR<sup>ER</sup> response to the intestine. However, this signal has not been identified yet (32). Moreover, expression of constitutively active form of XBP1s transcription factor in a specific subset of astrocyte-like glia cells extends lifespan of *C. elegans*. Glial XBP-1s initiate a cell non-autonomous UPR<sup>ER</sup> activation in peripheral cells that renders these transgenic worms more resistant to proteotoxic stress and chronic ER stress (33).

Notably, UPR<sup>ER</sup> cell non-autonomous activation has also been observed in mammals. Expression of XBP-1s in the pro-opiomelanocortin neurons of mice leads to XBP-1 splicing and hence activation of the UPR<sup>ER</sup> in the liver (34). Moreover, a recent study reported that mice sensory food perception is sufficient to induce rapid morphological ER remodeling in the liver, through melanocortin-dependent cell non-autonomous activation of hepatic mTOR signaling and Xbp1 splicing. In particular, activation of Xbp1 splicing by food perception induces expression of ER-stress genes and phosphatidylcholine synthesis (35).

### 4.3 The unfolded protein response of mitochondria

Another cellular stress response pathway is the unfolded protein response of the mitochondria (UPR<sup>mt</sup>), which can also be activated in a cell non-autonomous manner. The mitochondrial electron transport complex (ETC) can cause formation of ROS, which perturb protein folding. Thus, unfolded proteins can accumulate in the mitochondrial membrane, where they are recognized and cleaved by the ATP-dependent protease ClpP (36). The resulting peptides are released from the mitochondria matrix into the cytoplasm through the transporter protein HAF-1. The accumulation of these peptides in the cytoplasm results in the activation of the proteins ATFS-1, DVE-1 and UBL-5, which translocate into the nucleus. Here, DVE-1 and UBL-5 form a transcriptionally active complex (DVE-1/UBL-5) that, together with ATPF-1, induce the transcription of the mitochondrial chaperones HSP60 and HSP70, which in turn trigger the UPR<sup>mt</sup> stress response activation (**Fig. 2**) (36).

In *C. elegans*, knockdown of ETC components in neurons can induce the UPR<sup>mt</sup> in non-neuronal tissues. Indeed, neuronal-specific depletion of the Cytochrome C Oxidase CCO-1 protein (CCO-1) leads to the activation of mtHSP70 protein in the intestine and induces lifespan extension (37). Moreover, expression of expanded polyQ proteins (polyQ40) in neurons is sufficient to induce UPR<sup>mt</sup> activation in somatic tissues through a cell non-autonomous communication that requires both the serotonergic signaling and the retromer-

---

dependent Wnt pathway (38). In fact, polyQ40 proteins form protein aggregates that accumulate in the outer mitochondrial membrane of neurons, affecting mitochondrial function. Neuronal mitochondrial dysfunction triggers the release from these cells of dense core vesicles containing the ELG-20 mitokine. Mitokines act as cell non-autonomous signal, which induce UPR<sup>mt</sup> response in distal tissues (38).

In mice, perturbation of mitochondria in muscles causes the release into the plasma of FGF-21 (fibroblast growth factor). This factor induces the activation of UPR<sup>ER</sup> in distal tissues via PERK signaling (39). In addition, brain-specific SIRT1 protein overexpression increases, cell non-autonomously, mitochondria skeletal muscle and mitochondrial functional gene expression. In turn, this process extends mice lifespan of 10–15% (40).

#### **4.5 Cell non-autonomous regulation of proteostasis by non-neuronal tissues**

Although the nervous system plays a central role in the cell non-autonomous regulation of proteostasis, non-neuronal tissues can also initiate inter-organ communication pathways. Both reduction of insulin signaling and the germline-mediated pathway (22, 24) are two examples of inter-organ communication elicited from non-neuronal tissues that modulate proteostasis systemically.

The insulin and IGF1-like signaling (IIS) pathway is a powerful cell non-autonomous regulator of lifespan. It acts through the release of insulin and IGF1-like peptides and their major downstream effectors, the FOXO transcription factors. In *C. elegans*, tissue-specific intestinal inactivation of the FOXO transcription factor DAF-16 activates the expression of target genes in muscle cells that boosts proteostasis and protects muscles from protein aggregation-associated damage (41). Moreover, specific expression of DAF-16 in muscles, influences gene expression in the intestine (41).

Recently, transcriptional microarray analysis identified an insulin-like peptide, *ins-7*, which acts as a signaling molecule in insulin-mediated cell non-autonomous communication from the nervous system to the intestine resultin in lifespan extension (42).

Importantly, the FOXO-dependent cell-non-autonomous effects on organismal proteostasis are evolutionary conserved. For instance, knockout of IGF-1 receptor in adipose tissue of mice, which controls FOXO activity, is sufficient to extend lifespan (43) and reduce proteotoxicity of protein aggregates, as reported in murine Alzheimer's disease models (44).

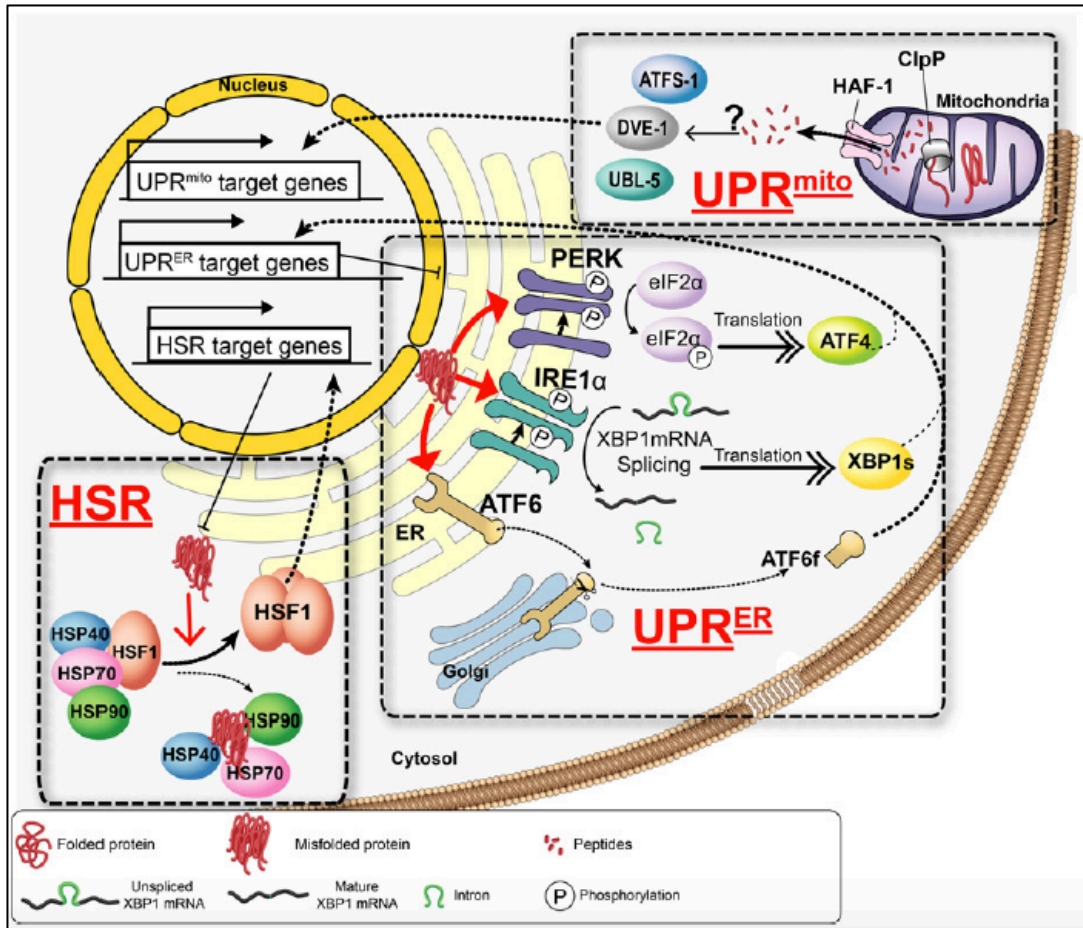


**Fig. 2. Cellular stress signaling pathways.** Adapted from Daniel O'Brien et al (2016).

Environmental challenges cause protein folding defects and accumulation of misfolded proteins, which in turn activates cellular stress response pathways. The HSR is regulated by HSF1. Formation of misfolded proteins in the cytosol leads to the release HSF1 from its inhibitory interactions with HSP90, HSP70 and HSP40. Free HSF1 multimerize and translocate into the nucleus where it activates the expression of heat-shock genes. Protein folding stress in the ER lumen triggers the UPR<sup>ER</sup>, activating the transmembrane proteins IRE1, PERK or ATF6. Activation of IRE1 induces XBP-1 mRNA splicing in the cytosol and translation of the active form XBP-1s in the nucleus, where it promotes the expression of UPR-specific proteostasis components. Protein misfolding in the mitochondrial matrix activates the UPR<sup>mt</sup>, which induces to cleavage of misfolded peptides by ClpP and subsequent transport into the cytosol by HAF-1. This results in activation of the transcriptional complex formed by ATFS-1, DVE-1 and UBL-5, inducing transcription of mitochondria-specific chaperones

Similarly to somatic tissues, the reproductive system can also elicit cell non-autonomous mechanisms to control somatic proteostasis. The theory of *the disposable soma theory of ageing* hypothesizes that the only presence of germline is sufficient to cause somatic deterioration and lifespan reduction (45). This theory was formulated by Kirkwood in 1977 and it has been supported by many experimental studies (46). In nature, the amount of external resources is limited and living organisms have to distribute the available energy between the germline and the soma. According to this theory, living organisms preferentially reallocate

---

resources to the reproductive system, in order to prevent, repair or eliminate damage in the germline, and thus ensuring a healthy and fit progeny. Therefore, a lower fraction of resources is used for the maintenance of the soma, which inevitably undergoes a progressive deterioration and ageing (45, 46). Accordingly, germline removal leads to lifespan extension in different animals. For example, gonad ablation in *C. elegans* prolongs lifespan (47). In particular, lifespan extension is not induced by sterilization itself but it takes effect through the removal of proliferating germline stem cells (GSCs), which are responsible for the generation of the signal that modulates longevity (47). Germline ablation not only increases lifespan but also improves proteostasis through the regulation of DAF-16 (45, 48). In presence of germline, the IIS signaling pathway triggers the insulin/IGF-1 receptor that activates the PI3-kinase/PDK/ATK signaling cascade, which induces the phosphorylation of DAF-16 transcriptional factor, preventing its nuclear localization. Upon germline removal, IIS signaling is downregulated and DAF-16 can translocate into the nucleus, where it promotes the expression of genes that extend lifespan and increase stress resistance (**Fig. 3**) (45, 48). Thus, gonad ablation enhances cell non-autonomously proteostasis in somatic tissues via DAF-16 activation. Notably, IIS pathway downregulation is sufficient to delay polyglutamine aggregation toxicity in *C. elegans*, (49). Moreover, the enhanced somatic proteostasis that occurs in the germline-lacking worms it is explained by the upregulation of both the ubiquitin proteasome system and autophagy. Consistently, germline lacking-worms show higher proteasome activity in somatic tissues (50). A consequence of DAF-16 activation is the somatic upregulation of the 19s proteasome subunit RPN-6. RPN-6 subunit stabilizes the interaction between the 20s and the 19s, thus improving proteasome activity (**Fig. 3**) (51). Accordingly, somatic RPN-6 overexpression is sufficient to protect from protein aggregates toxicity in Huntington's disease models (50, 51). In addition, germline-lacking worms exhibit increased autophagy. In fact, these worms display upregulation of the autophagy transcription factor HLH-30/TFEB, which modulates the expression of many ATGs, thus enhancing autophagy upon gonad removal (**Fig. 3**) (52, 53). Finally, somatic proteostasis could also be enhanced by an increase in chaperones levels and by stress response pathways induction (45).

Moreover, gonad removal not only increases somatic proteostasis but also remodels organismal metabolism. In fact, the absence of GSC signaling leads to the cell non-autonomous activation of intestinal transcription factors like *skn-1/Nrf2* (54). In particular, GCS ablation contributes to increase circulating fatty acids (FAs) that are normally accumulated in the intestine. Increased circulating FAs may lead to *skn-1* nuclear translocation that, in turn, controls lipid metabolism and enhances lifespan.

---

The ‘germline DNA-damage-induced systemic stress resistance’ (GDISR) pathway represents another example of germline-induced cell non-autonomous communication in *C. elegans* (55). When DNA damage occurs in germ cells, the ERK MAP kinase MPK-1 pathway is induced. This event triggers the activation of the innate immune response, which leads to the secretion of putative signal peptides from germ cells. This signal communicates the germline DNA damage to the somatic tissues, where the ubiquitin proteasome system is upregulated and proteostasis enhanced (55). Thus, germline DNA damage in the germline induces a systemic stress resistance improvement triggered by a cell non-autonomous mechanism.

Finally, the link between low temperature, germline fitness and organismal longevity represents another example of how germline influences somatic tissues via cell non-autonomous communication in *C. elegans*. Although extreme cold-shock has a detrimental effect on living organisms, a moderate decrease in body temperature induces a remarkable lifespan extension (56). A recent study, where I participated, reports that low temperature ameliorates the exhaustion of the GSC pool in *C. elegans*, which normally diminishes with ageing (56). Concomitantly, GSC robust proliferation upon mild cold shock induces the release of prostaglandin E2 (PGE2) signal from the germline. PGE2 induces the expression of the CBS-1 protein in somatic tissues, such as the intestine. Subsequently, CBS-1 increases the somatic production of hydrogen sulfide, a gaseous signaling molecule that induces lifespan extension (56).

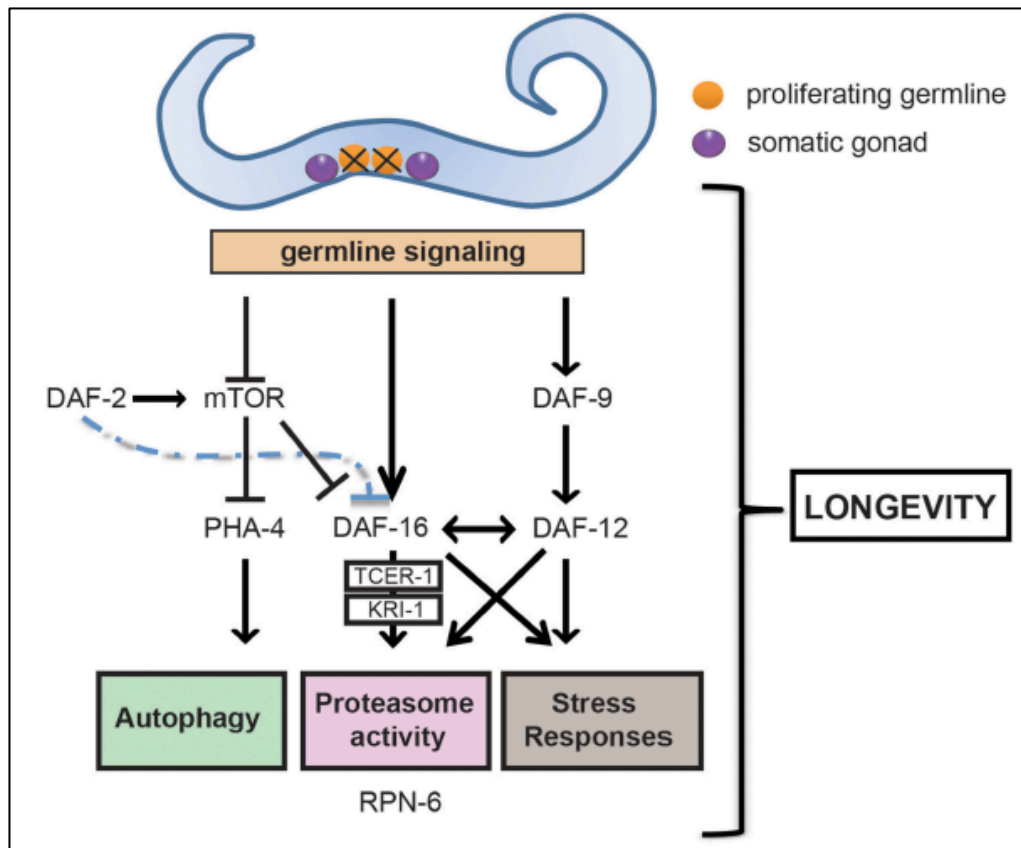


**Fig. 3. Germline ablation extends lifespan** . Adapted from Khodakarami et al (2015)

Ablation of proliferating germ cells, but not somatic cells, promotes lifespan extension in *C. elegans*. Germline ablation induces a signaling pathway that culminates with the activation of FOXO transcription factor DAF-16. Active DAF-16 translocates into the nucleus where it regulates expression of genes that increase stress resistance, proteasome activity and autophagy, thus inducing lifespan extension. DAF-16 is negatively regulated by the *daf-2*/insulin/insulin-like growth factor (IGF) signaling (IIS) pathway.

## 5. P granules

An intrinsic characteristic of germline cells is the assembly of germ granules, specific membrane-less ribonucleoprotein organelles (MLOs), which are constitutively found in the germline cytoplasm of all animals (**Fig. 4**) (57, 58). Although germ granules have a precise cytoplasmic localization, other MLOs can be found in both the nucleus and cytoplasm. Indeed, MLOs contribute to modulate gene expression, controlling for instance transcription, post-transcriptional events, translation and post-translational events such as splicing and degradation (59). Examples of other MLOs are P-bodies, stress granules (SGs), Paraspeckles, nucleolus and Cajal bodies (59).

Germ granules represent the first MLOs discovered and most of the knowledge about this organelle has emerged from studies in *C. elegans*. Indeed, the strong conservation of

---

germline granules among species and the relatively simplicity to edit the nematode genome, render *C. elegans* as a perfect model to study germline granules. Germline granules are also called P granules (PGs) in *C. elegans*. The structure and localization of PGs is conserved from invertebrates to mammals (49). PGs are composed of a heterogeneous mix of proteins and RNAs and reside in the cytoplasm of germ cells (57, 58). Particularly, P granules localize in close proximity of the nucleus periphery.

### 5.1 Function of P granules

P granules carry out several functions critical for germline differentiation, identity or maintenance and, thus, for organismal fertility. For instance, loss of function mutations in single PG components, such as *desp-1*, *pgl-1* and *glh-1*, cause temperature-sensitive sterility with defects in germ cells proliferation and gametogenesis (60). Moreover, simultaneous knockdown of four main PGs components (PGL-1, PGL-3, GLH-1, GLH-4), results in a germline that lacks PGs (61). In this model, germ line cells proliferate normally through larval stages but fail to initiate oogenesis during larval-adult transition, resulting in sterile adult worms, which do not generate oocytes (61). Thus, P granules are essential to secure germline fertility of adult animals. Furthermore, PG-lacking germlines show aberrant expression of somatic genes in germ cells. Transcriptomic analyses of PG-lacking germline revealed thousands of misregulated genes (62). In addition, some germ cells differentiate into a neuron-like cell type. Therefore, PGs control the gene expression landscape of germ cells during their development, preventing somatic gene expression and ensuring the proper germ cell identity fate.

In addition, PGs are a site for RNA biogenesis. Silencing of somatic genes could take effect through small RNA pathways in the germline (63). Small RNA may recognize unwanted transcripts and target them for degradation. Furthermore, enzymes required for small RNA biogenesis co-localize to PGs (63). Although many PG factors are associated to RNA destabilization and degradation, recent studies revealed that other PG components protect and stabilize transcripts to assure translation of specific mRNAs only at a precise moment during development of the germline (64). Consistent with a role in mRNA surveillance, several members of the RNA regulator Argonaute family are enriched in P granules. As such, the newly synthesized transcripts are captured by PGs prior diffusing into the cytosol. Thus, PGs can select which transcripts should be translated and which ones should be silenced. For example, PGs deliver maternal mRNAs to germline blastomers during early development,

---

enabling the correct gene expression and protecting germline blastomeres from adopting somatic fates (57, 65). Finally, PGs can also control the translation process by retaining protein translation components. For instance, the sequestration into PGs of IFE-1, a germline-enriched isoform of eukaryotic initiation factor 4E (eIF4E), causes translation inhibition (57).

## 5.2 Generation of P granules

PGs take their name from the P lineage, which gives rise to the germ cells (57). In the arrested oocytes, PGs are semi circular structures surrounding the nuclei. After fertilization, PGs became highly dynamic and diffuse to the cytoplasm. Subsequently, PGs segregate asymmetrically in the posterior part of the primordial one-cell zygote (P0). The P0 cell divides progressively four times (66). Every time the P cell divides, it generates two daughter cells. One is the P cell that contains all the PGs, which always segregate asymmetrically into the P cells after every division (67). The other cell is the precursor of somatic line and generally does not receive PGs from the mother P cell.

In the P2 cell, PGs change their localization, moving from the cytoplasm to the nuclear periphery. After the four divisions, P4 cell nuclei are completely surrounded by large PGs. Then, the P4 cell divides into the two primordial germ cells (PGS) Z2 and Z3, which both receive PGs. Then, the Z2 and Z3 cells divide symmetrically to eventually produce about 1500 germ cells that constitute the adult gonad. PGs remain associated to the nuclear envelope during all germ cell development into gametes and diffuse back to the cytoplasm only upon oocyte fertilization (**Fig. 4**) (58, 68).

## 5.3 Composition of P granules

Most of PGs components are rich in intrinsically disordered regions (IDR). IDRs contain low complexity and repetitive regions, rich in aminoacids as glycine, serine, and arginine (68, 69). Proteins harboring these IDRs are named intrinsically disordered proteins (IDPs). The abundance of such IDPs confers to PGs the ability to be extremely dynamic, being able to switch back and forth between liquid, gel and solid state (70, 71). In addition, P granules occasionally could fuse with one another and exchange mobile components with the cytoplasm.

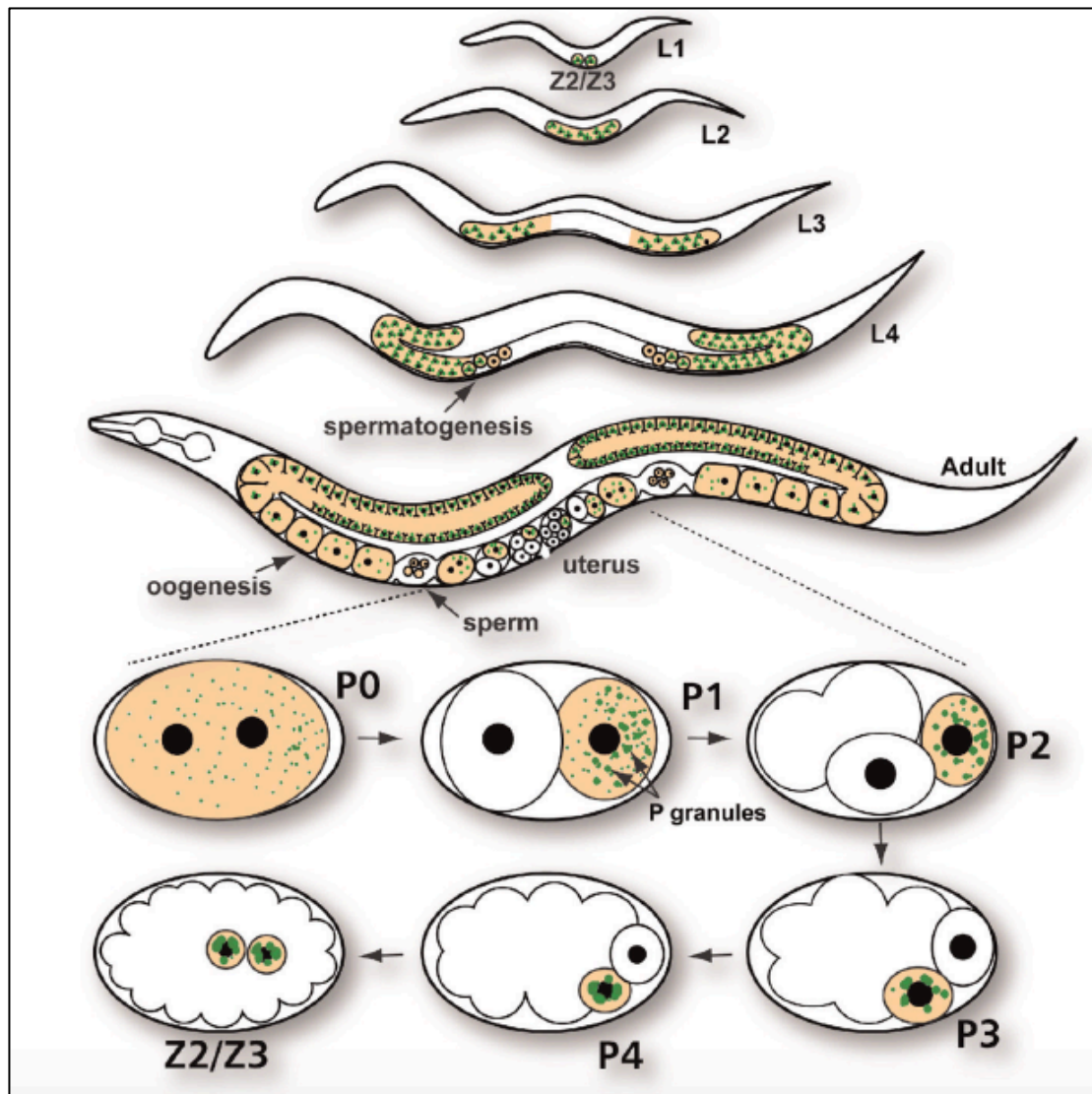


**Fig. 4. P granules.** Adapted from Updike and Strome (2010).

The 2 primordial germ cells (Z2/Z3) start to proliferate at the end of the first larval stage (L1). In the following larval stages, the primordial germ cells continue dividing, giving rise to the mature germline in the adult worm. After fertilization (P0 zygote), P granules segregate to the germ line blastomeres P1 to P4. Then, the primordial germ cell P4 divides into the daughter cells (Z2/Z3).

To date, over 40 different proteins have been reported to be part of PGs (57, 58). Many of these PG components are RNA-binding proteins. Some are constitutively part of PGs, while others only associate to the granules at precise stages of germline development. The list of components includes proteins that have roles in translation initiation and RNA metabolism like splicing, deadenylation and decapping. However, the defining components of P granules that associate to PGs throughout all germline life are two classes of RNA-binding proteins: the DEAD-box proteins GLH-1–4 and the RGG-domain proteins, PGL-1 and PGL-3 (57, 58).

---

## 5.4 The germline helicases protein family

The first PG component identified was the *Drosophila* DEAD-box RNA helicase Vasa (57). Vasa proteins are highly conserved through species and play important roles in germline development and fertility in all animals. *C. elegans* has four VASA proteins, which are named germline helicases (GLH): GLH-1, 2, 3 and 4 (72). Among them, GLH-1 plays a predominant role in PGs, compared to the other GLH members.

GLH proteins contain a FGG region, which consists of a sequence rich in glycine, where arginine residues are interspersed in regularly spaced intervals (68). The FGG domain is responsible for the association of PGs to the nuclear periphery, through an interaction with nuclear pore proteins. In *C. elegans*, the 75% of all nuclear pores of germline cells interact with PGs (73). Thus, GLH proteins play a central role in localizing PGs at the nuclear periphery. Accordingly, depletion of GLH-1 and GLH-2 causes partial PG detachment from nuclear pores (74). Furthermore, another essential function of GLH-1 is the recruitment of all PGL proteins to P granules (75). In fact, GLH-1 deficiency causes PGL-1 diffusion in the cytosol.

GLH-1 is important to assure germline fertility. In fact, *glh-1* null mutants show temperature-dependent sterility due to defects in proliferation and gametogenesis at 25°C. On the contrary, *glh-2*, *glh-3* and *glh-4* single null mutants do not show sterility at any temperature (60, 75).

## 5.5 The PGL protein family

The PGL family of proteins includes three paralogous proteins: PGL-1, 2 and 3 (65). All PGL proteins are able to interact with each other *in vitro*. However, PGL-1 and PGL-3 have 77% amino acid similarity and can interact directly with each other *in vivo* (65). Moreover, PGL-2 is absent in PGs during embryogenesis (68), whereas PGL-1 and PGL-3 associate to PGs throughout all germ cell life.

PGL-1 and PGL-3 proteins have a RGG domain in the C-terminal region, whereas PGL-2 lacks this part. The RGG domain, a type of IDR, is a region rich in glycine, while arginine residues are interspersed in regularly spaced intervals (68). The RRG domain enables PGL proteins to interact with RNAs, through polyvalent interactions between arginine residues and RNA molecules. This interaction is essential for the P granule core formation (76, 77). In addition, the RGG boxes have been shown to bind RNA with low sequence preference.

---

Therefore, PGL proteins are likely to bind via the RGG box to diverse mRNAs and mRNA protein complexes (mRNPs) that contain other protein components of P granules (76).

Interestingly, it has been proposed a model to explain how PGs form, which consists of two steps (76). First, PGL proteins interact, through the RGG domain, with various mRNAs and mRNPs, subsequently PGL proteins interact with each other, through the self-interaction domains, thus forming the globular structure that characterizes P granules (76). Therefore, PGL proteins act as a scaffold during the assembly of PGs.

PGL-1 plays a predominant role in PG assembly, compared to the other PGL proteins. Accordingly, *pgl-1* null mutant shows defects in germ cell proliferation and gametogenesis that causes temperature-dependent sterility (60, 65). On the contrary, deletions of single *pgl-2* and *pgl-3* do not cause germline defects but enhances the sterility when depleted together with *pgl-1*. In addition, PGL-1 is the only PGL protein that binds IFE-1, which is essential for spermatogenesis (65).

## 5.6 P granule association to mitochondria

In adult animals, germ granules exhibit a perinuclear distribution. Interestingly, PGs also reside close to mitochondria, forming complexes with germline-specific structures such as the mitochondrial cloud and intermitochondrial cement (57, 78, 79). For example, germ granules are associated to mitochondria at different development stages in *Drosophila* (78). In insects, the polar granule represents a certain type of germ granule that gives rise to the primordial germ cells. In *Drosophila immigrans*, polar granules are attached to mitochondria during the early stages of the embryo, whereas during oogenesis and immediately after fertilization, polar granules are attached to mitochondria in every *Drosophila* species studied except in *D. hydei* (78).

The biological reason of this close proximity is not clear yet, but it has been suggested that mitochondria could serve as extra energy source for the germ granule (78). Furthermore, PGs can also contain cytoplasmic components, such as microtubules and centrioles. When the P granule grows, it can randomly engulf cytoplasmic elements or other neighbor P granules as well (57). However, this event happens infrequently during P granule growth. In addition, PG proteins are also prone to aggregation and can lead to aberrant granules (59, 80, 81).

---

## 5.7 P granule phase transition

Formation of PGs, as well as of other MLOs, occurs through a process called phase transition. During phase transition macromolecules separate in a dense phase, rich in proteins and nucleic acids, and in a diffuse phase, where molecules are less concentrated (82). Hence, this event gives rise to new cellular sub-compartments: a cytoplasmic area poor in molecules and the MLO that remains separated from the surrounding environment. High energy is required to obtain phase transition, resulting in entropy decrease (59).

In physiological conditions, MLOs are highly dynamic structures due to their composition abundant in RNA-binding proteins. Indeed, RNA-binding proteins are rich in IDRs and low complexity sequences that contribute to form electrostatic and hydrophobic interactions (68, 59). Thus, reversible multivalent interactions allow MLOs to transit among diffuse, liquid, or solid states (supramolecular levels).

Importantly, MLOs can polymerize into solid structures and induce toxic protein aggregation (59, 81, 83). When MLOs assume a solid structure they could cause neurodegenerative disorders, such as ALS and frontotemporal dementia. Therefore, the supramolecular level of MLOs needs to be strictly controlled by mRNP regulators or cellular control pathways (59). Accordingly, the PGs supramolecular level appears to be rigorously monitored also in the *C. elegans* germline. Thousands of reversible interactions render PGs highly dynamic, so PGs assume different structures, compositions and morphologies during the distinct phases of germ cell development (81).

For instance, PGs undergo phase transition from viscoelastic semiliquid structures to more dynamic liquid droplets upon oocyte fertilization. Furthermore, it appears that specific RNA-binding proteins (RBPs) modulate this phase transition (81). In arrested oocytes, PGs are highly viscous perinuclear structures that contain RBPs such as CGH-1, the Lms protein CAR-1, as the mRNA-binding translational repressors PUF-5 and MEX-3, which contribute to retain specific subsets of mRNAs within the granule (81).

Upon oocyte fertilization, RBPs form new interactions while others are lost. Thus, new subsets of mRNA are free to diffuse into the cytosol, where they are translated, whereas other new mRNAs are captured in the granule and repressed (81). These changes cause a germ granule remodeling that leads to PGs phase transition from viscous to more dynamic liquid-like structures. This phenomenon represents also a strategy to modulate mRNA expression, which finely controls cell identity specification. Therefore, phase transition depends on RBPs that are responsible for the formation of new interactions. In particular, RBPs, such as PUF protein and

---

CAR-1, determine which mRNAs are retained in the granules and which are released into the cytosol (81).

Importantly, CGH-1 helicase prevents germ granules phase transition into solid polymers and maintain semiliquid subdomains. Accordingly, loss of CGH-1 lead to abnormal structures that accumulate into large sheet-like granules (81). Sheet size vary up to ~10 um and all sheets retain a square geometry. Their precise geometry strongly suggests that these arrays result from specific interactions and not random aggregation. Therefore, CGH-1 modulates granule fluidity and organization. On the contrary, depletion of specific PUF proteins (PUF-3, 5 and 11) in *cgh-1* mutant worms prevents the formation of these abnormal squared sheet-like granules. These findings suggest that PUF proteins could be required for mRNPs to co-assemble into either semiliquid droplets or solid polymers, while the CGH-1 could act to prevent a nondynamic solid state (81). Another group of proteins that control PGs dynamics and prevent germline granules aggregation is the *C. elegans* Y-box binding protein (CEY) family (84).

## 6. The *C. elegans* Y-box binding protein family

The *C. elegans* Y-box binding protein (YBX) family includes four members CEY-1, 2, 3 and 4 (84). CEYs are relatively small proteins: CEY-1 consists of around 200 aminoacids, CEY-4 of approximately 300 aminoacids, whereas CEY-2 and CEY-3 are both composed of around 270 aminoacids (84). Importantly, these four members share in common a high conserved region of about 70 aminoacids called cold shock domain (CSD) (**Fig. 5**).

The CSD is highly conserved among species, sharing more that 40% similarity and 60% identity from bacteria to vertebrates (85). The CSD takes its name from the bacterial cold shock protein (Csps), which consists only of the CSD sequence. Csps are believed to act as chaperones, which are activated in response to cold shock and prevent potential toxic folding events (86). Moreover, the CSD consists of five antiparallel  $\beta$ -strands that form a  $\beta$ -barrel structure, which enables interactions with single stranded DNA and RNA molecules (87). The two motifs RNP1 and RNP2, located respectively in the  $\beta$ -strands 2 and 3 of the CDS, are responsible for this interaction with nucleic acid molecules (88).

Although CEYs share identical CSDs, the rest of their protein structure presents differences. For instance, CEY-1 and CEY-4 show arginine rich RG/RGG regions, whereas both CEY-2 and CEY-3 lack this domain (84). However, CEY-2 and CEY-3 share a 70% of

---

homology and, since their expression pattern overlaps, they probably display redundant functions (**Fig. 5**) (84).

Although the CSD enables interactions with RNA and DNA molecules, CEYs are also capable to interact with other proteins through other domains present at the N and C-terminal protein regions. Furthermore, except for CEY-2 and CEY-3, CEY proteins exhibit different localization patterns. Importantly, all four CEYs are expressed in germline, however CEY-1 and CEY-4 localize also in the soma, whereas CEY-2 and CEY-3 are absent in somatic tissues (84). In somatic tissues, CEY-1 is highly expressed in neurons, while CEY-4 in the intestine (**Fig. 5**).

In addition, CEY-2 and CEY-3 germline expression pattern shows a gradient that coincides with oocyte maturation; it increases from the distal to the proximal part of germline and disappears with oocyte fertilization and embryo development (84).

## **6.1 Function of YBX proteins**

In contrast to YBX proteins of other organisms, which localize to both cytosol and nucleus, CEY proteins appear to be located only in the cytoplasm (84). Therefore, whereas YBX proteins act at both transcriptional and post-transcriptional levels, CEYs are supposed to operate exclusively at post-transcriptional levels. In the nucleus, YBXs are involved in the transcription process as well as in DNA repair and pre-mRNA splicing, whereas YBXs control RNA stability and regulate protein translation in the cytosol.

The best-studied Y-Box protein is YBX-1, which represents a bona fide example to understand how YBX proteins act. Besides the CSD, YBX-1 holds a domain rich in alanine/proline at the N-terminal region, whereas the C-terminal consists of positively and negatively charged clusters that enable YBX-1 to oligomerize. Contrarily to the CDS, both N-terminal and C-terminal regions are intrinsically disordered sequences, which confer to YBX-1 the ability to play multiple diverse functions (89). In the nucleus, YBX-1 is involved in gene transcription, DNA repair and mRNA splicing, whereas in the cytoplasm YBX-1 is essential to control mRNA translation and stability, but it is also a major polysome component. Furthermore, YBX-1 can either induce or repress mRNA translation and these events depend on the ratio mRNA/YBX-1. At low mRNA/YBX-1 ratios, individual YBX-1 proteins interact, through the CDS domain, with free mRNA molecules leading to their unwinding and subsequently exposing these transcripts to either translation or decay machineries (90).

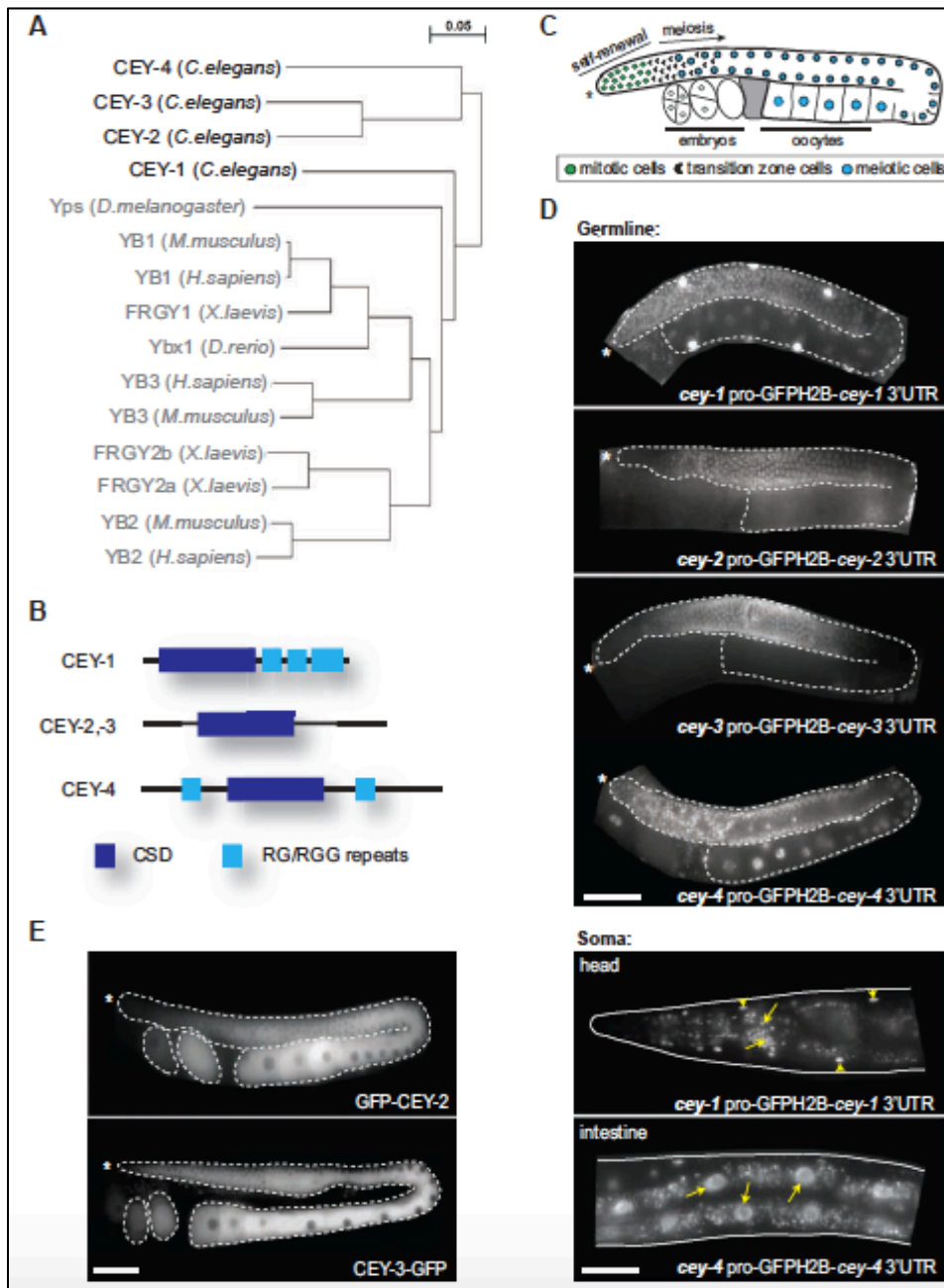


**Fig. 5. The *C. elegans* Y-box binding protein family (CEY).** Adapted from Arnold *et al* (2014).

(A) The YBX protein family is highly conserved among species and the closest CEY ortholog is the Yps protein of *Drosophila melanogaster*. (B) All CEYs share the CSD. However, CEY-1 and CEY-4 contain RG/RGG repeats, which are absent in CEY-2 and CEY-3. (D) Transgenic worms expressing reporter constructs for each of the *cey* genes reveal that all four CEY factors are expressed in germline. Here, whereas *cey-1* and *cey-4* are highly expressed in the distal most region of the gonad, *cey-2* and *cey-3* are very lowly expressed distally but become strongly upregulated more proximally. In the soma, although *cey-1* and *cey-4* are expressed in all tissues, *cey-1* reporter expression is higher in neurons and muscles, whereas *cey-4* reporter expression is strongly expressed in the intestinal cells. (E) Transgenic worms expressing GFP-tagged CEY-2 and CEY-3 confirm that GFP-CEY-2 and CEY-3-GFP are exclusively expressed in the germline.

---

However, at high mRNA/YBX-1 ratios, YBX-1 still interact with mRNAs but its C-terminal promotes YBX-1 multimerization and leads to mRNPs packaging, protecting mRNAs from translation (90). However, other studies show that YBX-1 can also recognize specific protein sequences and modulate translation of individual mRNA targets (89). Thus, YBX-1 plays roles in several different cellular processes (89). For instance, YBX-1 regulates cell proliferation, through its control on cyclins translation. Moreover, YBX-1 has roles in apoptosis and cell differentiation. For these reasons, YBX-1 has often been associated to cancer, acting as an oncogene. Finally, YBX-1 is involved in stress responses and plays important functions in controlling the formation of SGs (91, 92).

## 6.2 Role of YBX proteins on germ granules

YBX proteins localize prevalently to the reproductive system of many animals, where they play a pleiotropic role. Accordingly, several studies reveal that YBX proteins are associated to germline granules (93). In fact, YBXs package maternal mRNA in cytoplasmatic mRNPs, where transcripts are stored and kept translationally silent until they are needed. Thus, YBXs orchestrate, post-translationally, the correct gene expression pattern necessary for the precise cell identity specification of germ cells. For instance, the Yps *Drosophila* YBX variant controls the localization and translation of the maternal oskar transcript, which is essential for correct development (94). In *Xenopus*, the FRGY-2 ortholog has the important function to bind newly transcribed maternal mRNAs and repress their translation (95). In mouse, MSY-2 controls maternal mRNAs stability (96). Finally, YBX-1 regulates the sqt1 mRNA translation in zebrafish (97).

Similarly, CEY proteins are involved in many aspects of germline function in *C. elegans*. CEYs display a central role in controlling the spatial and temporal maternal mRNA translation during oogenesis in *C. elegans*. Moreover, as their YBX orthologs, CEYs do not interact with specific subsets of mRNA, on the contrary the binding occurs in a more unspecific fashion (84).

Furthermore, it has emerged that CEYs are not only PG component but they are also crucial for germ granules organization and dynamics. Accordingly, co-immunoprecipitation experiments reveal that CEYs interact in a RNA-dependent fashion with many PGs component, such as GLH-1, GLD-1, CAR-1 and PAB-1 (84). Importantly, CEY proteins seem to prevent PG aggregation. In fact, the germline of quadruple *cey-1, 2, 3* and *4* null mutant worms show formation of aberrant aggregate-like P granules, which colocalize with PGs components such

---

as CGH-1, CAR-1 and GLD-1 (84). Therefore, CEYs act as guardian factors that avoid phase transition of germ granule and protect germline proteostasis from collapse.

Moreover, *cgh-1* depletion also induces formation of abnormal PGs that aggregate into squared-sheet solid structures (81, 84). These aberrant germ granule aggregates colocalize with CEY-3, supporting the idea that CEYs are also PGs components (84). Interestingly, the mammalian ortholog YBX-1 is also part of SGs and it can protect from abnormal mRNPs aggregation (91).

Under normal conditions, the population of mRNA not associated to polysomes is lower compared to the polysomal transcripts (91). The non-polysomal mRNA is associated with specific cytoplasmic proteins, as YBX-1, which prevents SG formation (98). Under stress conditions, translation is inhibited and polysomal mRNAs are released into the cytoplasm. Thus, the amount of free non-polysome mRNA increases and the mRNA-stabilizing proteins, like YBX-1 that prevent mRNA aggregation, result to be outnumbered. This event triggers SG formation. However, when aggregation-prone proteins or misfolded proteins form, they can gain access to mRNA and induce mRNA aggregation and abnormal SG formation (91). Therefore, YBX-1 acts as guardian to protect from abnormal SG formation. Accordingly, YBX-1 overexpression prevents SG induction (91).

Another study revealed that YBX-1 competes with TDP-43 and FUS in binding mRNA molecules *in vitro* (99). As previously discussed, TDP-43 and FUS are RBPs that can cause neurodegenerative diseases like ALS and frontotemporal lobar degeneration (FTLD). Both TDP-43 and FUS have long self-attractive low complexity domains (LCD), which confer a prion-like behavior to these RBPs. Therefore, TDP-43 and FUS can be responsible for the formation of abnormal aggregate-like SGs. *In vitro*, TDP-43 and FUS are able to interact to free mRNA molecules and multimerize, resulting in mRNPs aggregation (99). However, YBX-1 is capable to compete with TDP43 and FUS in binding mRNAs, and replace them from mRNPs. In fact, the only addition of YBX-1 molecules to these mRNPs is sufficient to cause the dissociation of TDP-43 and FUS proteins from the mRNAs (99).

### **6.3 Functions of CEY proteins in the *C. elegans* germline**

Through controlling mRNA translation, CEY proteins indirectly regulate many aspects of germline development. In addition, CEY-2 and CEY-3 seem to play a major role in the germline compared with CEY-1 and CEY-4. Accordingly, the double loss of *cey-1* and *cey-4* does not disturb fertility, whereas the loss of both *cey-2* and *cey-2* partially affects worm

---

fertility, causing a reduction in the progeny number (84). In fact, *cey-2* and *cey-3* double mutant worms present premature oocytes maturation. Finally, the quadruple CEYs mutant causes total sterility (84). Furthermore, double *cey-2* and *cey-3* mutant worms have a significant reduction in proliferating mitotic germ cells in the distal region of germline and increased germ cell apoptosis (84). In contrast, CEY-1 and CEY-4 are also expressed in the soma, where they appear to regulate the formation of large polysomes (84). The double *cey-1* and *cey-4* knockout results in a dramatic loss of large polysomes with a concomitant increase in monosomes and disomes. However, this difference in polysomes organization does not affect the global translation rate levels. In fact, the *cey-1* and *cey-4* double mutant worms have neither development defects nor shorten in lifespan (84).

---

## **OBJECTIVES OF THIS WORK**

- 1.** Determine if CEY proteins influence germline proteostasis.
- 2.** Investigate if germline proteostasis status can be communicated to the soma via cell non-autonomous mechanisms.
- 3.** Unravel the mechanism behind a novel inter-organ communication between germline and soma.
- 4.** Discover the signal molecule responsible for the germline-soma communication.

---

## RESULTS

Aggregation-prone mutations challenge the integrity of the cellular proteome, leading to protein aggregates that cause malfunction and death of post-mitotic cells such as neurons (2, 3). This demise in protein homeostasis (proteostasis) contributes to the onset of distinct disorders, including Alzheimer's disease, Huntington's disease (HD) and amyotrophic lateral sclerosis (ALS) (2, 3). Besides intracellular deficits in proteostasis, growing evidence indicates that the proteostasis status can be communicated between somatic tissues (32, 38). Since the germline can influence somatic function (47, 55, 56), we asked whether proteostasis alteration in germline cells affects somatic tissues such as the nervous system.

### 1. Depletion of *cey-2* and *cey-3* proteins induces PGL-1 aggregation.

To assess whether perturbation of germline proteostasis induces cell non-autonomous mechanisms, we targeted Y-box binding proteins (YBX), which have been reported to prevent aberrant aggregation of germ granules (84, 91, 92). The *C. elegans* genome encodes four YBX proteins, i.e. CEY1-4 (84). Whereas CEY-1 and CEY-4 are present in both the soma and the germline (21), CEY-2 and CEY-3 are only expressed in the germline similar to PGL-1 (84).

To further confirm these findings, we performed quantitative PCR (qPCR) on RNA samples isolated from either wild-type strain or temperature-sensitive *glp-4* mutant, which lacks germline when grown at 25°C. Accordingly to previous results, we observed that *cey-2* and *cey-3* expression, similarly to *pgl-1*, was not detectable in *glp-4* mutant (**Fig. 6**). This result confirms that CEY-2 and CEY-3 factors are exclusively present in germline and their expression is totally undetectable in the soma. Contrarily, *cey-1* and *cey-4* expression, similarly to *act-2*, was unchanged in germline-lacking mutant compared to wild-type strain (**Fig. 6**). This result corroborates the finding that CEY-1 and CEY-4 are expressed in both soma and germline of *C. elegans*. Thus, we focused on CEY-2 and CEY-3 to circumvent direct effects of CEY proteins on somatic tissues.

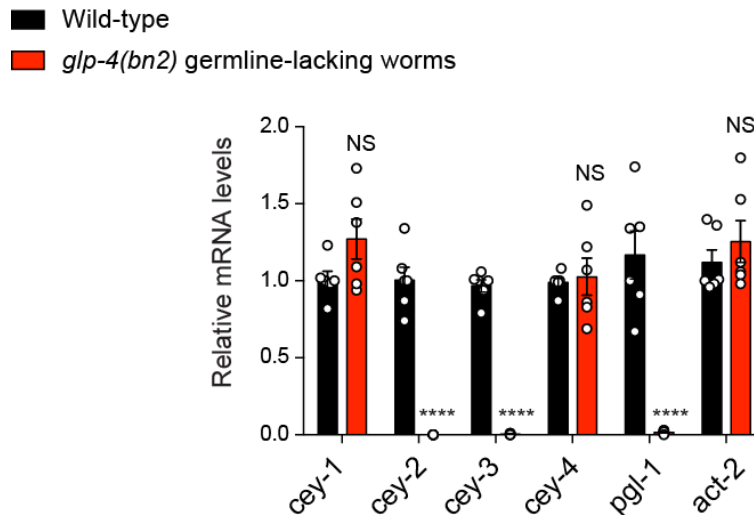


**Fig. 6. *cey-2* and *cey-3* are only expressed in the germline.** qPCR analysis of germline-specific *cey-2*, *cey-3*, and *pgl-1* as well as ubiquitously-expressed *cey-1*, *cey-4*, and *act-2* ( $\beta$ -actin) normalized by the geometric mean of the housekeeping genes *cdc-42* and *Y45F10D.4* in germline-lacking worms (*glp-4(bn2)*). Graph represents the mean  $\pm$  s.e.m. of the relative mRNA levels to wild-type worms (n= 6 independent experiments). Statistical comparisons were made by two-tailed Student's t-test for unpaired samples, \*\*\*\*(P< 0.0001). NS= not significant (P> 0.05).

Remarkably, qPCR experiments revealed that RNAi knockdown of either *cey-2* or *cey-3* was specific for the respective CEY target and did not cause depletion of other unspecific CEY factors. Notably, knockdown of either *cey-2* or *cey-3* was extremely efficient, resulting in a approximately 100% reduction of their expression level (**Fig. 7**). Furthermore, single depletion of both *cey-2* and *cey-3* did not affect the expression level of any other CEY factors.

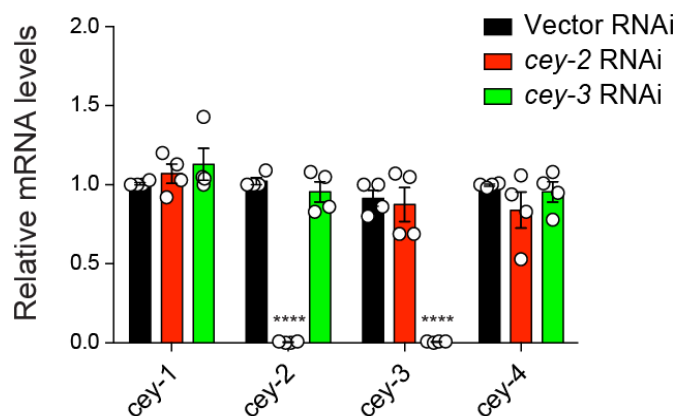


**Fig. 7. Knockdown efficiency and specificity of *cey-2* and *cey-3* RNAi.** qPCR analysis of day 3-adult wild-type worms upon either *cey-2* or *cey-3* RNAi treatment. Graph represents the relative expression to Vector RNAi control (mean  $\pm$  s.e.m., n= 4). Statistical comparisons were made by two-tailed Student's t-test for unpaired samples. P-value: \*\*\*\*(P<0.0001).

To validate the role that CEY proteins exert on P granule dynamics, we targeted PGL-1 protein, as it represents one of the main PG regulators (76, 77). Importantly, PGL-1 immunostaining experiments revealed that single knockdown of either *cey-2* or *cey-3* was sufficient to trigger the accumulation of PGL-1 into aberrant foci in the germline, particularly in the mitotic region where germline stem cells (GSCs) are located (**Fig. 8A**). Likewise, we observed a similar phenotype in *cey-2* functional null mutant worms (**Fig. 8B**). Moreover, filter trap assays, of GFP-tagged PGL-1 reporter strain, showed accumulation of PGL-1 aggregates upon germline-specific CEYs depletion, without affecting the total amounts of PGL-1::GFP protein (**Fig. 9**). This result confirmed that PGL-1 aberrant foci display an insoluble aggregate behavior.

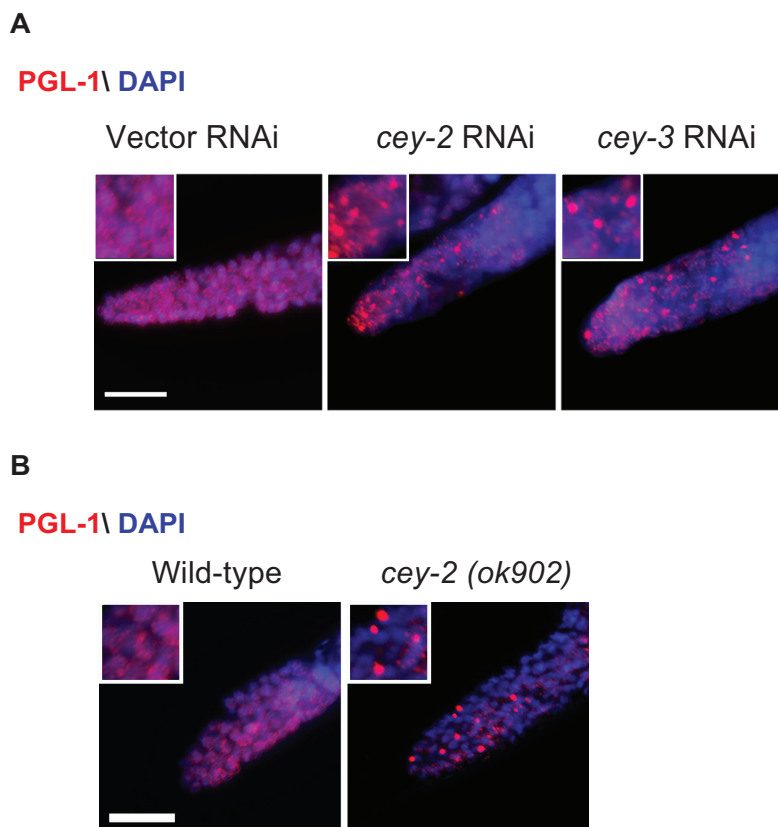


**Fig. 8 PGL-1 aggregation upon *cey-2* and *cey-3* knockdown.** (A) Immunostaining of germlines with antibody to PGL-1 and DAPI (nuclei). Knockdown of germline-specific CEY proteins triggers aggregation of endogenous PGL-1 in GSCs of the germline mitotic region (that is, the first 20 rows of cells in the most distal part of the germline). Scale bar, 20  $\mu$ m. Images are representative of three independent experiments. (B) Immunostaining with antibody to PGL-1. *cey-2* functional null mutant worms exhibit PGL-1 aggregates in germline stem cells (GSCs). Cell nuclei were stained with DAPI. Scale bar, 20  $\mu$ m. Images are representative of two independent experiments.

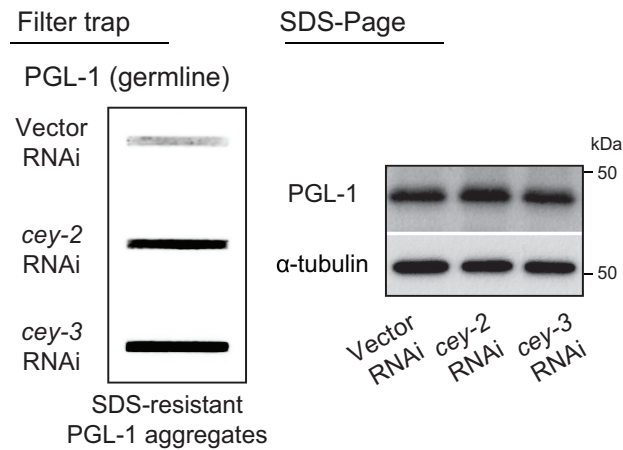


**Fig. 9 Filter trap assay of *cey-2* and *cey-3* knockdown worms shows increased PGL-1 aggregation.** Knockdown of germline-specific CEY proteins triggers aggregation of PGL-1::GFP (detected by anti-GFP antibody) expressed under germline-specific promoter *pie-1*. Right panel: SDS-PAGE analysis with antibodies to GFP and  $\alpha$ -tubulin loading control. The images are representative of three independent experiments.

## 2. Depletion of *cey-2* and *cey-3* does not affect organismal lifespan and fecundity

Since PGL-1 aggregates localize in the mitotic region of germline, we asked if such aberrant PGL-1 foci could affect germ stem cells. However, we did not detect changes neither in the proliferation nor in the total number of GSCs in germline of single CEY-2 and CEY-3 depleted worms (**Fig. 10A, B, C**).

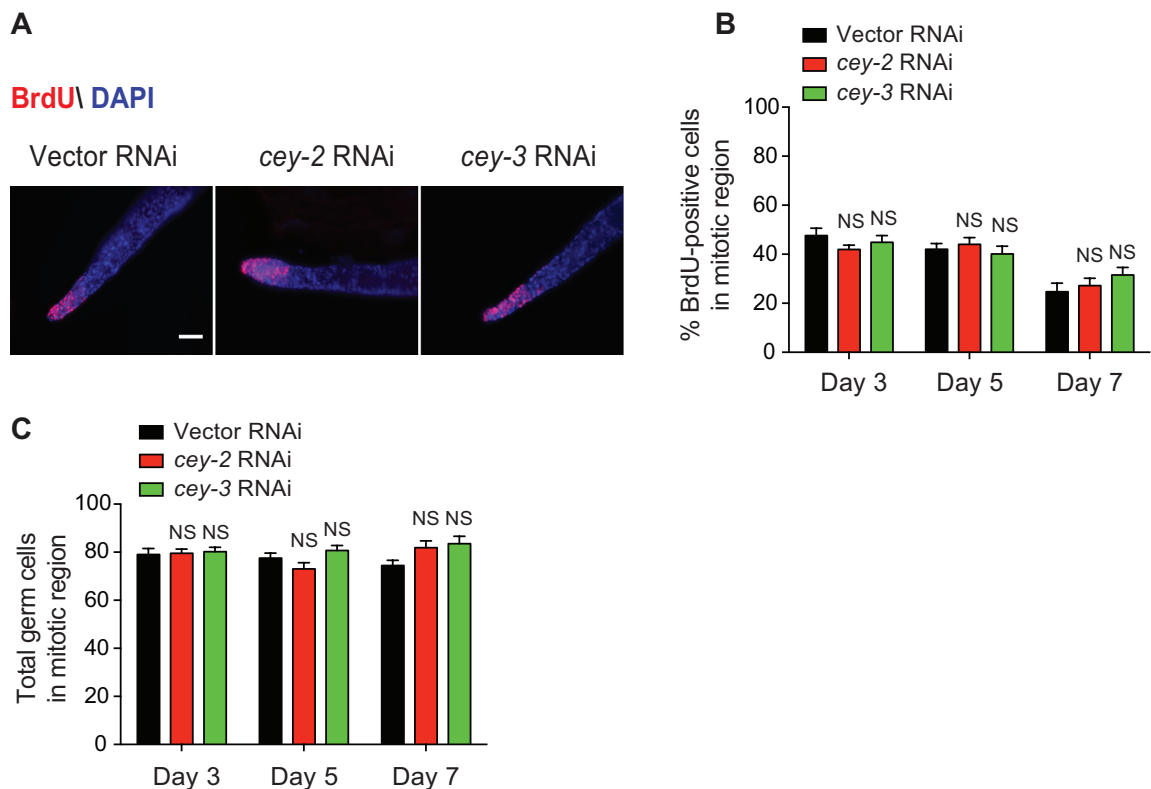


**Fig. 10 *cey-2* and *cey-3* knockdown does not impair proliferation of GSCs.** (A) 5 bromodeoxyuridine (BrdU) staining of proliferating GSCs in the mitotic region. The mitotic region consists of the first 20 rows of cells in the most distal part of the germline. *C. elegans* germlines were extruded after 2 h of BrdU treatment at day 3 of adulthood. Cell nuclei were stained with DAPI. Scale bar, 20  $\mu$ m. The images are representative of two independent experiments. (B) Percentage of BrdU-positive cells per total nuclei within the mitotic region (mean  $\pm$  s.e.m., n= 16 germlines scored per condition from two independent experiments). (C) Total number of germ cells within the mitotic region (mean  $\pm$  s.e.m., n= 16 germlines scored per condition from two independent experiments).

Subsequently, we asked if formation of abnormal PGL-1 aggregates could affect germline by altering fecundity. However, single depletion of *cey-2* and *cey-3* did not alter either the number of eggs laid or the number of eggs etched (Fig. 11A, B, C). Therefore, the accumulation of PGL-1 aggregates did not diminish GSC proliferation and fecundity rates, indicating that these worms conserve a functional germline.

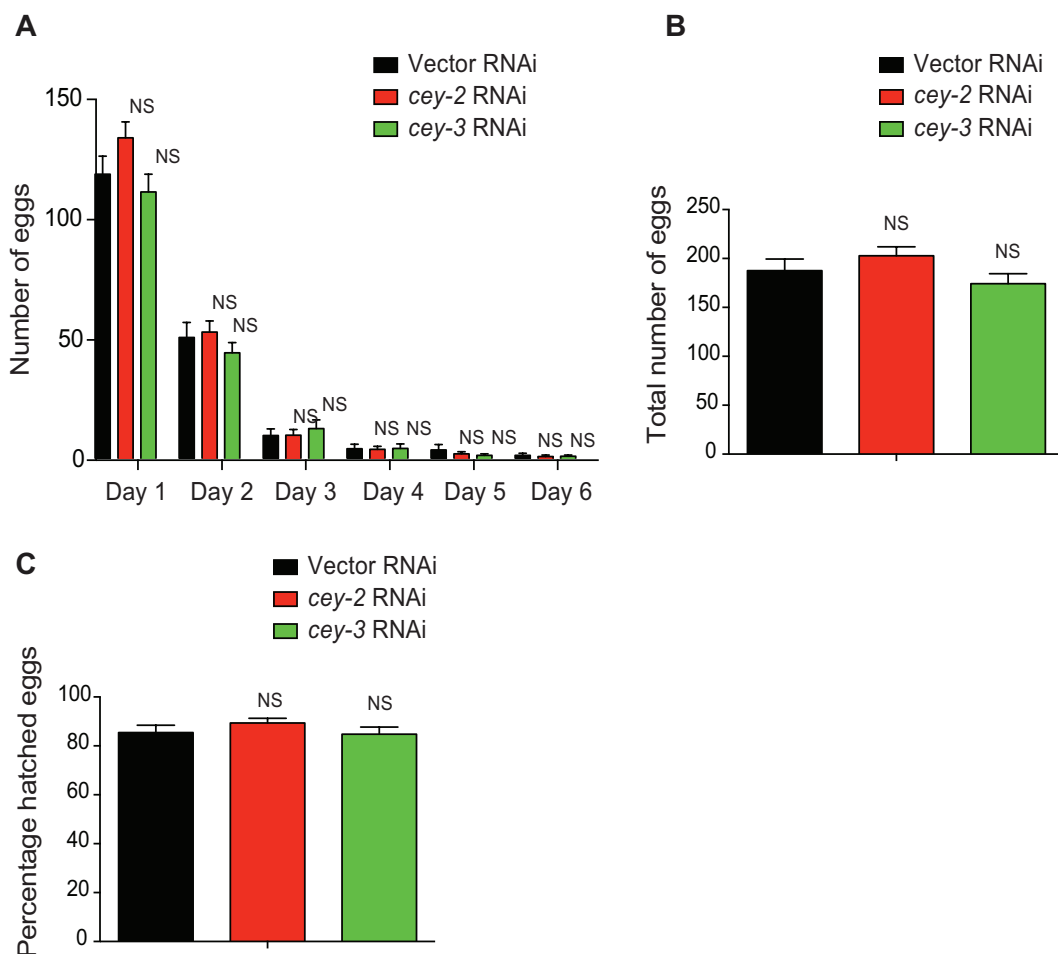


**Fig. 11. *cey-2* and *cey-3* knockdown does not impair fecundity.** (A) Number of eggs laid per wild-type hermaphrodite every 24 h during the first 6 days of adulthood (mean  $\pm$  s.e.m., n= 10 worms scored per condition from 3 independent experiments). (B) Total number of eggs laid per wild-type hermaphrodite (mean  $\pm$  s.e.m., n=

---

10 worms scored per condition from 3 independent experiments). (C) Percentage of hatched eggs (mean  $\pm$  s.e.m.,  $n=10$  worms scored per condition from 3 independent experiments). All the statistical comparisons were made by two-tailed Student's *t*-test for unpaired samples, NS= not significant ( $P > 0.05$ ).

Finally, we investigated if either *cey-2* or *cey-3* depletion could affect worm lifespan. Importantly, loss of germline-specific CEYs did not shorten lifespan, suggesting that PGL-1 aggregates do not induce organismal sickness or mortality (**Fig. 12**). Thus, single knockdown of either *cey-2* or *cey-3* did not impair features such as organismal viability, reproduction and GSC self-renewal, providing a mean to examine whether the proteostasis status of GSCs modulates protein aggregation in the soma.

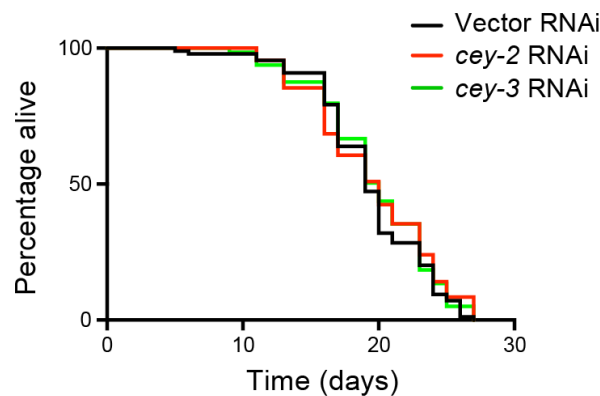


**Fig. 12. Single knockdown of germline-specific CEYs does not shorten lifespan.** Lifespan analysis of wild-type worms on either *cey-2* or *cey-3* RNAi (log-rank test,  $n=96$  worms/condition). See **Supplementary Data 1** for statistical analysis and replicate data.

### 3. Depletion of germline-specific CEYs induces protein aggregation in the nervous system.

In order to determine if single depletion of *cey-2* and *cey-3* could affect somatic proteostasis, we used *C. elegans* that express expanded polyglutamine repeats (polyQ) throughout the nervous system, a bona fide model of neuronal protein aggregation (*100-101*). In these worms, neurotoxicity and protein aggregation correlate with increased length of the polyQ peptide, with a pathogenic threshold of 40 repeats (*100*). Notably, knockdown of germline-specific CEYs triggered a pronounced increase of polyQ67 aggregation in neurons, without affecting the total amounts of polyQ peptides (**Fig. 13A**). We further confirmed neuronal polyQ67 aggregation in single *cey-2* and double *cey-2*, -3 functional null mutant worms (**Fig. 13C**). On the contrary, loss of CEY proteins did not induce aggregation of control polyQ19-peptides (**Fig. 13B**).

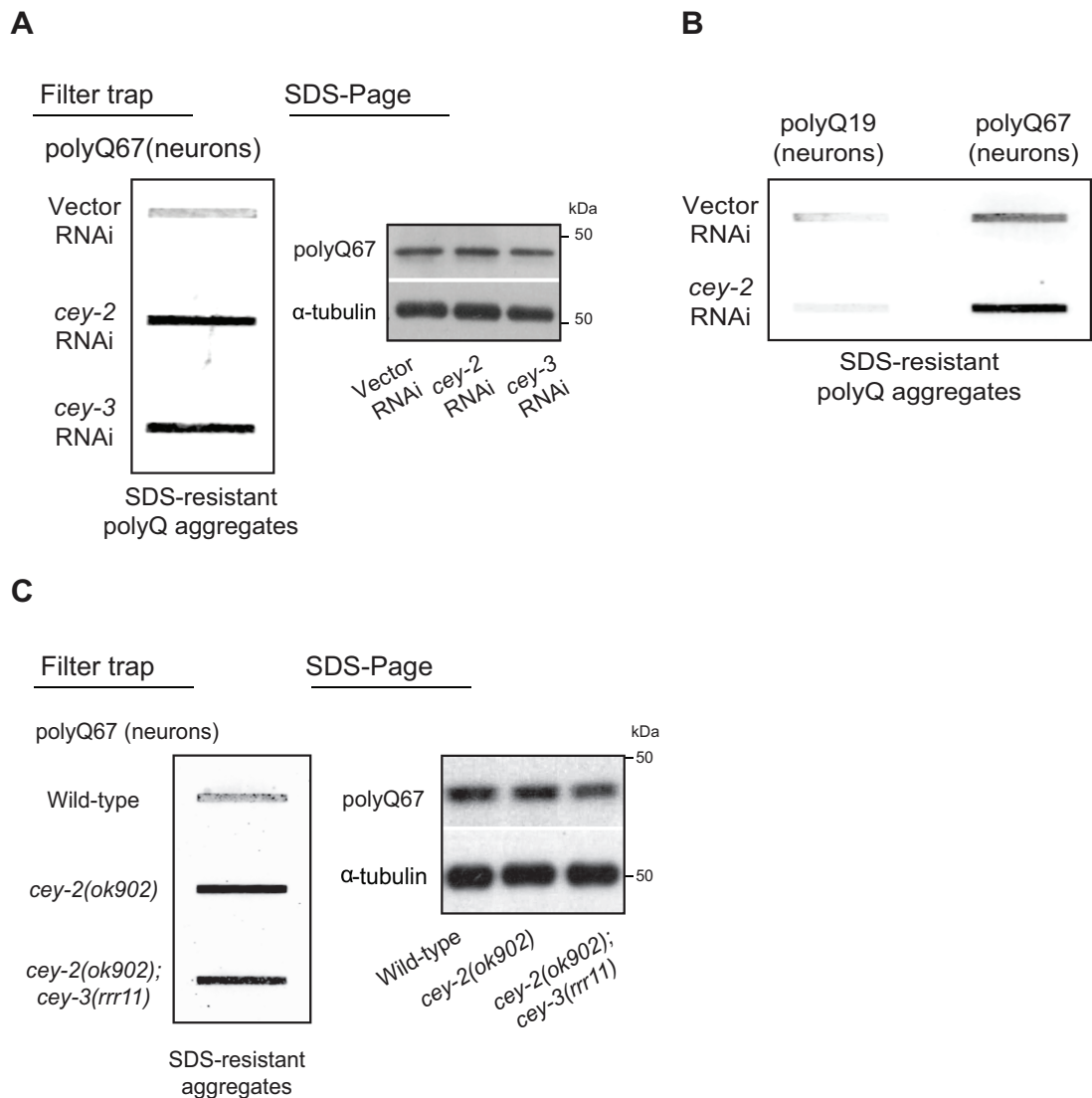


**Fig. 13. Either knockdown or loss-of-function mutation of CEY factors increases protein aggregation in neurons.** (A) Loss of germline-specific CEYs induces aggregation of polyQ67::YFP (detected by anti-GFP antibody) expressed under neuronal-specific F25B3.3 promoter. Worms were analysed at day 3 of adulthood. The images are representative of 4 independent experiments. (B) Filter trap analysis with anti-GFP antibody of neuronal polyQ19 and polyQ67-expressing models. The images are representative of 3 independent experiments. (C) Loss-of-function mutations in germline-specific CEYs induces aggregation of polyQ67 in neurons (detected by anti-GFP antibody). Right panel: SDS-PAGE analysis with antibodies to GFP and  $\alpha$ -tubulin loading control. The images are representative of two independent experiments.

Since the neurotoxic effects of expanded-polyQ aggregation correlate with impairment of coordinated movement (100), we performed motility assays and found that loss of germline-specific CEY proteins hasten the motility defects induced by polyQ67 expression (Fig. 14). However, loss of *cey-2* or *cey-3* did not affect the motility of control polyQ19-expressing worms (Fig. 14).

Therefore, we deduced that single depletion of CEY-2 and CEY-3 is sufficient to affect somatic proteostasis via a cell non-autonomous mechanism.

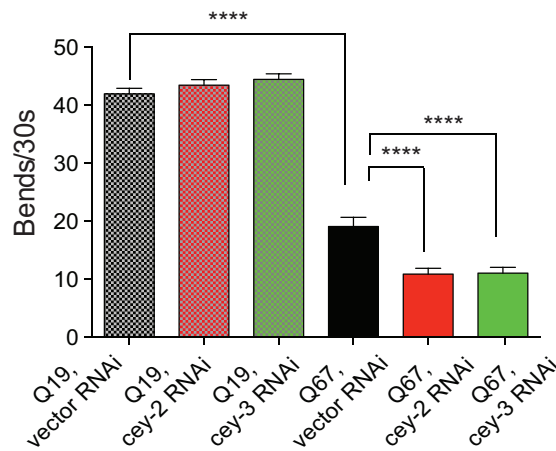


**Fig. 14. Knockdown of *cey-2* and *cey-3* reduces motility of polyQ expressing worms.** Loss of germline-specific CEYs hastens the motility defects of neuronal polyQ67-expressing worms, but does not affect control polyQ19 worms. Bar graphs represent average ( $\pm$  s.e.m.) thrashing movements over a 30 s period on day 3 of adulthood (n=160 worms per condition from three independent experiments). Statistical comparisons were made by two-tailed Student's t-test for unpaired samples, P values: \*\*\*\*(P<0.0001).

#### 4. Depletion of *cey-1* induces protein aggregation in the nervous system via a cell non-autonomous mechanism.

Similarly to the germline-specific CEYs, RNAi against *cey-1* also impaired germline proteostasis (**Fig. 15A**), displaying formation of PGL-1 aggregates. Moreover, CEY-1 deficiency also triggers polyQ67 aggregation in neurons (**Fig. 15B**). However, CEY-1 factor is expressed in both germline cells and nervous system. Therefore, in order to discern if the effect of CEY-1 deficiency on somatic proteostasis was induced cell autonomously or cell non-autonomously, we utilized a neuronal-specific RNAi strain, which permits CEY-1 knockdown exclusively in neurons. Thus, we crossed the polyQ67-expressing strain with the TU340 strain that carries the *sid-1* null mutation, which is rescued only in neurons by SID-1 neuronal-specific overexpression. SID-1 protein is essential for RNA import into the cell (102). Thus, in the TU3401 strain RNAi molecules reach exclusively neuronal cells, rendering this strain sensitive to RNAi specifically in neurons. As further confirmation, neuronal RNAi specificity was corroborated by qPCR analysis. In fact, whereas in control worms (polyQ67) RNAi efficiently depleted *cey-1*, *cey-2* and *cey-3* (**Fig. 16A**), it failed to knockdown *cey-2* and *cey-3* in the neuronal-sensitive strain (Neuronal-specific RNAi; polyQ67), confirming that CEY-2 and CEY-3 are not expressed in neurons (**Fig. 16B**). Contrarily, accordingly with the finding

that CEY-1 is also expressed in the nervous system, *cey-1* resulted partially depleted in the neuronal-sensitive strain (**Fig. 16B**), similar to the TRiC/CCT chaperonin complex (**Fig. 16C**), a direct regulator of expanded-polyQ proteostasis (*101*).

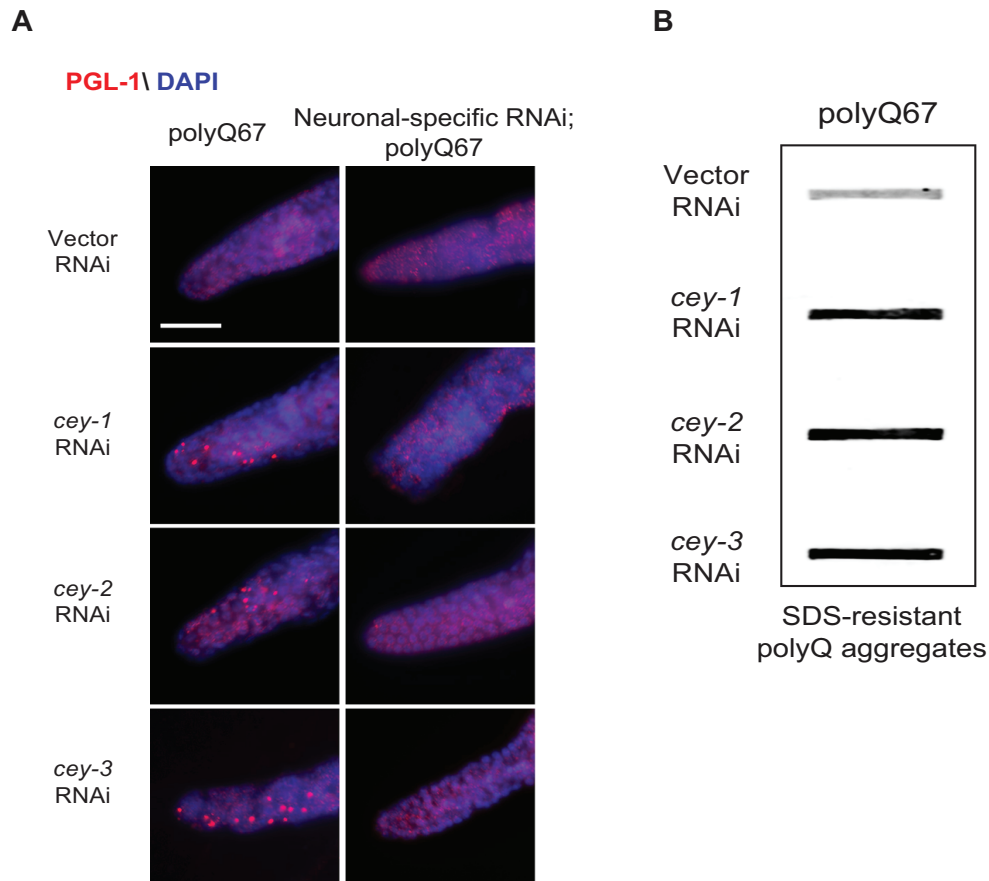


**Fig. 15. Knockdown of *cey-1* induces PGL-1 aggregation in germline and enhances protein aggregation in the soma.** (A) Immunostaining of germlines in polyQ67-expressing worms with antibody to PGL-1 and DAPI (nuclei). On the left, knockdown of *cey-1* induces aggregation of PGL-1 in the germline. On the right, neuronal-specific RNAi against CEY factors does not impair proteostasis of PGL-1 in the germline. Scale bar, 20  $\mu$ m. Images are representative of three independent experiments. (B) Knockdown of *cey-1* increases polyQ67 aggregation in neurons (detected by anti-GFP antibody). The images are representative of four independent experiments.



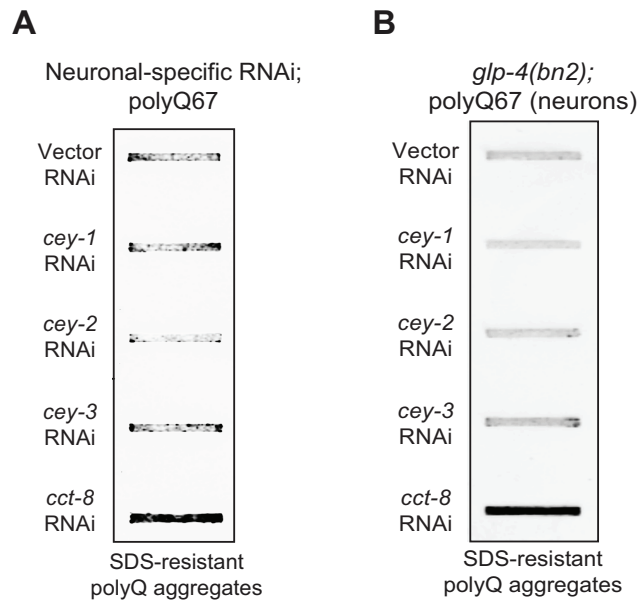


**Fig. 17. Knockdown of *cey-1* in neurons does not increase protein aggregation.** (A) Neuronal-specific knockdown of *cey-1* does not induce polyQ67 aggregation in neurons. In contrast, neuronal-specific knockdown of *cct-8*, a subunit of the TRiC/CCT chaperonin complex, promotes polyQ67 aggregation in neurons. The images are representative of four independent experiments. (B) RNAi against CEY factors does not induce polyQ67 aggregation in neurons of germline-lacking worms (*glp-4(bn2)*). In contrast, knockdown of *cct-8* promotes neuronal polyQ67 aggregation. The images are representative of three independent experiments.

## 5. PGL-1 aggregation in germline causes disruption of somatic proteostasis.

To assess if PGL-1 aggregation in germline is responsible for somatic proteostasis disruption, we performed rescue experiments using *pgl-1* RNAi. Given that germline-specific PGL proteins have redundant roles, loss of PGL-1 alone does not impair the formation of germ granules or germline function (75). Notably, knockdown of aggregation-prone PGL-1 was sufficient to ameliorate neuronal polyQ67 dysregulation in *cey-2* mutants. In fact, filter trap assays showed a significant reduction of CEY-2-dependent protein aggregation, upon *pgl-1* depletion (Fig. 18). This result further supports a role of cell non-autonomous signals triggered by defects in germline proteostasis.

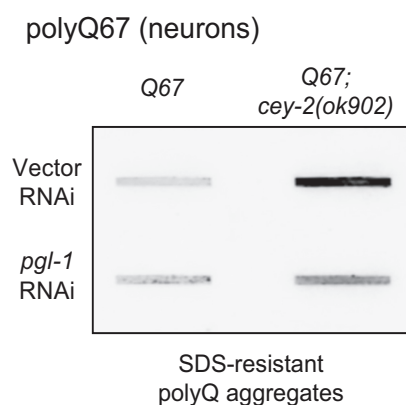


**Fig. 18. PGL-1 knockdown rescues CEY-2-dependent protein aggregation.** Knockdown of germline-specific *pgl-1* rescues the increased polyQ67 aggregation phenotype in neurons of *cey-2* mutants. The images are representative of three independent experiments.

## 6. Depletion of either *cey-2* or *cey-3* induces an overall somatic proteostasis disruption.

In order to determine if somatic proteostasis imbalance, induced by germline-specific CEY factors deficiency, was restricted to the nervous system or it was extended to other somatic tissues, we utilize *C. elegans* strains expressing expanded-polyQ peptides in other somatic tissues, such as muscle and intestine. Importantly, filter trap assays revealed that loss of either *cey-2* or *cey-3* also triggered increased aggregation in both intestine and muscle strains (**Fig. 19A, B**). Therefore, we concluded that the effect of PGL-1 aggregation on somatic proteostasis is not limited to the nervous system, but it also affects proteostasis of other somatic tissues.

Moreover, we asked if somatic proteostasis imbalance, occurring upon germline-specific CEYs knockdown, was specific for expanded-polyQ peptides or it was the result of an overall proteostasis disruption. To answer this question, we studied the effect of CEYs knockdown on proteostasis in other neurodegenerative diseases, such as ALS. Therefore, we utilized ALS model strains expressing human mutant FUS (P525L, R522G) and TDP43 proteins (M331V), in the nervous system. Importantly, besides expanded-polyQ peptides, knockdown of germline-specific CEYs induced aggregation of ALS-related mutant variants of FUS and TDP-43 in neurons (**Fig. 20A, B, C**). Thus, we concluded that knockdown of either *cey-2* or *cey-3* induces an overall proteostasis collapse in the soma of *C. elegans*. Altogether, our results indicate that the proteostasis status of the germline determines aggregation of disease-related proteins in the soma, a process impaired by the accumulation of PGL-1 aggregates in germline cells upon loss of CEY proteins.

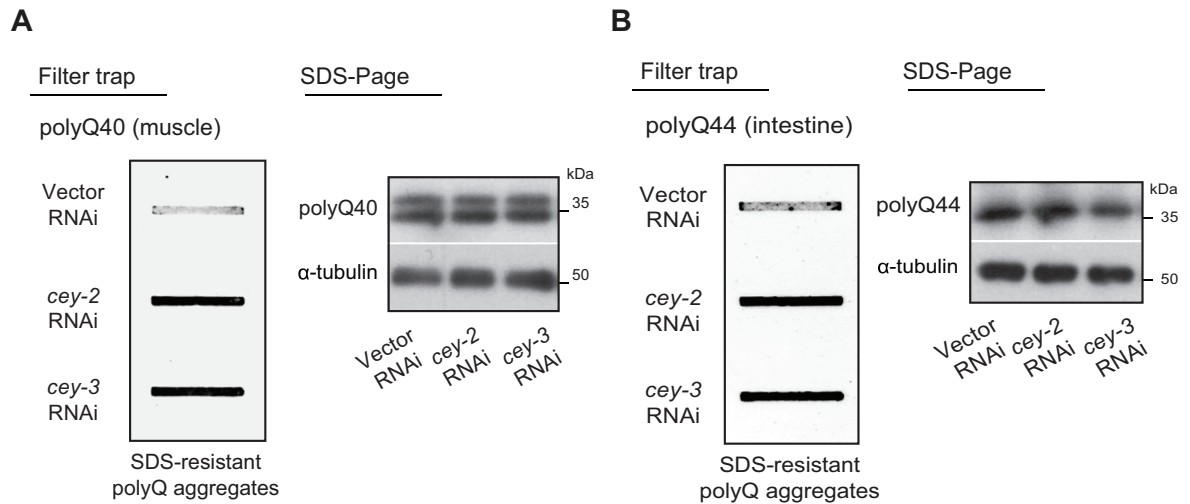
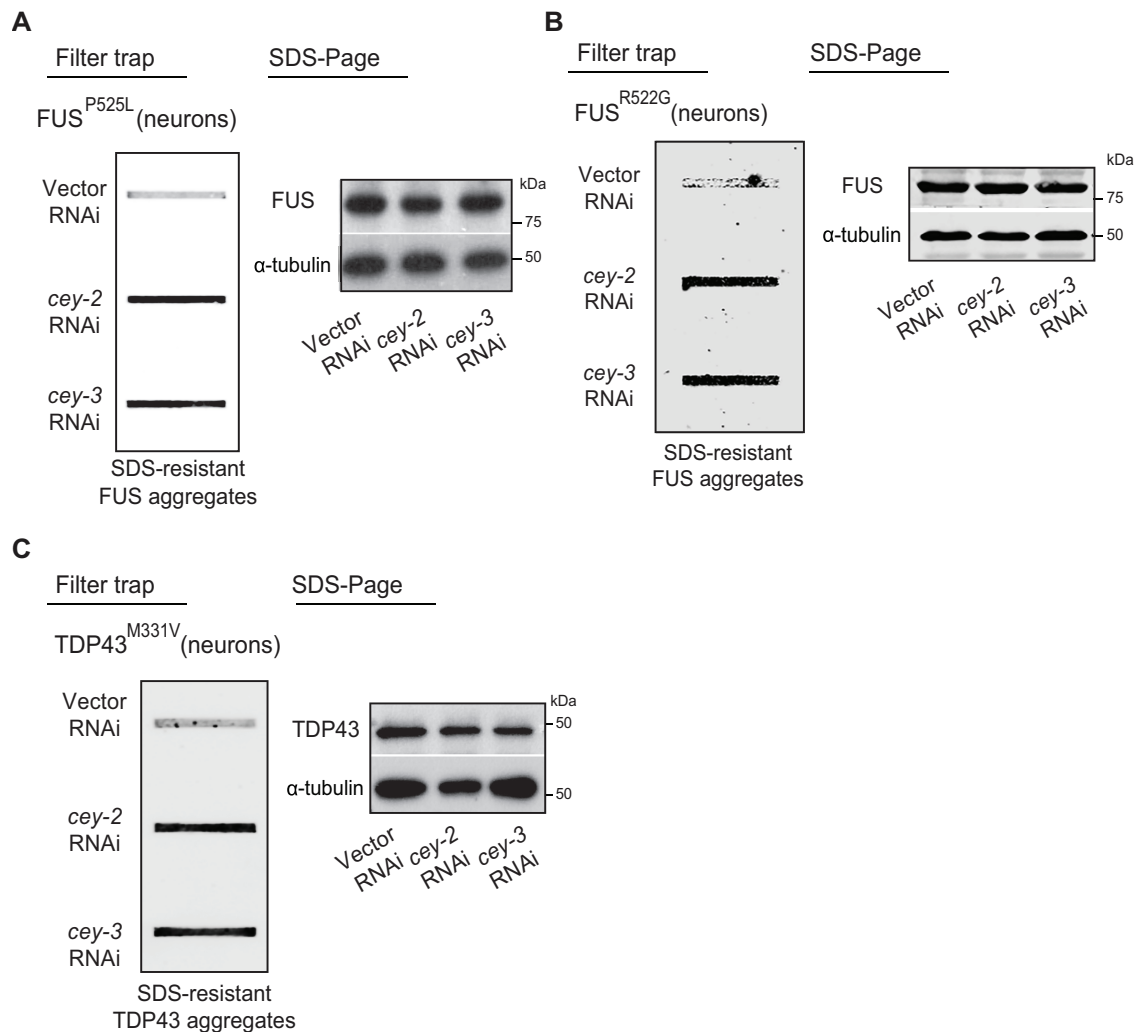


**Fig. 19. Knockdown of *cey-2* and *cey-3* enhances protein aggregation in muscle and intestine.**

(A) Knockdown of germline-specific CEYs increases polyQ aggregation in *C. elegans* that express polyQ40::YFP in the muscle (detected by anti-GFP antibody). Right panel: SDS-PAGE analysis with antibodies to GFP and  $\alpha$ -tubulin loading control. The images are representative of three independent experiments. (B) Knockdown of germline-specific CEYs increases polyQ aggregation in *C. elegans* that express polyQ44::YFP in the intestine (detected by anti-GFP antibody). Right panel: SDS-PAGE analysis with antibodies to GFP and  $\alpha$ -tubulin loading control. The images are representative of three independent experiments.



---

**Fig. 20 Knockdown of *cey-2* and *cey-3* enhances protein aggregation in ALS models.** (A) Knockdown of germline-specific CEYs increases aggregation of ALS-related mutant FUSP525L variant in *C. elegans* neurons (detected by anti-FUS antibody). Right panel: SDS–PAGE analysis with antibodies to FUS and  $\alpha$ -tubulin loading control. The images are representative of two independent experiments. (B) Loss of germline-specific CEYs triggers aggregation of ALS-related mutant FUSR522G variant in neurons. Knockdown of either *cey-2* or *cey-3* promotes aggregation of mutant FUSR522G variant in *C. elegans* neurons (detected by anti-FUS antibody). Right panel: SDS–PAGE analysis with antibodies to FUS and  $\alpha$ -tubulin loading control. The images are representative of two independent experiments. (C) Knockdown of germline-specific CEYs increases aggregation of ALS-related mutant TDP43M331V variant in *C. elegans* neurons (detected by anti-TDP43 antibody). Right panel: SDS–PAGE analysis with antibodies to TDP43 and  $\alpha$ -tubulin loading control. The images are representative of two independent experiments.

## 7. Depletion of either *cey-2* or *cey-3* causes mitochondria perturbation in germline.

To determine how proteostasis defects in the germline influence somatic tissues, we first assessed the intracellular changes induced by PGL-1 aggregation in germline cells. For this purpose, we examined the proteome of isolated germlines from *C. elegans* following *cey-3* knockdown. Besides CEY-3 levels, quantitative proteomics analysis revealed that another 73 proteins were significantly downregulated on *cey-3* knockdown. Remarkably, Gene Ontology Cellular Component (GOCC) analysis of downregulated proteins indicated strong enrichment for numerous mitochondrial components required for mitochondrion organization and function (**Fig. 21**). Among them, we found factors involved in the mitochondrial electron transport chain (ETC) such as components of complex I/NADH-ubiquinone oxidoreductase (NUO-5, NDUF-9, NDUF-2.2, C33A12.1, Y63D3A.7, Y94H6A.8, Y54F10AM.5), complex III/ubiquinol-cytochrome c reductase (ISP-1, UCR-1), complex IV/cytochrome c oxidase (COX-6A, COX-7C) and complex V/proton-transporting ATP synthase complex (ATP-4, ASB-1, HPO-18, ASG-1, Y69A2AR.18) (**Fig. 21**). In addition, we observed a decrease in components of complexes that regulate mitochondrial biogenesis and morphology, such as prohibitin (PHB-1), mitochondrial ribosomes (MRPL-44) or translocases of the outer (TOMM-20) and inner mitochondrial membrane (TIM-16) (**Fig. 21**).

To confirm that *cey-3* deficiency induces downregulation of mitochondria components, we performed qPCR experiments. Notably, we observed that the reduction in protein level of several mitochondria components, detected by proteomics analysis, correlated with a decrease of the mRNA levels in the *cey-3* depleted germline (**Fig. 22**).

## GOCC of downregulated proteins in the germline upon *cey-3* RNAi

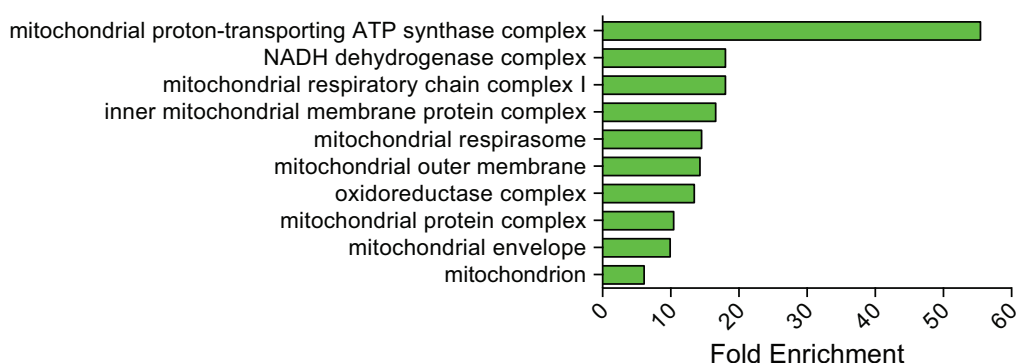


**Fig. 21. Proteomics analysis of *cey-3* knockdown worms show downregulation of several mitochondria proteins.** Gene Ontology Cellular Component (GOCC) analysis of downregulated proteins in extruded germlines from *C. elegans* following *cey-3* knockdown (false discovery rate (FDR) < 0.05). 10 of the most enriched GOCC terms are shown. Please see Supplementary Data 3 for the complete list of enriched GOCC terms.

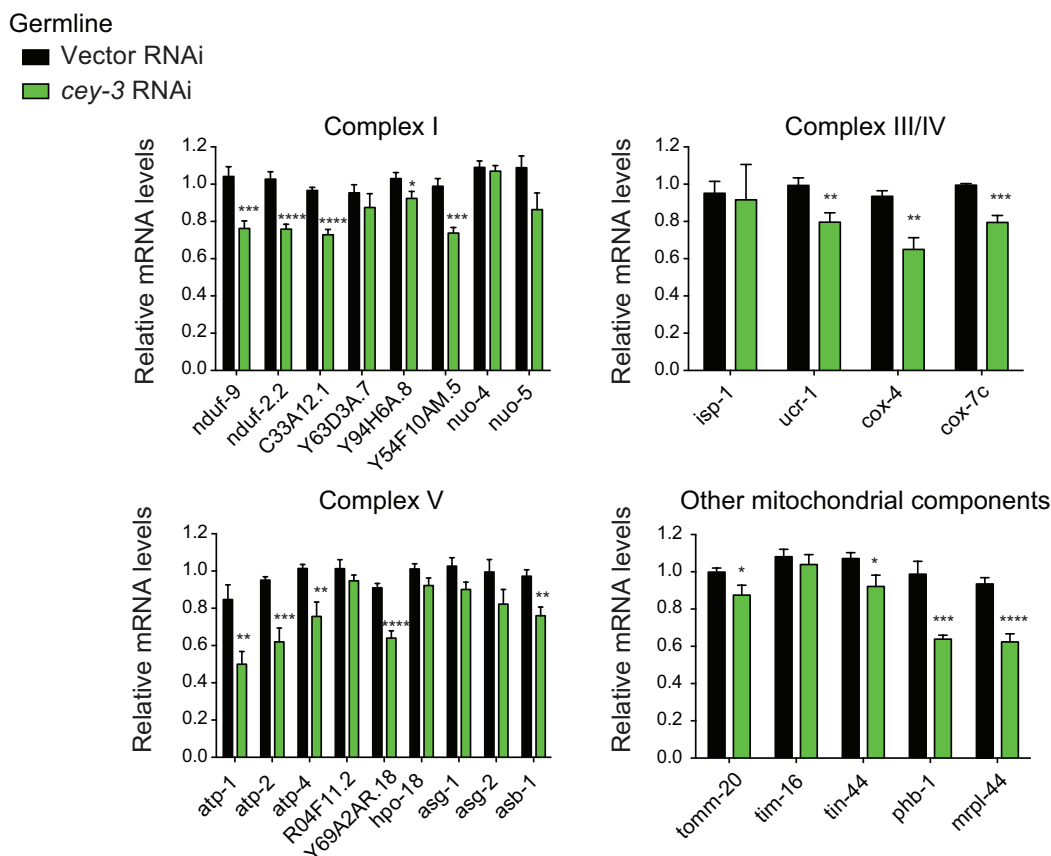


**Fig. 22. qPCR analysis confirms downregulation of mitochondria proteins in *cey-3* depleted germline.** qPCR analysis of mitochondrial components in isolated germlines. Graphs represent the relative expression to Vector RNAi control (mean  $\pm$  s.e.m. of 8 independent experiments). statistical comparisons were made by two-tailed Student's t test for unpaired samples. P values: \*P < 0.05, \*\*P < 0.01, \*\*\*P < 0.001, \*\*\*\*P < 0.0001, NS= not significant (P > 0.05).

To further study the effect of single CEY-2 and CEY-3 deficiency on mitochondria, we performed germline immunostaining of the mitochondria ATP-1 protein. Of note, in line with proteomics results, we also found changes in the morphology of mitochondrial networks that became more diffused through the cytoplasm of germline cells upon either knockdown (**Fig. 23A, B**) or loss-of-function mutation (**Fig. 24A, B**) of CEY factors.

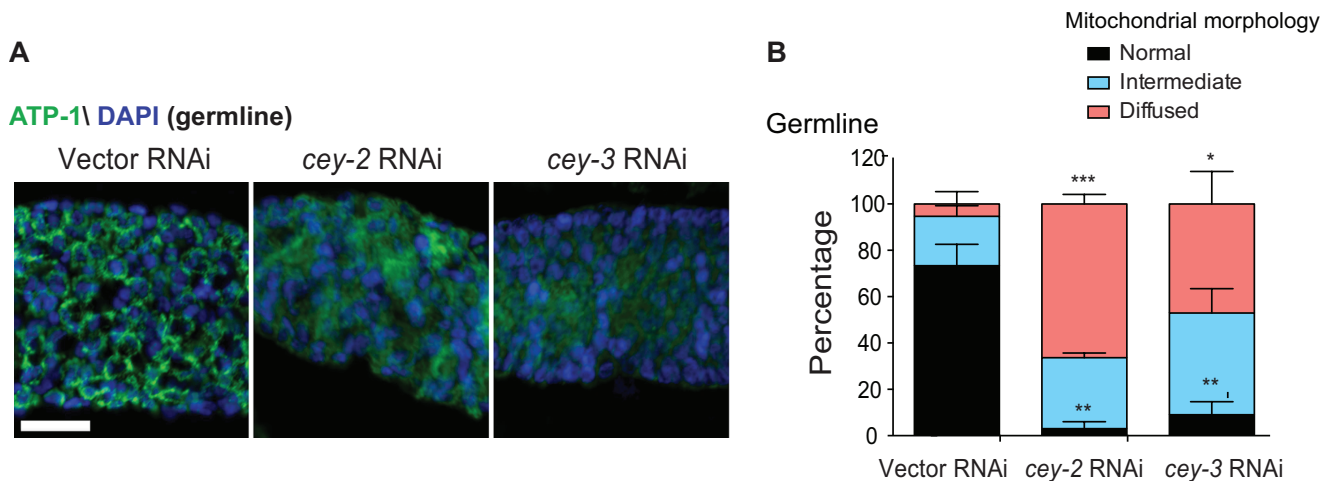


**Fig. 23. Single *cey-2* and *cey-3* knockdown induces mitochondria morphological defects in germline.** (A) Immunostaining of germline cells with antibody to mitochondrial marker ATP-1. Cell nuclei were stained with DAPI. Scale bar, 20  $\mu$ m. Images are representative of 3 independent experiments. (B) Percentage of germlines with normal, intermediate or diffused mitochondrial network morphology (mean  $\pm$  s.e.m. of 3 independent experiments, Vector RNAi= 50 germlines, *cey-2* RNAi= 43 germlines, *cey-3* RNAi= 52 germlines). statistical comparisons were made by two-tailed Student's t test for unpaired samples. P values: \*P < 0.05, \*\*P < 0.01, \*\*\*P < 0.001, \*\*\*\*P < 0.0001, NS= not significant (P > 0.05).

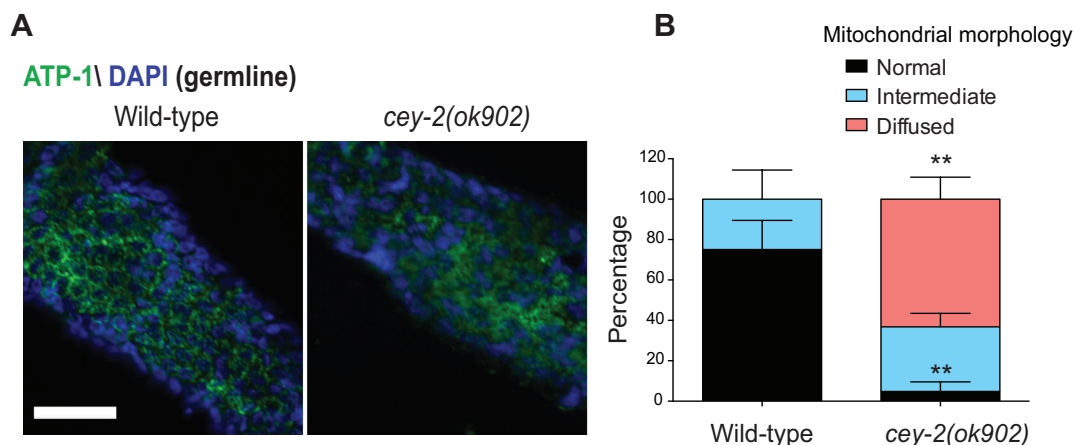


**Fig. 24. The germline cells of *cey-2* functional null mutant animals exhibit changes in the morphology of mitochondrial networks.** (A) Immunostaining of germline cells with antibody to mitochondrial marker ATP-1. Cell nuclei were stained with DAPI. Scale bar, 20  $\mu$ m. (B) percentage of germlines with normal, intermediate or diffused mitochondrial network morphology (mean  $\pm$  s.e.m. of 3 independent experiments, wild-type= 14 germlines, *cey-2(ok902)*= 18 germlines). Statistical comparisons were made by two-tailed Student's t test for unpaired samples. P-values: \*\*P < 0.01.

Importantly, loss of *pgl-1* rescued the low levels of mtDNA content in *cey-2* mutants (**Fig. 25**), supporting that aggregation of PGL-1 impinges on the mitochondrial network of germline cells.

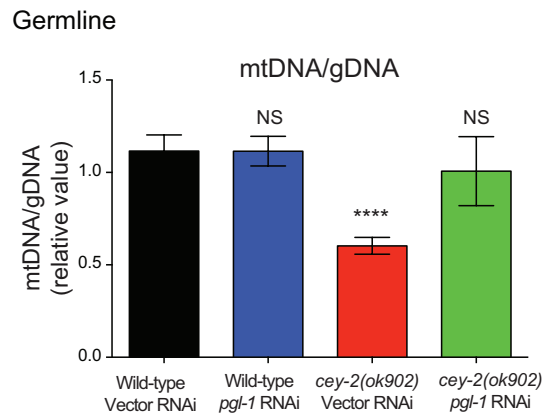


**Fig. 25. PGL-1 knockdown rescues the low mtDNA content in the germline of *cey-2* null mutant.** Relative DNA (mtDNA)/genomic DNA (gDNA) ratio in isolated germlines to wild-type + Vector RNAi (mean  $\pm$  s.e.m., wild-type + Vector RNAi (n= 15 biological replicates from three independent experiments), wild-type + *pgl-1* RNAi (n= 13), *cey-2(ok902)* + Vector RNAi (n= 14), *cey-2(ok902)* + *pgl-1* RNAi (n= 19)). Statistical comparisons were made by two-tailed Student's t test for unpaired samples. P values: \*P < 0.05, \*\*P < 0.01, \*\*\*P < 0.001, \*\*\*\*P < 0.0001, NS= not significant (P > 0.05).

## 8. Depletion of either *cey-2* or *cey-3* induces a cell non-autonomous disruption of mitochondria in the soma.

Remarkably, single CEY-2 and CEY-3 depletion not only cause mitochondria perturbation in germline but also in the soma. In fact, worms with PGL-1 aggregates in the germline also exhibited changes in the mitochondrial network of distal somatic tissues, suggesting a cell non-autonomous process mediated by the germline. Accordingly, ATP-1 immunostaining experiments showed increased mitochondria fragmentation in the intestine of germline-specific CEYs depleted worms (**Fig. 26A, B**).

Moreover, imaging analysis of the transgenic *myo-3p::GFP(mit)* reporter strain, which expresses, GFP fused to a mitochondria targeting sequence (MTS) in muscle, confirmed increased fragmentation of somatic mitochondria, upon either *cey-2* or *cey-3* knockdown (**Fig. 27A, B**). Thus, mitochondria formed more fragmented structures in muscle and intestinal cells upon knockdown of germline-specific CEY proteins, through a cell non-autonomous mechanism.

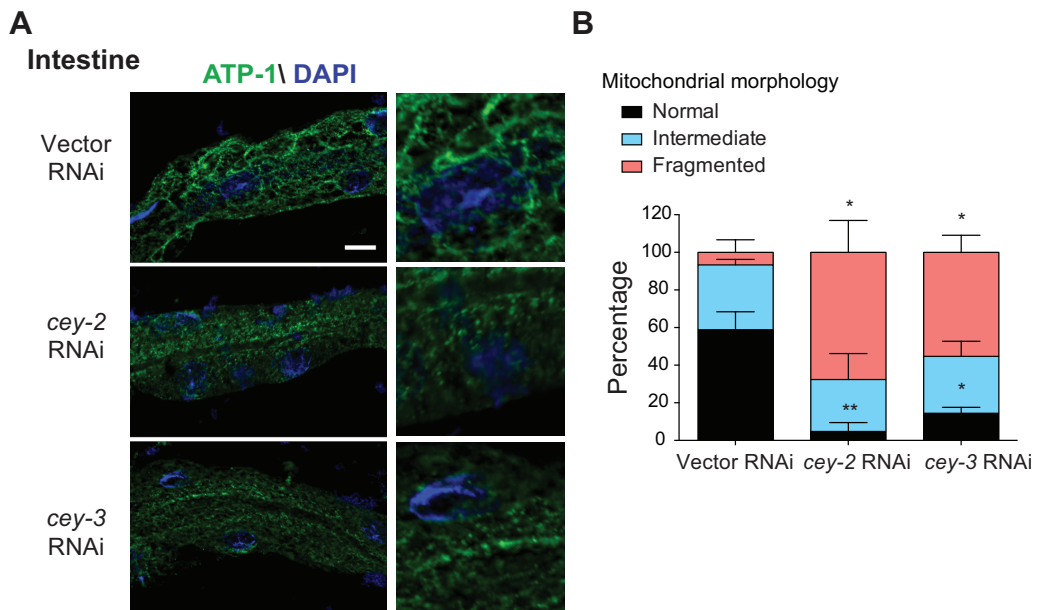


**Fig. 26. Single knockdown of *cey-2* and *cey-3* induces mitochondria fragmentation in intestine.** (A) Immunostaining of the intestine with antibody to mitochondrial marker ATP-1. Cell nuclei were stained with DAPI. Scale bar, 20  $\mu$ m. On the right, higher magnification of intestinal cells. Images are representative of three independent experiments. (B) Percentage of animals with normal, intermediate or fragmented mitochondrial network morphology in the intestine (mean  $\pm$  s.e.m. of 3 independent experiments, Vector RNAi= 34 animals, *cey-2* RNAi= 20 animals, *cey-3* RNAi= 32 animals).

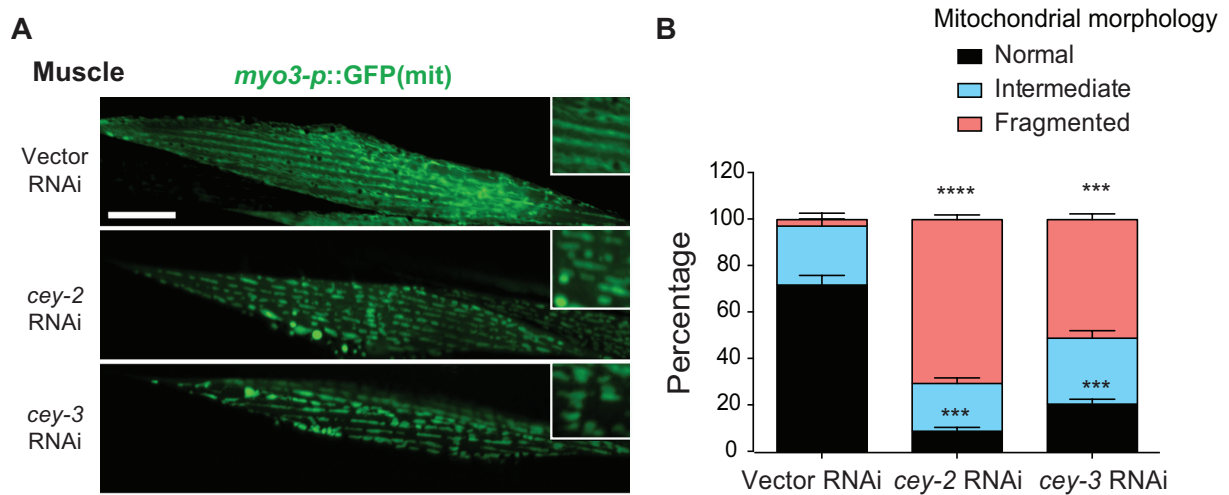


**Fig. 27. Single knockdown of *cey-2* and *cey-3* induces mitochondria fragmentation in muscles.** (A) Representative images of mitochondrial morphology in muscle cells marked by *myo-3p::GFP(mit)* upon knockdown of germline-specific CEYs. Scale bar, 20  $\mu$ m. Images are representative of 3 independent experiments. (B) Percentage of animals with normal, intermediate or fragmented mitochondrial network morphology in the muscle (mean  $\pm$  s.e.m. of 3 independent experiments, Vector RNAi= 30 animals, *cey-2* RNAi= 45 animals, *cey-3* RNAi= 41 animals).

Similar to the intracellular effects caused by PGL-1 aggregation in the germline, we also observed reduced expression of mitochondrial components (Fig. 28, Fig. 29) and lower mtDNA content in somatic tissues (Fig. 30).

Importantly, knockdown of PGL-1 in the germline was sufficient to rescue low mtDNA levels (Fig. 30) and mitochondrial morphology (Fig. 31) alterations in the soma of *cey-2* mutant worms.

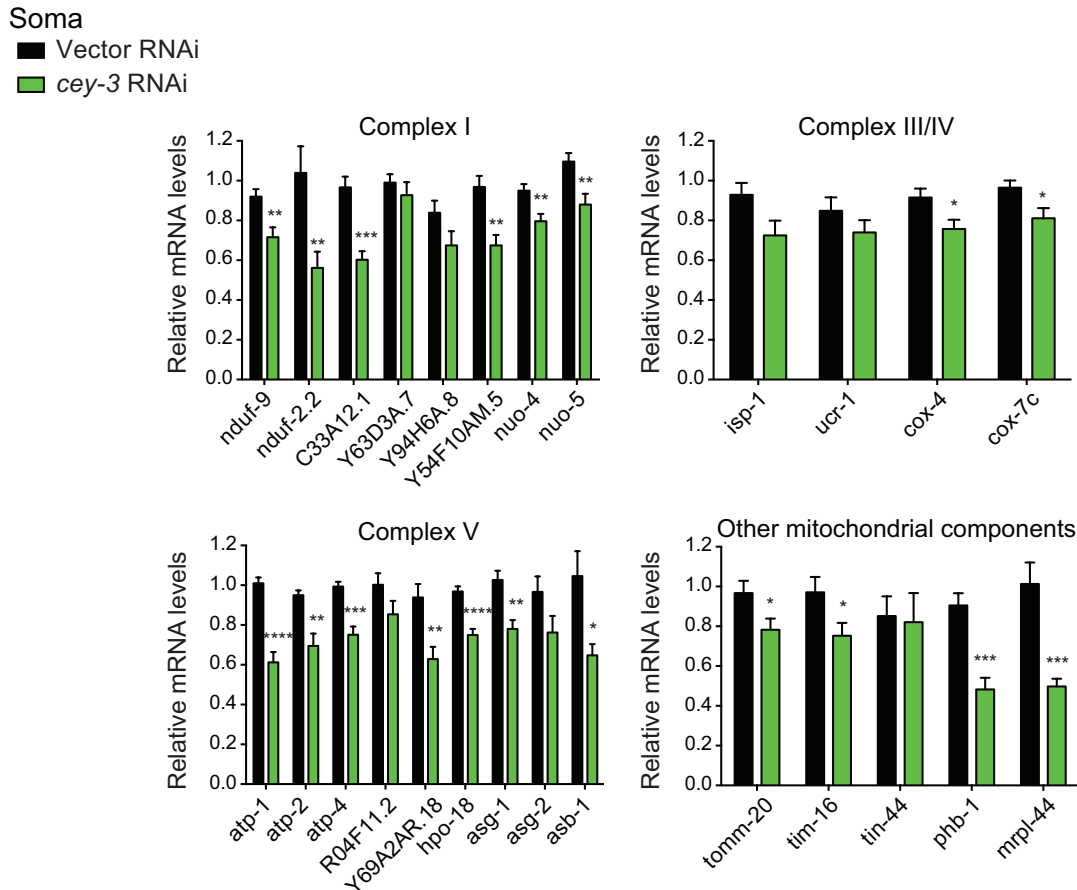


**Fig. 28. Knockdown of germline-specific *cey-3* results in decreased expression of mitochondrial components in the soma.** qPCR analysis of mitochondrial components in somatic tissues (isolated intestines + heads). Graphs represent the relative expression to Vector RNAi control (mean  $\pm$  s.e.m. of 8 independent experiments).

Vector RNAi  
 *cey-2* RNAi

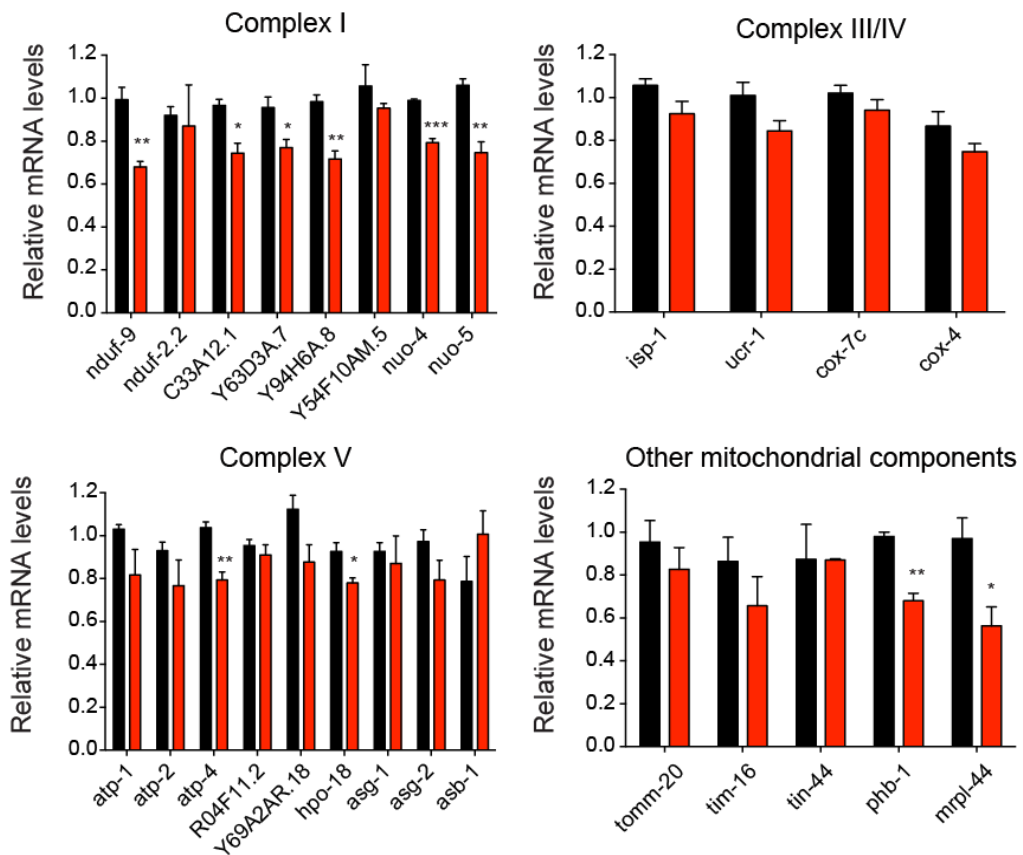


**Fig. 29. Knockdown of germline-specific *cey-2* results in decreased expression of mitochondrial components in the soma.** qPCR analysis of mitochondrial components in somatic tissues (isolated intestines + heads). Graphs represent the relative expression to Vector RNAi (mean  $\pm$  s.e.m. of 3 independent experiments). Statistical comparisons were made by two-tailed Student's t test for unpaired samples. P values: \*P < 0.05, \*\*P < 0.01, \*\*\*P < 0.001.

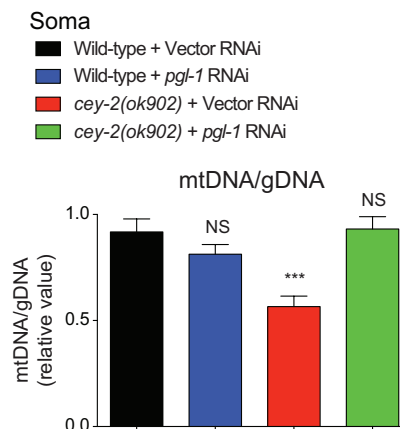


**Fig. 30. PGL-1 knockdown rescues the low mtDNA content in the soma of *cey-2* null mutant.** Relative DNA (mtDNA)/genomic DNA (gDNA) ratio in somatic tissues to wild-type + Vector RNAi (mean  $\pm$  s.e.m., wild-type + Vector RNAi (n= 13 biological replicates from three independent experiments), wild-type + *pgl-1* RNAi (n= 11), *cey-2(ok902)* + Vector RNAi (n= 14), *cey-2(ok902)* + *pgl-1* RNAi (n= 19)).

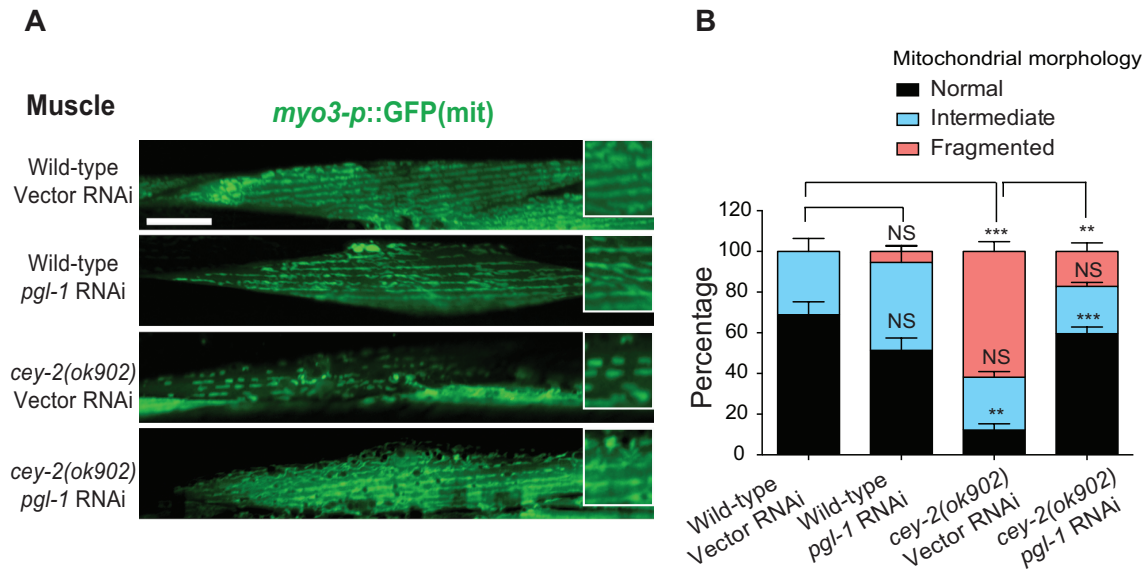


**Fig. 31. PGL-1 knockdown rescues the mitochondria fragmentation in muscles of *cey-2* null functional mutant.** (A) Knockdown of *pgl-1* partially rescues changes in muscle mitochondrial morphology induced by loss of *cey-2* function. Scale bar, 20  $\mu$ m. Images are representative of 3 independent experiments. (B) Percentage of animals with normal, intermediate or fragmented mitochondrial network morphology in the muscle (mean  $\pm$  s.e.m. of 3 independent experiments, wild-type + Vector RNAi= 44 worms, wild-type + *pgl-1* RNAi= 38 worms, *cey-2(ok902)* + Vector RNAi= 62 worms, *cey-2(ok902)* + *pgl-1* RNAi= 78 worms).

Despite the systemic mitochondrial changes induced by loss of germline-specific CEY factors, the animals maintained similar basal mitochondrial oxygen consumption rates when compared with control worms (Fig. 32A, B).

Likewise, *cey-2* mutant worms did not exhibit decreased levels of nicotinamide adenine dinucleotide (NAD<sup>+</sup>) and ATP compared with wild-type worms (Fig. 33A, B). Thus, these results suggest an upregulation of the basal activity of mitochondria to compensate for the lower mitochondrial content, a process that could challenge the integrity of the mitochondrial proteome and activate proteostasis responses in the organelle.

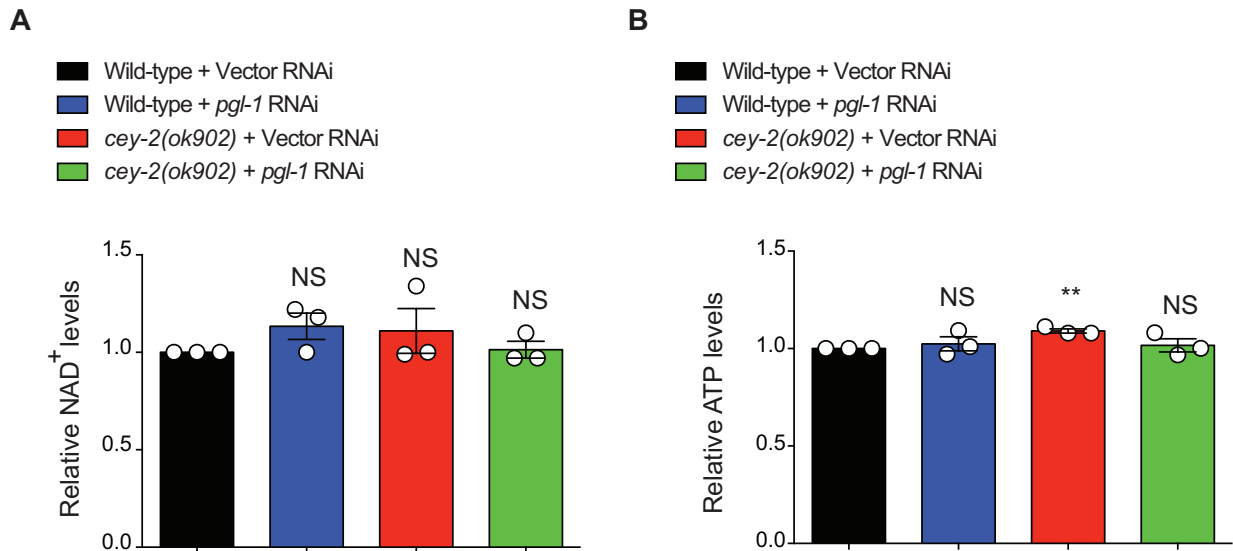


**Fig. 31. Loss of germline-specific CEY factors does not impair basal mitochondrial oxygen consumption rates, NAD<sup>+</sup> levels and ATP levels.** (A) Relative NAD<sup>+</sup> levels to wild-type + Vector RNAi (mean ± s.e.m., n= 3 independent experiments). (B) Relative ATP levels to wild-type + Vector RNAi (mean ± s.e.m., n= 3 independent experiments). In all the experiments, we assessed day 3-adult worms. Statistical comparisons were made by two-tailed Student's t-test for unpaired samples. P values: \*\*P < 0.01, NS= not significant (P > 0.05).

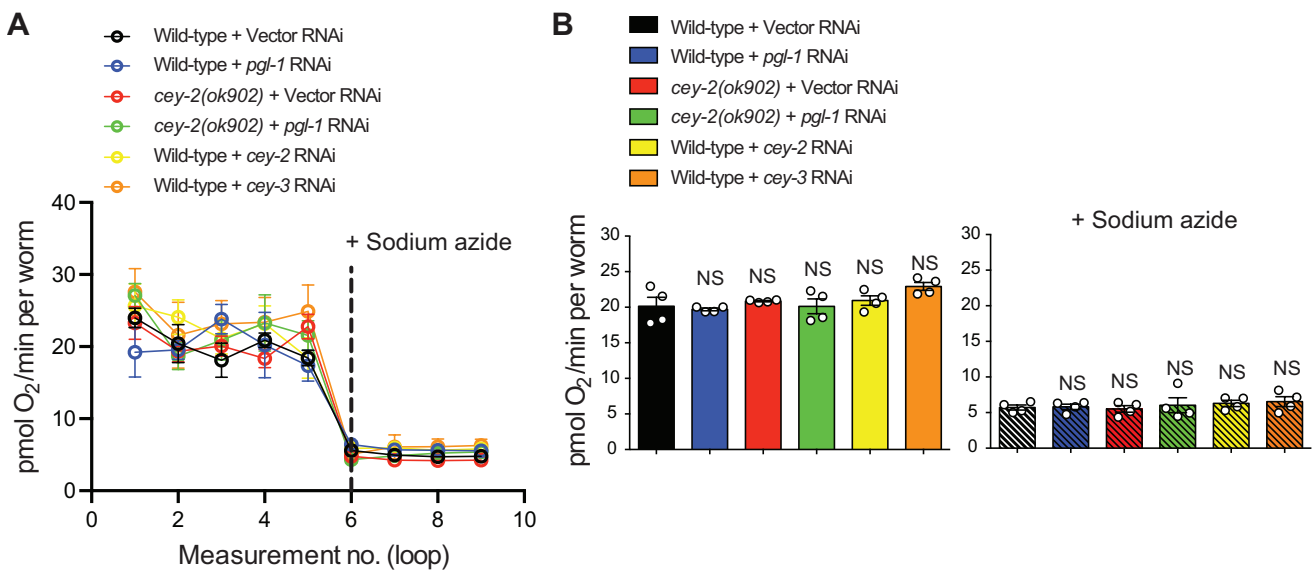


**Fig. 33. Loss of germline-specific CEY factors does not impair basal mitochondrial oxygen consumption rates, NAD<sup>+</sup> levels and ATP levels.** (A) Graph shows a representative experiment of basal oxygen consumption rates from day 3 adult worms treated with the indicated RNAis (mean ± s.e.m., n= 5-6 technical replicates). We added sodium azide, an inhibitor of complex IV, to fully block mitochondrial respiration and measure non-mitochondrial oxygen consumption. Each measurement loop represents 4.5 min (mix for 2 min, wait for 0.5 min, measure for 2 min). The graph is representative of four independent experiments. (B) Bar graphs represent the average (± s.e.m.) oxygen consumption rates from four independent experiments.

## 9. Depletion of either *cey-2* or *cey-3* induces $UPR^{mt}$ in the soma via a cell non-autonomous mechanism.

To assess this hypothesis, we used transgenic worms that express in somatic tissues *hsp-6p::GFP*, a specific reporter of the activation of the mitochondrial unfolded protein response ( $UPR^{mt}$ ) (103, 104). Notably, knockdown of germline-specific *cey-2* or *cey-3* induced the expression *hsp-6p::GFP* in the soma (Fig. 34).

Besides induction of *hsp-6p::GFP*, knockdown of either *cey-2* or *cey-3* also increased the somatic expression of *hsp-60p::GFP* (Fig. 35), a distinct specific reporter of  $UPR^{mt}$  (103, 104).

On the contrary, knockdown of germline-specific CEY factors did not induce the UPR of the endoplasmic reticulum (105) or the cytosolic heat shock response (106) (Fig. 36), indicating specific activation of the  $UPR^{mt}$ .

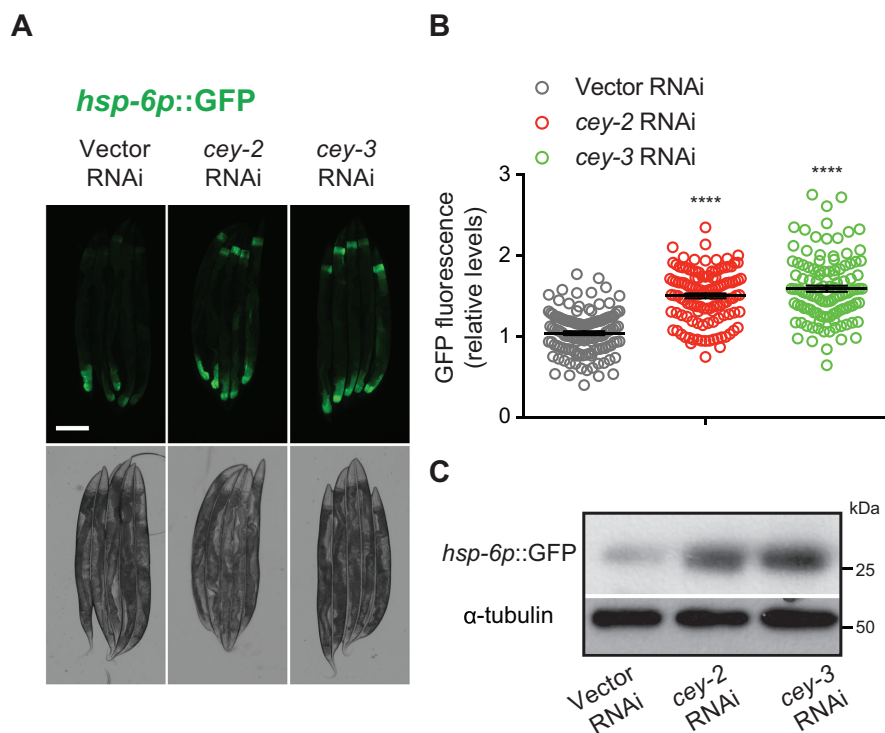


**Fig. 34. Loss of germline-specific CEY factors induces *hsp-6* expression in the soma.** (A) Knockdown of germline-specific CEY factors induces somatic *hsp-6p::GFP* expression. Scale bar, 200  $\mu$ m. (B) Quantification of *hsp-6p::GFP* fluorescence relative to vector RNAi (mean  $\pm$  s.e.m., vector RNAi (n= 128 worms), *cey-2* RNAi (n= 122 worms), *cey-3* RNAi (n= 114 worms) from four independent experiments). (C) Western blot analysis of *hsp-6p::GFP* worms with antibodies to GFP and  $\alpha$ -tubulin loading control. The images are representative of three independent experiments.

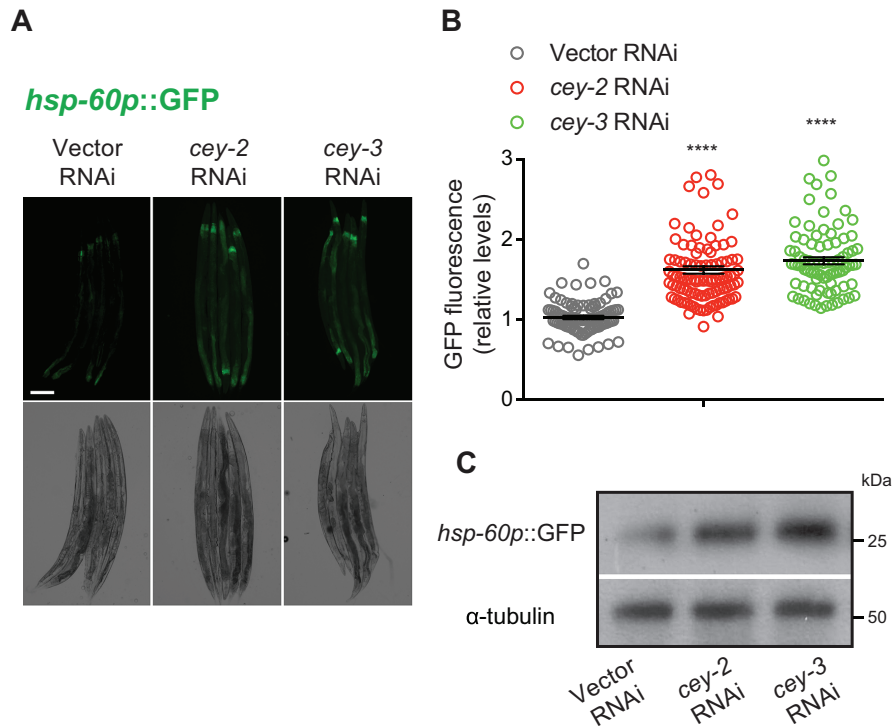


**Fig. 35. Loss of germline-specific CEY factors induces *hsp-6* expression in the soma.** (A) Knockdown of germline-specific CEY factors induces somatic *hsp-60p::GFP* expression. Scale bar, 200  $\mu$ m. (B) Quantification of *hsp-60p::GFP* fluorescence relative to vector RNAi (mean  $\pm$  s.e.m., vector RNAi (n= 93 worms), *cey-2* RNAi (n= 103 worms), *cey-3* RNAi (n= 83 worms) from four independent experiments). (C) Western blot analysis of *hsp-60p::GFP* worms with antibodies to GFP and  $\alpha$ -tubulin loading control. The images are representative of three independent experiments. Statistical comparisons were made by two-tailed Student's t test for unpaired samples. P-values: \*P < 0.05, \*\*P < 0.01, \*\*\*P < 0.001, \*\*\*\*P < 0.0001, NS= not significant (P > 0.05).

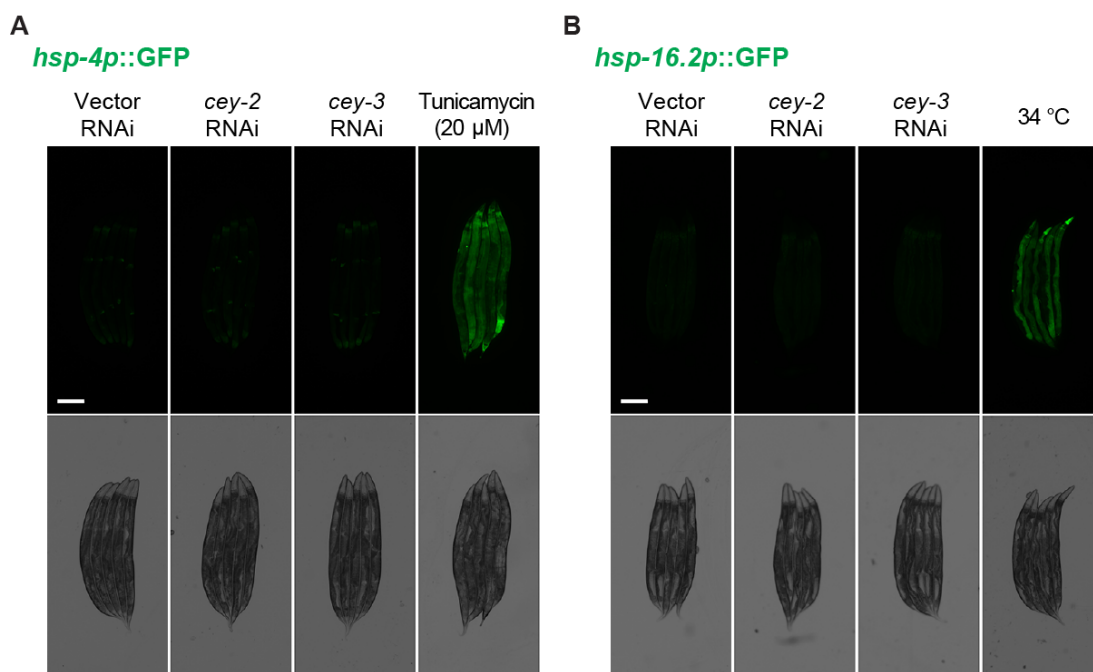


**Fig. 36. Knockdown of germline-specific CEY factors does not induce either the UPR<sup>ER</sup> or the cytosolic heat shock response in somatic tissues.** (A) Representative images of *hsp-4p::GFP* worms at day 3 of adulthood. Knockdown of *cey-2* or *cey-3* does not trigger the UPR of the endoplasmic reticulum. As a positive control, worms were treated with 20  $\mu$ M tunicamycin for 24 h to induce the UPR<sup>ER</sup>. Scale bar, 200  $\mu$ m. The images are representative of six independent experiments. (B) Representative images of *hsp-16.2p::GFP* worms at day 3 of adulthood. Knockdown of *cey-2* or *cey-3* does not induce the cytosolic heat shock response reporter *hsp-16.2p::GFP*. As a positive control, worms were placed at 34 °C for 3 h to induce the cytosolic heat shock response. Scale bar, 200  $\mu$ m. The images are representative of five independent experiments.

## 10. The Wnt/ELG-20 signaling is responsible for the cell non-autonomous communication induced by CEYs depletion.

The Wnt signaling pathway acts as a mitokine signal to communicate information about mitochondrial changes between tissues (107). In *C. elegans*, EGL-20 is the only Wnt ligand that can induce long-range, cell non-autonomous events (107, 108). While knockdown of *egl-20* did not prevent the intracellular reduction of mitochondria content induced by PGL-1 aggregation in the germline (Fig. 37A), it was sufficient to rescue the lower mitochondrial content in somatic tissues (Fig. 37B).

Likewise, loss of either *egl-20* Wnt ligand or its receptor *mig-1* rescued changes in the mitochondrial morphology of somatic tissues triggered by PGL-1 aggregation in the germline (Fig. 38).

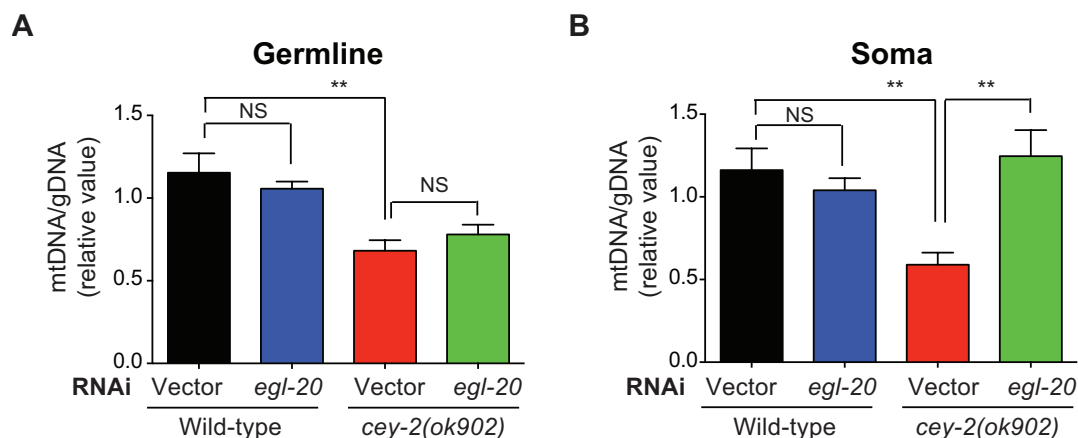


**Fig. 37. Knockdown of *egl-20* rescues the low mtDNA content in the soma but not in the germline of *cey-2* null functional mutant.** (A) Relative DNA (mtDNA)/genomic DNA (gDNA) ratio in isolated germlines to wild-type + Vector RNAi (mean  $\pm$  s.e.m., n= 6 biological replicates from three independent experiments). (B) Relative mtDNA/gDNA ratio in somatic tissues (isolated intestines + heads) to wild-type + Vector RNAi (mean  $\pm$  s.e.m., n= 5 biological replicates from three independent experiments).

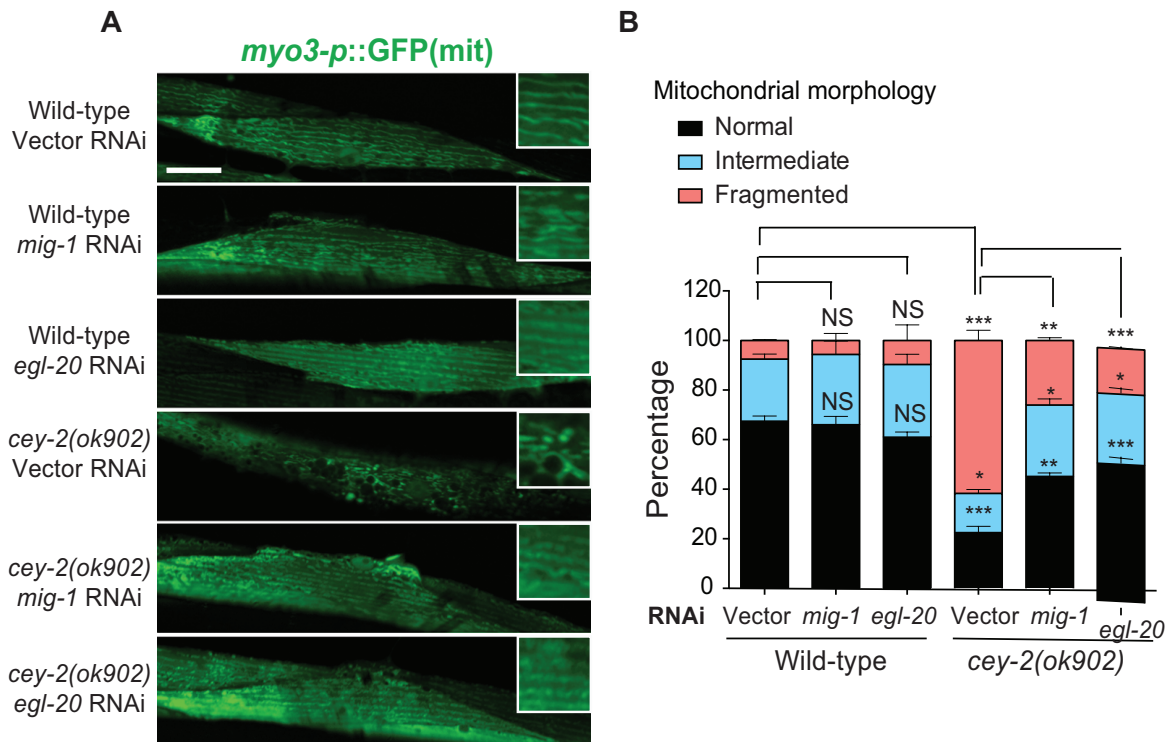


**Fig. 38. Knockdown of *egl-20* and *mig-1* rescues the mitochondria fragmentation in muscles of *cey-2* null functional mutant.** (A) Knockdown of either Wnt/mitokine signal *egl-20* or its receptor *mig-1* ameliorates changes in the mitochondrial morphology of the muscle induced by loss of *cey-2* function. Scale bar, 20  $\mu$ m. Images are representative of 3 independent experiments. (B) Percentage of animal with normal, intermediate or fragmented mitochondrial network morphology in the muscle (mean  $\pm$  s.e.m. of 3 independent experiments, wild-type + Vector RNAi= 40 worms, wild-type + *mig-1* RNAi= 35 worms, wild-type + *egl-20* RNAi= 41 worms, *cey-2(ok902)* + Vector RNAi= 75 worms, *cey-2(ok902)* + *mig-1* RNAi= 73 worms, *cey-2(ok902)* + *egl-20* RNAi= 89 worms).

Since growing evidence links mitochondrial alterations with the accumulation of protein aggregates in neurodegenerative diseases (38, 110, 111), we asked whether systemic mitochondrial changes induced by loss of proteostasis in the germline promote the aggregation of disease-related proteins in neurons. Remarkably, knockdown of either *egl-20* or *mig-1* ameliorated polyQ67 aggregation in the neurons of *cey-2* mutant worms (Fig. 39), indicating that the Wnt/mitokine signaling pathway communicates proteostasis deficits from germline cells to somatic tissues.

Taken together, we find that depletion of germline-specific CEY proteins induces aggregation of the germ granule component PGL-1, which, in turn, causes germline mitochondria perturbation. This process triggers the Wnt/ELG-20 signaling pathway that affects mitochondria of somatic tissues. Somatic mitochondria perturbation, in turn, triggers protein aggregation, contributing to somatic proteostasis collapse. Thus, ELG-20 acts as signal

molecule of a cell non-autonomous mechanism, mediated by mitochondria alteration, which permit to communicate the germline proteostasis status to somatic tissues.

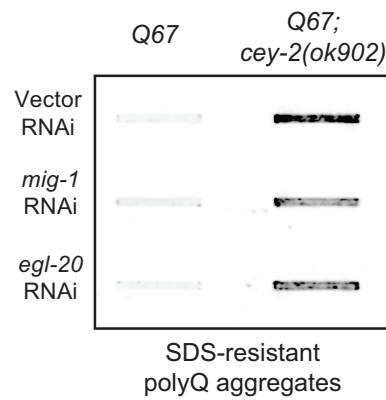


**Fig. 39. Knockdown of *egl-20* rescues the neuronal protein aggregation of *cey-2* null functional mutant.** Knockdown of either *egl-20* or *mig-1* ameliorates increased polyQ67 aggregation phenotype in the neurons of *cey-2* mutants. The images are representative of three independent experiments. Analysis by two-tailed Student's t-test for unpaired samples: \*P < 0.05, \*\*P < 0.01, \*\*\*P < 0.001, NS= not significant (P > 0.05).

---

## DISCUSSION

To date, extensive evidence demonstrates that proteostasis can be regulated through cell non-autonomously mechanisms (22, 23, 24). This process has been reported in different model organisms, demonstrating that this phenomenon is conserved among species, from nematodes to mammals. However, many of these studies were performed in *C. elegans*, as it represents a simple model to study tissue communication. Moreover, although the nervous system has been considered the main tissue capable to orchestrate distant proteostasis regulation, also other somatic tissues, such as muscle and intestine, can play a similar role (22, 23, 24).

Similarly to the soma, the reproductive system has also been reported to be capable to modulate cell non-autonomously proteostasis of distant somatic tissues. In fact, germline ablation, DNA damage and GSC pool diminution affect the soma, leading for instance to lifespan extension and improved stress resistance (47, 51, 55, 56).

Moreover, whereas the effects of somatic proteostasis imbalance on other somatic peripheral tissues are partially known and subject of study, no research was so far conducted to study the effect on somatic proteostasis induced by germline proteostasis perturbation.

Thus, we asked whether proteostasis deficits in germline cells impinge on distal tissues such as the nervous system. To answer this question, we targeted the *C. elegans* Y-box binding proteins (CEYs), a typical component of ribonucleoprotein granules that prevents aberrant aggregation of self-interacting proteins. Accordingly, germline of quadruple CEYs mutant worms displays PGs aggregation in abnormal foci structures. However, these abnormal granules differ from the squared sheet structures previously observed upon depletion of *cgh-1* (81, 84), which is a DEAD-box RNA helicase that controls mRNPs to prevent phase transition to nondynamic solids. Moreover, *cey-2* knockdown accelerates PGs aggregates formation in the germline of *cgh-1* mutant worms (81).

Similarly, we observed formation of analogues PGs foci aggregates upon depletion of either *cey-2* or *cey-3* proteins, showing that single knockdown of germline-specific CEYs is sufficient to trigger abnormal PGs formation. These abnormal granules showed a bigger size than regular PGs and colocalized with PGL-1 protein.

Formation of abnormal granules induced by CEYs depletion is in agreement with the role that these proteins play on PG organization. The role that CEYs exert on mRNP granules is conserved among species, as CEY orthologs control mRNP organization in many different animals (84, 94, 95, 96, 97). Therefore, it is not surprising that PGs structure and dynamics results affected in absence of CEY proteins.

---

Furthermore, CEY proteins control both positively and negatively protein translation, therefore CEY deficiency may affect the protein level of essential PG components, causing indirectly consequences on PGs structure. For instance, knockdown of either *cey-2* or *cey-3* could alter the protein abundance of PGL-1 protein. Due to PGL-1 capacity to self-associate and recruit other mRNPs, PGL-1 may act as a nucleating factor for the aggregation of other PG components (60, 75, 76). Therefore, increased PGL-1 protein levels could lead to formation of bigger and abnormal structures. Accordingly with this hypothesis, depletion of PGL-1 protein from early *C. elegans* embryos causes dispersal of other germ granule components in the cytoplasm (76). Germline-specific PGL-1 overexpression experiments could shed light on this hypothesis. In the case PGL-1 overexpression would be sufficient to trigger PGs aggregation, it would signify that PGL-1 concentration plays a critical role on PGs dynamics regulation.

Alternatively, CEYs depletion could affect translation of PG modulators, which are known to modulate and control PG dynamics. Examples of PG modulators are the PUF proteins, which have been identified as suppressors of PG aggregation. Accordingly, *puf-3* and *puf-11* depletion transforms square sheets aggregates to small, rounded granules, in *cgh-1* mutant (81). Therefore, reduced levels of PUF proteins could enhance PGs capacity to aggregate into bigger aberrant foci.

Finally, CEY proteins may be involved in recruiting RBPs to PGs, as CEYs are supposed to interact directly or indirectly with other PGs components. Accordingly, CEYs have been shown to interact, in a RNA-dependent fashion, with other PGs factors such as CAR-1 and PAB-1 (84). Depletion of CAR-1 and PAB-1 proteins prevents PGs aggregation in *cgh-1* mutant worms (81). Therefore, CEYs depletion may alter the recruitment of such proteins to granules and indirectly cause PG aggregation.

Interestingly, we observed that knockdown of CEYs induce abnormal PG foci exclusively in the tip of the distal germline region, where the GSC pool is located. Importantly, whereas double *cey-2* and *cey-3* mutant worms display reduced total number and proliferation of GSCs, single *cey-2* and *cey-3* depletion did not alter either the total number or the proliferation rate of GSC cells, ruling out perturbation of GSC niche as a cause of abnormal PGs formation upon CEYs deficiency.

Moreover, contrarily to double mutant CEY-2 and CEY-3 worms that show reduction in egg laid (84), single *cey-2* and *cey-3* did not cause fertility defects. Therefore, either *cey-2* or *cey-3* depleted worms conserve a functional germline.

CEY-2 and CEY-3 are supposed to carry out redundant functions, as they hold 70% identity and present similar localization (84). Moreover, CEY-2 and CEY-3 protein levels show

---

an expression pattern that increases from the distal to the proximal region of the germline. Therefore, the tip of the distant germline is the region displaying the lowest amount of CEY-2 and CEY-3 protein levels. Thus, depletion of either *cey-2* or *cey-3* could have a stronger effect in this region, since the amount of the not depleted CEY could not be sufficient to compensate the effect of the lacking CEY. Therefore, the tip of the distal germline may be more susceptible to single CEYs knockdown and this could explain the presence of abnormal PGs exclusively in this area. An alternative explanation could be that the distal germline, being the region where the mitosis takes place, hold a different gene expression pattern. Thus, the presence of some proteins rather than others could render this region more susceptible to form aberrant granules.

Importantly, we observed that PGL-1 abnormal foci display an insoluble aggregate behavior, as these PGL-1 granules were SDS resistant and could be isolated by filter trap assay. For this reason, single depletion of *cey-2* and *cey-3* is sufficient to induce PG solid phase transition and challenge germline proteostasis. Phase separation events can be prompted by interactions between the RGG/RG domains, often present in RBPs, and mRNA molecules (59). Thus, alteration in PG composition could be a critical event that triggers phase transition of PGs into solid aggregates. For instance, an increase in PGL-1 protein, which carries a RGG domain, could cause an increment in the recruitment of mRNA molecules, and indirectly of other proteins bound to mRNAs, to the granule triggering PG condensation and formation of less dynamic structure. Therefore, depletion of either *cey-2* or *cey-3* affects PG dynamics, causing PG phase transition, which leads to the formation of solid insoluble structures. Future experiments could be carried out in order to further confirm the proteostasis impairment observed in CEYs depleted germline. For instance, it could be important to determine if the cellular clearance mechanisms, such as the proteasome and the autophagy pathway, would be compromised upon knockdown of CEY factors. An additional experiment could be directed to analyze the overall proteome aggregation status of germline using the Proteostast kit, which permits the detection of endogenous protein aggregates (112). Finally, to confirm the aggregate behavior of aberrant PGL-1 aggregates, FRAP experiments could be performed to evaluate the compromise dynamics of such abnormal granules.

Importantly, depletion of either *cey-2* or *cey-3* challenge proteostasis not only in germline but also in somatic tissues such as nervous system, muscles and intestine. Therefore, since CEY-2 and CEY-3 proteins are expressed exclusively in germline, a cell non-autonomous mechanism should be responsible for such somatic proteostasis disruption. In fact, upon single *cey-2* and *cey-3* depletion, we observed increased protein aggregation and neurodegeneration, as indicated by animal decreased motility in HD model worms.

---

Remarkably, somatic proteostasis defects were observable not only in HD models but also in ALS models. Since HD and ALS are caused by different kind of protein aggregates, we deduced that somatic proteostasis, caused by germline CEYs depletion, results overall challenged and it does not fail to cope only with a specific subtype of protein aggregate. Therefore, this increased susceptibility of soma to form protein aggregates must be linked to a general proteostasis disruption. For instance, downregulation of chaperones could trigger misfolding events and accelerate the formation of protein aggregates. Alternatively, a disruption of protein clearance mechanisms could lead to protein aggregates accumulation (2, 3, 4). For example, defective proteasome activity, caused by decreased expression or inactivation of proteasome subunits, as well as autophagy downregulation could contribute to increase the accumulation of protein aggregates. It will be fascinating to perform further experiments to shed light on this regard. For instance, specific kits, that permit to measure proteasome activity, could be utilized to assess if CEYs depletion affects the proteasome. In addition, autophagy activity could be monitored by using GFP-fused LGG-1 and LGG-2 reporter strains, which allow to examine the autophagosomes formation (113).

Of note, single knockdown of CEY factors did not induce HSR in the intestine, demonstrating that, although somatic proteostasis is perturbed, heat shock response is not activated. This event is in line with recent evidence showing that overexpression of various aggregation-prone proteins do not induce HSR activation in neuronal-like mammalian cells (114). This failure of HSR activation is explained by the capacity of such pathogenic protein in either evading detection or impairing induction of the HSR. Therefore, defective HSR induction may be a further explanation for the increased protein aggregation observed in the soma of CEYs depleted worms.

Importantly, somatic proteostasis disruption was rescued upon *pgl-1* knockdown. This data suggest that the effect of germline-specific CEYs deficiency on somatic proteostasis is mediated by PGL-1 and that PGL-1 acts downstream *cey-2* and *cey-3* depletion. To note, PGL-1 protein is exclusively express in the germline, thus, its knockdown does not directly impact on other tissues. Therefore, we speculate that PGL-1 germline aggregates, and subsequent germline proteostasis perturbation, could be responsible to induce a cell non-autonomous mechanism that affects somatic proteostasis, causing its disruption.

Remarkably, cell non-autonomous disruption of somatic proteostasis is not only induced by deficiency of germline-specific *cey-2* and *cey-3* but also by *cey-1* depletion. Although, CEY-1 is expressed in both soma and germline, a CEY-1 cell autonomous effect was ruled out using HD model strains that do not permit *cey-1* knockdown in germline. In fact, in these

---

models, we did not observe increased aggregation upon neuronal-specific *cey-1* depletion. Thus, similarly to germline-specific CEYs, also *cey-1* deficiency affects somatic proteostasis through a cell non-autonomous mechanism originated from the germline.

Notably, quantitative proteomics analysis of isolated germlines revealed that single CEY factors depletion induces mitochondria defects in germline. Several components of different mitochondria respiratory chain complexes were downregulated upon knockdown of germline-specific CEY factors. This difference in mitochondrial protein expression correlates with mitochondrial structural defects, as mitochondria appear to be more disorganized, showing disruption in functional mitochondrial networks. Finally, we observed a reduction in the total amount of mitochondria.

This decrease in mitochondria abundance could be the consequence of prohibitin downregulation, which occurs upon CEY depletion. In fact, a reduction of prohibitin has been shown to influence mitochondrial proliferation (115).

Mitochondria have also been described to hold capacity in controlling programmed cell death in mammals (116). In accordance with our observation, a previous publication reports that double *CEY-2* and *CEY-3* mutant worms display increased germ cells apoptosis (84), which could be the consequence of defective germline mitochondria.

Importantly, we show that these mitochondria defects are linked to germline proteostasis collapse mediated by PGL-1 aggregates. In fact, *pgl-1* knockdown rescued the reduction in the amount of germline mitochondria, showing that PGL-1 acts downstream CEYs depletion and upstream mitochondria perturbation. Therefore, in the germline of single *cey-2* and *cey-3* depleted worms, PGL-1 forms aggregates that affect proteostasis, which subsequently causes mitochondria alterations.

Accordingly, several evidences link proteostasis and mitochondria disruption. In fact, it has been reported that proteostasis imbalance affects mitochondrial function with dramatic consequences for organismal health (117). Moreover, in neurodegenerative disease models, mitochondrial dysfunction shows various parameters that include a decline in energy production, impaired tricarboxylic acid cycle activity, decreased electron chain function, and aberrant mitochondrial dynamics (118, 119). Furthermore, similarly to our results, mitochondria from HD patients have reduced levels of complex II and III (120). In addition, polyQ40 proteins accumulate in the outer mitochondrial membrane and thus impact mitochondrial import and membrane potential in *C. elegans*. In mammalian cells, toxic polyQ proteins interact with the mitochondrial membrane and perturb membrane potential (121). Finally, protein aggregates have been also associated with excessive production of ROS and

---

accumulation of mtDNA mutations (122). Therefore, germline proteostasis imbalance appears to be the cause of germline mitochondria defects.

Since PGs and mitochondria reside close to each other in germline (47, 78, 79), additional experiments could be carried out to study if PG aggregates colocalize with mitochondria, as protein aggregates may cause mitochondria disruption by interacting and accumulating in the mitochondria membrane, thus perturbing membrane potential. Moreover, some PGs regulators, like CGH-1, are known to affect PGs dynamics and cause aggregation, thus depletion of these proteins could provide evidences to confirm the link between germline proteostasis imbalance and mitochondria perturbation. Alternatively, mitochondria defects could be an indirect consequence of PGL-1 aggregates formation. As previously described, PGs sequester mRNAs and, by controlling translation, assure a correct spatiotemporal gene expression pattern. For instance, aberrant PGs aggregates could sequester and/or retain mRNAs essential for correct mitochondrial functionality. Thus, these sequestered transcripts may not be translated and cause mitochondria dysregulation. Accordingly with this hypothesis, proteomics analysis of *cey-3* depleted germline revealed several downregulated mitochondria components. This depletion could be the consequence of the sequestration, by PGL-1 aggregates, of the respective mRNAs of mitochondria depleted-components, with subsequent protein downregulation.

Surprisingly, these mitochondria defects were not only limited to germline but were also observed in somatic tissues. Similarly to germline, the soma also displayed downregulation of several respiratory complexes components, mitochondria fragmentation and reduction of total mitochondria number. As for defective somatic proteostasis, our results indicate that somatic mitochondria dysregulation is also a consequence of cell non-autonomous effect mediated by depletion of either *cey-2* or *cey-3* in germline. Moreover, these somatic mitochondrial defects were dependent on PGL-1 aggregation. Indeed, *pgl-1* depletion could rescue not only the morphological and structural defects but also the total mitochondria number decrease in the soma. Therefore, PGL-1 aggregates impinge not only cell autonomously germline mitochondria but also cell non-autonomously mitochondria of somatic tissues. Again, PGL-1 is a germline-specific protein and its knockdown only takes place in the reproductive system. Thus, PGL-1 acts downstream single *cey-2* and *cey-3* depletion and upstream mitochondria dysregulation.

This mitochondria imbalance could represent another explanation for the previously described proteostasis collapse observed in the soma. In fact, not only proteostasis imbalance affects mitochondria but also mitochondria defects can contribute to proteostasis disruption. For instance, *hsp-6* depletion enhances cytoplasmic polyQ aggregation, indicating that the mitochondrial protein quality control system contributes to proteostasis balance (123).

---

Reduction in the levels of *hsp-6* abolishes mitochondrial import and lead to an accumulation of mitochondrial pre-proteins in the cytosol, thus enhancing the potential risk of protein aggregation. Accordingly, the overloading of mitochondrial membrane carriers is able to induce cytosolic protein aggregation of unimported mitochondrial proteins (124). Therefore, downregulation of mitochondria protein import machinery can cause cytosolic protein aggregation and proteostasis disruption. Accordingly with this hypothesis, we observed reduction of mitochondria import components such as TOMM-20 and TIN-44. Thus, downregulation of these proteins could increase protein aggregation and aggravate proteostasis disruption in neurodegenerative diseases, as we observed in HD and ALS worm models upon single CEY deficiency. In order to test this hypothesis, restoring the protein import machinery could represent a strategy to rescue somatic proteostasis collapse in CEY depleted worms. Import restoration could takes effect by overexpressing for instance TOMM-20 or TIN-44.

Surprisingly, although the somatic mitochondria defects of CEYs deplete worms, we did not detect alterations in either oxygen consumption or ATP and NAD production. A potential explanation for these results may be the limitation of the assays we have performed. In fact, these assays permit measurements of the entire worms. However, although we show that both germline and soma display mitochondria imbalance, some tissues could be more affected than others or not be affected at all, thus hiding to our measurements potential mitochondria alterations. Moreover, the lack of differences in oxygen consumption and ATP/NAD production could be explained by mitochondria compensatory mechanisms, taking place in order to balance CEY-dependent mitochondria defects. For instance, in Barth syndrome lymphoblastoid cells, a compensatory increase in the number of mitochondria prevents the loss of mitochondrial respiration and ATP synthesis (125). Interestingly, we have observed a decrease in the total mitochondria number. Therefore, the basal activity of mitochondria could be upregulated to compensate for the lower mitochondrial content. Increased ATP production could lead to increased ROS generation, which may contribute to protein aggregates formation and proteostasis imbalance. This event could be a potential explanation for the increased protein aggregation and somatic proteostasis disruption observed in CEYs depleted HD and ALS worm models. Thus, compensatory effects could challenge the integrity of the mitochondrial proteome and activate proteostasis responses in the organelle. Accordingly, we detected that the UPR<sup>mt</sup> response was activated in the soma of either *cey-2* or *cey-3* depleted worms. We observed increased activation of HSP-6 and HSP-60 in the intestine. This somatic activation represents a further confirmation of the cell non-autonomous effect of germline CEYs depletion.

---

The UPR<sup>mt</sup> activation could be the direct effect in response to somatic mitochondrial defects, such as the downregulation of mitochondria complexes components. Accordingly, the UPR<sup>mt</sup> is upregulated in response to RNAi against *cco-1*, which is an essential component of the complex IV of the respiratory chain. (104). However, the somatic UPR<sup>mt</sup> activation could also be the result of mitochondria dysfunction in germline, induced by a cell non-autonomous mechanism. Accordingly to this hypothesis, perturbation of *cco-1* in the nervous system and muscles induce the UPR<sup>mt</sup> activation in the intestine, via cell non-autonomous communication (33).

Alternatively, the UPR<sup>mt</sup> activation may result from cytoplasmic protein aggregates accumulation in the soma of CEYs depleted worms. Accordingly, it has been reported that the UPR<sup>mt</sup> activates in response to polyQ accumulation in the mitochondria outer membrane in both *C. elegans* and in mice (126). Therefore, increased ROS production or protein import dysregulation could contribute to the formation of cytoplasmic endogenous aggregates that could interfere with mitochondria and eventually causing UPR<sup>mt</sup> activation. To test this hypothesis, the ROS production could be measured using specific kits. Moreover, also the somatic presence of endogenous protein aggregates could be studied using the Proteostat assay kit, which allows for aggresome detection. Of note, other cellular stress response pathways as UPR<sup>ER</sup> and HSR did not result to be activated in the soma of either *cey-2* or *cey-3* depleted worms, showing the specificity of mitochondria involvement in the cell non-autonomous CEY-dependent pathway.

Importantly, it has been recently discovered that mitochondria can communicate their status, through molecules called mitokines, and thus influence mitochondria in other tissues. Accordingly, we found that the Wnt/ELG-20 mitokine is the responsible signal that permits mitochondria communication from the germline to the soma. In fact, we observed that downregulation of *elg-20* and its receptor *mig-1* rescued either mitochondria structural defects or decreasing mitochondria number in the soma but not in germline. These results confirm that EGL-20 is the signal required for the cell non-autonomous communication that triggers mitochondria defects in somatic tissues. On the other hand, these results suggest that germline must be the sender tissue of this signal, as it does not result affected by the rescue mediated by *elg-20* deficiency. Thus, EGL-20 must act downstream germline mitochondria perturbation but upstream somatic mitochondria alteration. In support to our results, it has been reported that neuronal expressed Q40 associates with mitochondria, causing local activation of the UPR<sup>mt</sup> that is further communicated extracellularly across the animal to promote UPR<sup>mt</sup> activation in non-neuronal tissues (38). The signal responsible for such UPR<sup>mt</sup> communication has been identified

---

as the Wnt/EGL-20 mitokine. In fact, neuronal-specific expression of ELG-20 is sufficient to trigger UPR<sup>mt</sup> in the distant intestine (107). Therefore, the UPR<sup>mt</sup> somatic activation, observed in CEYs depleted worms, may be triggered by ELG-20 signal. In order to test this hypothesis, HSP-6 and HSP-60 expression levels could be monitored upon knockdown of *elg-20* or *mig-1* in CEYs depleted worms, to observe potential rescue effects. Moreover, we found that blocking the cell non-autonomous communication, through ELG-20 or MIG-1 knockdown, was sufficient to reduce protein aggregation in CEYs-depleted HD model worms. Thus, this result reveals that ELG-20 signaling acts upstream somatic proteostasis collapse. Therefore, we speculate that somatic proteostasis disruption, caused by either *cey-2* or *cey-3* deficiency, is a consequence of somatic mitochondria dysfunction.

Previous studies have connected the Wnt signaling to neurodegenerative disease. In fact, Wnt signaling dysfunction has been implicated in a number of human diseases, including Alzheimer's and Parkinson's disease (127). Accordingly, it has also been proposed that Wnt signaling functions in a protective role against neurodegenerative diseases (128). In contrast with a protective role of the Wnt signal, we report that this signal is not protective but deleterious and it is responsible for a communication that affects mitochondria in distant tissues, and indirectly cause somatic proteostasis collapse. To confirm our results, further experiments could consist in overexpressing ELG-20 protein and monitor subsequent proteostasis status.

---

## CONCLUSION

Taken together, we find that dysregulation of germline-specific, non-mitochondrial CEY proteins induces aggregation of the germ granule component PGL-1 followed by intracellular changes in the mitochondrial network of germline cells. In turn, this process triggers a Wnt/mitokine signaling pathway that influences mitochondrial networks of somatic tissues. Thus, we identify a cell non-autonomous process that coordinates the proteostasis status of germline cells with systemic mitochondrial function, a capacity previously ascribed only to the nervous system. This cell non-autonomous mechanism originated in the germline can trigger protein aggregation in somatic tissues depending on the proteostasis status of germline cells, establishing a regulatory link between the fitness of the reproductive system with systemic mitochondrial function and proteostasis. Environmental and metabolic conditions such as stress or aging that impinge on proteostasis are tightly correlated with a decline of germline integrity in animals (45). Thus, we speculate that proteostasis deficits in germline cells ensued from stress conditions or aging could contribute to the dysregulation of mitochondrial function and aggregation of disease-related proteins that often appear in post-mitotic tissues such as muscle or nervous system with age.

---

## FUTURE PERSPECTIVE

Cell non-autonomous effects have been observed in different neurodegenerative diseases such as Huntington's disease, amyotrophic lateral sclerosis and Parkinson's disease. In fact, the phenotypes associated to these pathologies are not confined to the brain but they frequently involve non-neuronal peripheral tissues in ways that we are only starting to understand (23, 129). Unraveling the mechanisms behind cell non-autonomous control of proteostasis promises to shed light on both pathogenic mechanisms and future strategies for disease treatments. For instance, recent evidence from invertebrate models have demonstrated that stimulating somatic cells in the absence of stress can protect peripheral tissues that are affected by misfolded protein diseases through improving their folding capacity (27, 130).

Moreover, discovering the signal molecules and pathways involved in such interorgan communication represents a crucial aspect to better understand neurodegenerative diseases and shed light on new therapeutic approaches.

*C. elegans*, due to its simplicity, represents a perfect model to unravel the yet unknown signaling that controls cell-non-autonomous regulation of proteostasis. In fact, in this study we show a new cell non-autonomous mechanism that connects the reproductive system to the somatic periphery of *C. elegans*. In order to assess the significance of our findings, it would be important to verify if the here-reported cell non-autonomous communication is conserved in other model organisms and define whether this pathway contributes to aggravate the neurodegenerative phenotype of disease mammalian models.

Moreover, we found that Wnt/ELG-20 signal is the responsible molecule for the communication between germline and soma. Signal molecules, involved in inter-cellular communication, could represent targets for future innovative therapies. Thus, the Wnt signaling could represent a novel possible therapeutic approach. Blocking this signal may be a strategy to intervene in stopping the potential deleterious cell non-autonomous communication that affects the soma, thus preventing peripheral proteostasis disruption.

However, the signal that controls cell non-autonomous regulation of proteostasis may not be only one but an intricate network, consisting of a variety of molecules, such as secreted peptides, metabolites, and hormones, which could control distinct components of the organismal proteostasis network (24).

Accordingly, the ELG-20 mitokine could not be the only molecule responsible for here-described communication between germline and soma. In fact, *elg-20* deficiency only partially rescues the somatic mitochondrial structural defects observed in the soma of either *cey-2* or

---

*cey-3* depleted worms. More likely, ELG-20 acts in parallel with other molecules in orchestrating the interorgan communication started from germline mitochondria disruption. Therefore, further proteomics-based experiments could shed light on novel potential signal molecules and signaling pathways involved in the germline-soma communication and thus facilitate development of future treatments.

Moreover, contrarily to our findings, previous publications have shown that the Wnt/ELG-20 signaling holds a protective role, as it induces UPR<sup>mt</sup> activation in distant tissues (107). A possible explanation for such contradictory results could be related to the difference in the tissue inducing the Wnt/ELG-20 signaling. In fact, whereas we show that ELG-20 signaling is triggered by the reproductive system, previous studies report that the Wnt/ELG-20 signaling originates from somatic tissues. Thus, distinct tissues could induce differential ELG-20 mediated cell non-autonomous responses. However, future experiments would be required to better understand the role of ELG-20 in the cell non-autonomous regulation of proteostasis.

Furthermore, we show that the Wnt signaling is induced by germline mitochondria perturbation. Extensive evidence from model organisms and clinical studies suggests that mitochondria play a critical role in neurodegenerative diseases, such as Huntington's disease, Alzheimer's disease and Parkinson's disease. Mitochondria alterations, such as reduced mitochondrial fusion and increased mitochondrial fragmentation, are associated with mitochondrial dysfunction and cell death in age-related diseases.

However, most of the attention has focused on studying the cell autonomous effect of mitochondria dysfunction within the affected tissue. However only recently, the importance of cell non-autonomous mitochondria communication is emerging, as it contributes to control proteostasis of distant tissues. Therefore, investigating the mitochondria status not only in the affected tissue of disease models, but also in distant peripheral tissues could improve our knowledge on age-related diseases. Thus, acting on distant mitochondria and preventing their disruption, could be a new therapeutic strategy to ameliorate, cell non-autonomously, somatic proteostasis collapse.

Importantly, our results point out a novel role for the reproductive system in the context of neurodegenerative diseases, as germline proteostasis defects aggravate distant somatic proteostasis collapse that occurs in protein aggregation-related diseases. To date, no studies have taken in account the potential role of germline as sender of signal molecules, which could take part in the interorgan communication involved in age-related diseases. Thus, the reproductive system may represent a future target of study to deepen our knowledge on cell non-autonomous mechanisms that control neurodegenerative diseases.

---

In fact, we show that germ granule phase transition is the first event that triggers the cell non-autonomous mechanism, which culminates with somatic proteostasis collapse. Phase transition of mRNP complexes has been reported to display a crucial role in neurodegenerative diseases. Development of therapeutic strategies to control cellular phase transition is a powerful instrument to treat human diseases caused by protein aggregates. To date, like for mitochondria, the focus on phase transition events has been essentially on the tissue affected by the pathological phenotype, whereas we show that also distant tissues could be affected by phase transition events. Therefore, monitoring mRNPs status in distant tissues could be an innovative approach to study neurodegenerative diseases. As such, controlling mRNP phase transition in distant tissue could represent an alternative novel strategy to block potential cell non-autonomous communication responsible for the aggravation of diseases phenotype.

---

## METHODS

### *C. elegans* strains and maintenance

*C. elegans* strains were grown and maintained on standard nematode growth media (NGM) seeded with *E. coli* (OP50) bacteria (44). Wild-type (N2), SS104 (*glp-4(bn2)*I), SS747 (*bnIs1[pie-1p::GFP::pgl-1 + unc-119(+)]*), SJ4103 (*zcIs14[myo-3p::GFP(mit)]*), AM141 (*rmIs133[unc-54p::Q40::YFP]*), SJ4100 (*zcIs13[hsp-6p::GFP]*), SJ4058 (*zcIs9[hsp-60p::GFP + lin-15(+)]*), SJ4005 (*zcIs4[hsp-4p::GFP]*) and CL2070 (*dvIs70[hsp-16.2p::GFP] + rol-6(su1006)*) were provided by the *Caenorhabditis* Genetics Center (CGC) (University of Minnesota), which is supported by the NIH Office of Research Infrastructure Programs (P40 OD010440). RAF291 (*cey-2(ok902)*I) was provided by R. Ciosk and was generated by outcrossing the RB988 strain (*cey-2(ok902)*I) four times to wild-type N2 (19). RB988 (*cey-2(ok902)*I) was made by the *C. elegans* Gene Knockout Project at the Oklahoma Medical Research Foundation (Oklahoma, USA). RAF4 (*cey-3(rrr11);cey-2(ok902)*I) outcrossed twice to wild-type N2 was also a gift from R. Ciosk (19). AM23 (*rmIs298[F25B3.3p::Q19::CFP]*) and AM716 (*rmIs284[F25B3.3p::Q67::YFP]*) strains were provided by R. I. Morimoto (25). MAH602 (*sqIs61[vha-6p::Q44::YFP + rol-6(su1006)]*) was provided by M. Hansen (45). ZM5844 (*hpIs233[rgef-1p::FUS<sup>P525L</sup>::GFP]*) and ZM5842 (*hpIs228[rgef-1p::FUS<sup>R522G</sup>::GFP]*) were a kind gift from P. St George-Hyslop (46). IW46 (*Psnb-1::TDP-43-YFP M337V(iwEx28)*) was kindly provided by J. Wang (47). For neuronal-specific RNAi experiments, we used the TU3401 strain (*sid-1(pk3321)V;uIs69[pCFJ90(myo-2p::mCherry) + unc-119p::sid-1]*) provided by the CGC, in which RNAi treatment is only effective in neurons (48). DVG196 (*rmIs284[F25B3.3p::Q67::YFP]; sid-1(pk3321)V;uIs69[pCFJ90(myo-2p::mCherry) + unc-119p::sid-1]*) was generated by crossing AM716 to TU3401. Screening of *sid-1(pk3321)* homozygote worms was done by PCR using the following primers: GTGCATACACCGTCACGTC and TTCGGGAAATGGCGCTTAAC. Screening of *unc-119p::sid-1* was performed by using the following primers: TATAGGATCCTCATTTTTCCAGGTTCAACAATG and ATATAAGCGGCCGCAGAAAGGTGTCATGGTCTAGT. DVG195 strain (*rmIs284[F25B3.3p::Q67::YFP]; glp-4(bn2)*) was generated by crossing AM716 to SS104. For the generation of DVG180 (*rmIs284[F25B3.3p::Q67::YFP]; cey-2(ok902)*) and DVG183 (*rmIs284[F25B3.3p::Q67::YFP]; cey-3(rrr11); cey-2(ok902)*), AM716 was crossed to

---

RAF291 and RAF4, respectively. To generate DVG199 (*zcls14[myo-3p::GFP(mit)]; cey-2(ok902)*), we crossed SJ4103 to RAF291. Screening of *cey-2(ok902)* and *cey-3(rrr11);cey-2(ok902)* homozygote worms was done by PCR using the following primers: TGGGAAGAAGAGCAGAAGTCGAA, TTTTCACACTTTCCATCACGACACAT, GATCTCTCCATCGGCAAGAAAAGA, and ACCAAGGCCAGCATCGTCG.

### **RNAi constructs**

RNAi-treated worms were fed *E. coli* (HT115) containing an empty control vector (L4440) or expressing double-stranded RNAi. *pgl-1*, *cct-8*, *egl-20* and *mig-1* RNAi constructs were obtained from the Vidal RNAi library. *cey-1*, *cey-2*, and *cey-3* RNAi constructs were obtained from the Ahringer RNAi library. All RNAi constructs were sequence verified.

### **Lifespan studies**

Synchronized animals were fed from hatching on HT115 *E. coli* carrying empty vector or RNAi constructs. 96 adult animals were used per condition and scored every day or every other day (27). From the initial adult population, we censored the worms that are lost or burrow into the media as well as those that undergo bagging or exhibit ‘protruding vulva’ phenotypes.  $n = \text{total number of uncensored animals} / \text{total number (uncensored+censored) of animals}$  in each independent experiment. We used PRISM 6 software to determine median lifespan and generate lifespan graphs. To determine mean lifespan, we used OASIS software (49). *P* values were calculated using the log-rank (Mantel–Cox) method. The *P* values refer to experimental and control animals in a single experiment. In the main text, each graph presents a representative experiment. See **Supplementary Data 1** for statistical analysis and replicate data.

### **GSC proliferation assays**

Worms were incubated with 33 mM solution of 5-bromodeoxyuridine (BrdU) (Sigma-Aldrich) in S medium for 2 h at 20 °C. Worms were washed with EBT buffer (1X egg buffer, 0.2 % Tween 20, 20 mM sodium azide). Then, worms were decapitated to extract the germline on a coverslip and covered with a poly-lysine-coated microscope slide. The coverslip was

---

removed and the slide was fast frozen on dry ice. Then, the slide was fixed in methanol for 2 min at -20 °C and washed with PBST (1X PBS, 0.1% Tween 20). DNA was denatured in 2M HCl for 45 min at room temperature followed by washing using PBST. After blocking for 30 min in PBST containing 10% donkey serum, anti-BrdU antibody (Abcam, ab6326, 1:250) was added followed by overnight incubation in a humid chamber. Anti-Rat IgG secondary antibody (Life Technologies 1744742, 1:500) was added for 2 h at room temperature. Finally, slides were mounted with Precision coverslip (Roth) using DAPI fluoromount-G (Southern Biotech 0100-20).

### **Egg counting and percentage of viable eggs**

Synchronized L1 larvae were raised on HT115 *E. coli* carrying empty vector, *cey-2 RNAi* or *cey-3 RNAi* constructs. The number of eggs during the self-reproductive period was measured by singly plating late L4 worms and culturing them on the corresponding RNAi treatment. Each adult worm was then transferred to a new plate every 24 h and the previous plate was kept for another 24 h, when the number of alive progeny (that is, visible as L1 larvae) was scored to assess percentage of viable eggs. This procedure was repeated until no live progeny were counted.

### **Western blot**

Worms were lysed in protein lysis buffer (50 mM Tris-HCl, pH 7.8, 150 mM NaCl, 1% sodium deoxycholate, 1 mM EDTA, 0.1% SDS, 1% Triton X-100 and protease inhibitor (Roche)) using a Precellys 24 homogenizer. Worm lysates were centrifuged at 10,000 rpm for 10 min at 4 °C and the supernatant was collected. Protein concentrations were determined with standard BCA protein assay (Thermoscientific). 20 µg of total protein was separated by SDS-PAGE, transferred to nitrocellulose membranes (Millipore) and subjected to immunoblotting. Western blot analysis was performed with anti-GFP antibody (AMSBIO, TP401 1:5,000), FUS (Abcam, ab154141, 1:1000), TDP43 (Abcam, ab225710, 1:1000) and  $\alpha$ -tubulin (Sigma, T6199, 1:20,000).

---

### ***C. elegans* germline and gut immunostaining**

Day 3 adult worms were washed using EBT buffer (1X egg buffer, 20 mM sodium azide, 0.2 % Tween 20), decapitated to extract the germline and intestine on a coverslip and covered with a poly-lysine-treated slide. The microscope slide was then fast frozen on dry ice, fixed in methanol for 2 min at -20 °C and washed with PBST (1X PBS and 0.1 % Tween 20) followed by blocking with 10 % donkey serum in PBST for 30 min. Samples were incubated overnight with anti-PGL-1 antibody (DSHB, K76, 1:33) or anti-ATP5A (Abcam, ab14748, 1:100) at room temperature. Alexa Fluor 546 goat anti-Mouse IgM (Life Technologies, 2105681, 1:500) and Alexa Fluor 546 goat anti-Mouse IgG (Life Technologies, 1904466, 1:500) was added for 2 h. Slides were mounted with DAPI fluoromount-G (Southern Biotech 0100-20).

### **Imaging of *myo-3p::GFP(mit)* reporter**

For imaging of *myo-3p::GFP(mit)* reporter strain, day 3 adult worms were immobilized using 0.1% Azide in M9 buffer and covered with a coverslip. Images of worms were acquired with a Zeiss ApoTome Axio Imager Z.1 fluorescence microscope. Qualitative assessment of mitochondrial morphology was made by scoring animals based on three categories: normal (interconnected mitochondrial network), intermediate (combination of interconnected mitochondrial network and isolated smaller mitochondria) or fragmented (mostly fragmented mitochondria).

### ***hsp-6, hsp-60, hsp-4, hsp-16.2* transcriptional reporter experiments and imaging**

SJ4100 (*zcls13[hsp-6p::GFP]*), SJ4058 (*zcls9[hsp-60p::GFP + lin-15(+)]*), SJ4005 (*zcls4[hsp-4p::GFP]*) and CL2070 (*dvls70[hsp-16.2p::GFP] + rol-6(su1006)*) worms were cultured until day 3 of adulthood. For imaging, adult worms were immobilized using 0.1% Azide in M9 buffer and covered with a coverslip. Images of whole worms were acquired with a Zeiss Axio Zoom.V16 fluorescence microscope. To quantify GFP fluorescence, worms were outlined and quantified using ImageJ software.

---

## **NAD<sup>+</sup> and ATP detection**

200 age-synchronized day 3 adult worms were collected and washed with M9 buffer. For NAD<sup>+</sup> detection, we used a commercial colorimetric kit (NAD/NADH Assay Kit, #ab65348) following the manufacturer's instructions. Briefly, the animals were homogenized in NAD<sup>+</sup>/NADH extraction buffer. Enzymes that may consume NADH were removed by filtering the samples through a 10 kD spin column (ab93349) before performing the assay. Decomposition of NAD<sup>+</sup> for NADH detection in samples was done by heating the samples to 60 °C for 30 min. Quantification of NAD total and NADH was performed by colorimetric method (OD 450 nm) using standard curve derived from known NADH concentrations. For ATP quantification, we used a colorimetric/fluorometric ATP assay kit (Abcam, ab83355) following the manufacturer's instructions. First, worms were homogenized in ATP assay buffer followed by deproteinization using 4M Perchloric acid (Sigma-Aldrich, 244252) and 2M KOH (Sigma-Aldrich, P-1767) method. Then, pH was adjusted to 6.8-8. Samples were centrifuged at 13,000 g for 15 min at 4 °C and the supernatant was collected. Quantification of ATP content was measured by fluorometric (Ex/Em = 535/587 nm) method. ATP concentrations were determined using standard curve derived from fluorescence of known ATP concentrations. Levels of fluorescence were measured using multimode plate reader EnSpire (PerkinElmer). For both NAD<sup>+</sup> and ATP detection, protein levels were normalized by BCA protein assay kit (Pierce, Thermo Scientific).

## **Oxygen consumption rates**

Oxygen consumption rates (OCR) were measured and analyzed using the Seahorse XFe96 Analyzer (Agilent) using the protocol described in ref. (50). Briefly, synchronized worms at day 3 of adulthood were washed in M9 buffer three times to remove residual bacteria and then transferred into the Seahorse plate wells at around 20 worms/well with at least 5 technical replicates per condition. Oxygen consumption was measured at room temperature 20 °C. Sodium azide treatment (Sigma-Aldrich) was used at 40 mM.

---

## **Filter trap assay**

*C. elegans* strains were grown from hatching on HT115 *E. coli* carrying either empty vector or RNAi clones. At day 3 of adulthood, worms were collected with M9 buffer and worm pellets were frozen with liquid N<sub>2</sub>. Frozen worm pellets were thawed on ice and worm extracts were generated by glass bead disruption on ice in non-denaturing lysis buffer (50 mM Hepes pH 7.4, 1 mM EDTA, 150 mM NaCl, 1% Triton X100) supplemented with EDTA-free protease inhibitor cocktail (Roche). Worm debris was removed with 8,000g spin for 5 min. 100 µg of protein extract was supplemented with SDS at a final concentration of 0.5% and loaded onto a cellulose acetate membrane assembled in a slot blot apparatus (BioRad). Then, the membrane was washed with 0.2% SDS and SDS-resistant protein aggregates were assessed by immunoblotting using antibodies against GFP (AMSBIO, TP401 1:5,000), FUS (Abcam, ab154141, 1:1000) and TDP43 (Abcam, ab225710, 1:1000). Extracts were also analyzed by SDS-PAGE/Western blot with anti-GFP, anti-FUS, anti-TDP43 and anti- $\alpha$ -tubulin (Sigma, T6199, 1:20,000).

## **Motility assay**

Animals were grown on HT115 *E. coli* containing empty control vector or the indicated RNAi. At day 3 of adulthood, worms were transferred to a drop of M9 buffer. After 30 s of adaptation, the number of body bends was counted for 30 s. A body bend was defined as change in direction of the bend at the mid-body (25).

## **Sample preparation for label-free quantitative proteomics and analysis**

Extruded germlines of synchronized worms at day 3 of adulthood were lysed in urea buffer (8 M urea, 2 M Thiourea, 10 mM HEPES, pH 7.6) by sonication and cleared using centrifugation (13,000 rpm, 10 min). Supernatants were reduced (1 mM DTT, 30 min), alkylated (5 mM iodoacetamide, 45 min) and digested with trypsin at a 1:100 w/w ratio after diluting urea concentration to 2 M. One day later, samples were cleared (16,000g, 20 min) and the supernatant was acidified. Peptides were cleaned up using stage tip extraction (51). The liquid chromatography tandem mass spectrometry (LC-MS/MS) equipment consisted of an EASY nLC 1000 coupled to the quadrupole based QExactive instrument (Thermo Scientific) via a nano-spray electroionization source. Peptides were separated on an in-house packed 50

---

cm column (1.9  $\mu\text{m}$  C18 beads, Dr. Maisch) using a binary buffer system: A) 0.1% formic acid and B) 0.1% formic acid in acetonitrile. The content of buffer B was raised from 7% to 23% within 120 min and followed by an increase to 45% within 10 min. Then, within 5 min buffer B fraction was raised to 80% and held for further 5 min after which it was decreased to 5% within 2 min and held there for further 3 min before the next sample was loaded on the column. Eluting peptides were ionized by an applied voltage of 2.2 kV. The capillary temperature was 275  $^{\circ}\text{C}$  and the S-lens RF level was set to 60. MS1 spectra were acquired using a resolution of 70,000 (at 200 m/z), an Automatic Gain Control (AGC) target of  $3 \times 10^6$  and a maximum injection time of 20 ms in a scan range of 300-1750 Th. In a data dependent mode, the 10 most intense peaks were selected for isolation and fragmentation in the HCD cell using a normalized collision energy of 25 at an isolation window of 2.1 Th. Dynamic exclusion was enabled and set to 20 s. The MS/MS scan properties were 17,500 resolution at 200 m/z, an AGC target of  $5 \times 10^5$  and a maximum injection time of 60 ms. All label-free proteomics data sets were analyzed with the MaxQuant software (version 1.5.3.8) (52). We employed the label-free quantitative (LFQ) mode (53) and used MaxQuant default settings for protein identification and LFQ quantification. All downstream analyses were carried out on LFQ values with Perseus (version 1.5.2.4) (54). Statistically significant differences were determined with Perseus software after correction for multiple testing following the Benjamini–Hochberg procedure, which calculates false discovery rate (FDR) adjusted P values.

### **Quantitative RT–PCR**

Total RNA of whole animals was isolated from approximately 200 synchronized day 3 adult worms using RNAbee (Tel-Test Inc.). For analysis of mitochondrial components in germline, RNA of isolated germlines from 50 synchronized day 3 adult worms was extracted using RNAbee. In parallel, isolated intestines and heads were combined to extract RNA and examine expression of mitochondrial components in somatic tissues. cDNA was generated using qScript Flex cDNA synthesis kit (Quantabio). SybrGreen real-time qPCR experiments were performed with a 1:20 dilution of cDNA using a CFC384 Real-Time System (Bio-Rad). Data were analysed with the comparative  $2^{-\Delta\Delta C_t}$  method using the geometric mean of *cdc-42* and *Y45F10D.4* as housekeeping genes (55). See **Supplementary Data 4** for details about the primers used for this assay.

---

### **Mitochondrial DNA/genomic DNA ratio**

Isolated germlines or somatic tissues (intestines + heads) from 100 synchronized day 3 adult worms were incubated in lysis buffer (30 mM Tris-HCl, pH 8, 8 mM EDTA, 100 mM NaCl, 0.7% Nonidet P-40, 0.7% Tween 20, 100 mg/ml proteinase K) for 1 h at 65°C (56). Then, proteinase K was inactivated at 95°C for 15 min. The product was diluted 1:500 and 4 µl were loaded to quantify mitochondrial DNA (mtDNA) by SybrGreen real-time qPCR assay using the following primers for NADH dehydrogenase subunit 1 (*nd-1*): 5'-AGCGTCATTTATTGGGAAGAAGAC-3' and 5'-AAGCTTGTGCTAATCCCATAAATGT-3'. The results were normalized to genomic DNA (gDNA) using the following primers for *cox-4*: 5'-GCCGACTGGAAGAAGACTTGTC-3' and 5'-GCGGAGATCACCTTCCAGTA-3'. qPCR experiments were performed using a CFC384 Real-Time System (Bio-Rad) and data were analysed with the comparative  $2\Delta\Delta C_t$  method.

---

## REFERENCES

1. Carlos López-Otín, Maria A. Blasco, Linda Partridge, Manuel Serrano, Guido Kroemer, The Hallmarks of Ageing. *Cell* 153, 1194–1217 (2013).
2. M. S. Hipp, P. Kasturi, F. U. Hartl, The proteostasis network and its decline in ageing. *Nat Rev Mol Cell Biol* 20, 421-435 (2019).
3. D. Vilchez, I. Saez, A. Dillin, The role of protein clearance mechanisms in organismal ageing and age-related diseases. *Nat Commun* 5, 5659 (2014).
4. Saez, I. & Vilchez, D. The mechanistic links between proteasome activity, aging and age-related diseases. *Curr. Genomics* 15, 38–51 (2014).
5. Ferrington, D. A., Husom, A. D. & Thompson, L. V. Altered proteasome structure, function, and oxidation in aged muscle. *FASEB J.* 19, 644–646 (2005).
6. Vernace, V. A., Arnaud, L., Schmidt-Glenewinkel, T. & Figueiredo-Pereira, M. E. Aging perturbs 26S proteasome assembly in *Drosophila melanogaster*. *FASEB J.* 21, 2672–2682 (2007).
7. Andersson, V., Hanzen, S., Liu, B., Molin, M. & Nystrom, T. Enhancing protein disaggregation restores proteasome activity in aged cells. *Aging* 5, 802–812 (2013).
8. Vilchez, D. et al. RPN-6 determines *C. elegans* longevity under proteotoxic stress conditions. *Nature* 489, 263–268 (2012).
9. Tomaru, U. et al. Decreased proteasomal activity causes age-related phenotypes and promotes the development of metabolic abnormalities. *Am. J. Pathol.* 180, 963–972 (2012).
10. Martinez-Vicente, M. & Cuervo, A. M. Autophagy and neurodegeneration: when the cleaning crew goes on strike. *Lancet Neurol.* 6, 352–361 (2007).

- 
11. Yamamoto, Ai, and Anne Simonsen. “The elimination of accumulated and aggregated proteins: a role for aggrephagy in neurodegeneration.” *Neurobiology of disease* vol. 43,1 (2011)
  12. Garcia-Mata R, Gao YS, Sztul E., Hassles with taking out the garbage: aggravating aggresomes. *Traffic.*, 388-96 (2002).
  13. Rubinsztein, D. C., Marino, G. & Kroemer, G. Autophagy and aging. *Cell* 146, 682–695 (2011).
  14. Terman, A. The effect of age on formation and elimination of autophagic vacuoles in mouse hepatocytes. *Gerontology* 41, 319–326 (1995).
  15. Toth, M. L. et al. Longevity pathways converge on autophagy genes to regulate life span in *Caenorhabditis elegans*. *Autophagy* 4, 330–338 (2008).
  16. Simonsen, A. et al. Promoting basal levels of autophagy in the nervous system enhances longevity and oxidant resistance in adult *Drosophila*. *Autophagy* 4, 176–184 (2008).
  17. Mizushima, N. & Levine, B. Autophagy in mammalian development and differentiation. *Nat. Cell Biol.* 12, 823–830 (2010).
  18. Finkbeiner, S. Huntington’s Disease. *Cold Spring Harb. Perspect. Biol* 3, a007476 (2011).
  19. Holmberg, C. I., Staniszewski, K. E., Mensah, K. N., Matouschek, A. & Morimoto, R. I. Inefficient degradation of truncated polyglutamine proteins by the proteasome. *EMBO. J.* 23, 4307–4318 (2004).
  20. Zarei S, Carr K, Reiley L, Diaz K, Guerra O, Altamirano PF, et al. A comprehensive review of amyotrophic lateral sclerosis. *Surg Neurol Int* 2015;6:171 (2015).
  21. Yalda Baradaran-Heravi, Christine Van Broeckhoven, Julie van der Zee, Stress granule mediated protein aggregation and underlying gene defects in the FTD-ALS spectrum, *Neurobiology of Disease*, 104639, 0969-9961 (2020).

- 
22. R. C. Taylor, K. M. Berendzen, A. Dillin, Systemic stress signalling: understanding the cell non-autonomous control of proteostasis. *Nat Rev Mol Cell Biol* 15, 211-217 (2014).
23. Ilieva H, Polymenidou M, Cleveland DW. Non-cell autonomous toxicity in neurodegenerative disorders: ALS and beyond. *J. Cell Biol*, 187:761–772 (2009).
24. Daniel O'Brien and Patricija van Oosten-Hawle, Regulation of cell-non-autonomous proteostasis in metazoans. *Essays in Biochemistry* 60, 133–142 (2016).
25. Anckar, J. and Sistonen, L., Heat shock factor 1 as a coordinator of stress and developmental pathways. *Adv. Exp. Med. Biol.* 594 (2007).
26. Prahlad, V., Cornelius, T. and Morimoto, R. Regulation of the cellular heat shock response in *Caenorhabditis elegans* by thermosensory neurons, *Science* 70, 811–814 (2008).
27. Tatum M.C., Ooi, F.K., Chikka, M.R., Chauve, L., Martinez-Velazquez, L.A., Steinbusch, H.W.M., Neuronal serotonin release triggers the heat shock response in *C. elegans* in the absence of temperature increase. *Curr. Biol.* 25, 163–174 (2015).
28. Douglas PM, Baird NA, Simic MS, Uhlein S, McCormick MA, Wolff SC, Kennedy BK, Dillin A., Heterotypic signals from neural HSF-1 separate thermotolerance from longevity. *Cell Reports* 12, 1196–1204 (2015).
29. Fawcett, T.W., Sylvester, S.L., Sarge, K.D., Morimoto, R.I. and Holbrook, N.J. Effects of neurohormonal stress and aging on the activation of mammalian heat shock factor 1. *J. Biol. Chem.* 269, 32272–3228 (1994).
30. Conti B, Sanchez-Alavez M, Winsky-Sommerer R, Morale MC, Lucero J, Brownell S, Fabre V, Huitron-Resendiz S, Henriksen S, Zorrilla EP, de Lecea L, Bartfai T., Transgenic mice with a reduced core body temperature have an increased life span. *Science* 314, 825–828 (2006).

- 
31. Gardner, B.M., Pincus, D., Gotthardt, K., Gallagher, C.M. and Walter, P. Endoplasmic reticulum stress sensing in the unfolded protein response. *Cold Spring Harb. Perspect. Biol.* 5, a013169 (2013).
32. Taylor, R.C. and Dillin, A. XBP-1 Is a cell-nonautonomous regulator of stress resistance and longevity. *Cell* 153, 1435–1447 (2013).
33. A. E. Frakes *et al.*, Four glial cells regulate ER stress resistance and longevity via neuropeptide signaling in *C. elegans*. *Science* 367, 436-440 (2020).
34. Williams, K.W., Liu, T., Kong, X., Fukuda, M., Deng, Y., Berglund, E.D. et al. Xbp1s in Pomc neurons connects ER stress with energy balance and glucose homeostasis. *Cell Metab.* 3, 1–12 (2014).
35. Brandt, Claus et al. “Food Perception Primes Hepatic ER Homeostasis via Melanocortin-Dependent Control of mTOR Activation.” *Cell* 175,5 1321-1335 (2018).
36. Pellegrino, M.W., Nargund, A.M. and Haynes, C.M. Signaling the mitochondrial unfolded protein response. *Biochim. Biophys. Acta* 1833, 410–416 (2013).
37. Durieux, J., Wolff, S. and Dillin, A. The cell-non-autonomous nature of electron transport chain-mediated longevity. *Cell* 144, 79–91 (2011).
38. K. M. Berendzen *et al.*, Neuroendocrine Coordination of Mitochondrial Stress Signaling and Proteostasis. *Cell* 166, 1553-1563 e1510 (2016).
39. Kim, K.H., Jeong, Y.T., Oh, H., Kim, S.H., Cho, J.M., Kim, Y.-N. et al. Autophagy deficiency leads to protection from obesity and insulin resistance by inducing Fgf21 as a mitokine. *Nat. Med.* 19, 83–92 (2013).
40. Satoh A, Brace CS, Rensing N, Cliften P, Wozniak DF, Herzog ED, Yamada KA, Imai S., Sirt1 extends life span and delays aging in mice through the regulation of Nk2 homeobox 1 in the DMH and LH. *Cell Metabolism* 18, 416–430 (2013).

- 
41. Zhang, P., Judy, M., Lee, S.-J. and Kenyon, C. Direct and indirect gene regulation by a life-extending FOXO protein in *C. elegans*: roles for GATA factors and lipid gene regulators. *Cell Metab.* 17, 85–100 (2013).
42. Silva MC, Amaral MD, Morimoto RI., Neuronal reprogramming of protein homeostasis by calcium-dependent regulation of the heat shock response. *PLOS Genetics* 9: (2013).
43. Bluher, M., Kahn, B.B. and Kahn, C.R. Extended longevity in mice lacking the insulin receptor in adipose tissue. *Science* 299, 572–574 (2003).
44. Cohen E., Paulsson J.F. Blinder, P. Burstyn-Cohen, T. Du D., Estepa G. et al. Reduced IGF-1 signaling delays age-associated proteotoxicity in mice. *Cell* 139, 1157–1169 (2009).
45. Khodakarami Amirabbas, Isabel Saez, Johanna Melsand, David Vilchez, Mediation of organismal aging and somatic proteostasis by the germline, *Front.Mol.Biosci.* vol. 2 3. 23 (2015)
46. Kirkwood,T.B., Evolution of ageing. *Nature* 270, 301–304 (1977).
47. Arantes Oliveira N., Apfeld J., Dillin A.,and Kenyon,C..Regulation of lifespan by germline stem cells in *Caenorhabditis elegans*. *Science* 295, 502–505 (2002).
48. Panowski S.H., and Dillin A., Signals of youth: endocrine regulation of aging in *Caenorhabditis elegans*. *Trends Endocrinol. Metab.* 20, 259–264 (2009).
49. Morley J.F., Brignull H.R., Weyers J.J., Morimoto R.I., The threshold for polyglutamine expansion protein aggregation and cellular toxicity is dynamic and influenced by aging in *Caenorhabditis elegans*. *Proc.Natl.Acad. Sci.*, 99,1041710422 (2002)
50. Vilchez D., Morante I., Liu Z., Douglas P.M., Merkwirth C., Rodrigues A.P. et al, RPN-6 determines *C. elegans* longevity under proteotoxic stress conditions, *Nature* 489, 263–268 (2012b).

- 
51. Vilchez D., Boyer L., Morante I., Lutz M., Merkwirth C., Joyce D., et al Increased proteasome activity in human embryonic stem cells is regulated by PSMD11. *Nature* 489, 304–308 (2012a).
52. Lapierre L.R., Gelino S., Melendez A., Hansen M., Autophagy and lipid metabolism coordinately modulate lifespan in germline-less *C. elegans*. *Curr.Biol.* 21, 1507–1514 (2011).
53. Lapierre L.R., De Magalhaes Filho C.D., McQuary P.R., Chu C.C., Visvikis O., Chang J.T., The TFEB orthologue HLH-30 regulates autophagy and modulates longevity in *Caenorhabditis elegans*. *Nat.Comm.* 4, 2267 (2013).
54. Steinbaugh MJ, Sun LY, Bartke A, Miller RA. 2012. Activation of genes involved in xenobiotic metabolism is a shared signature of mouse models with extended lifespan. *American Journal of Physiology-Endocrinology and Metabolism* vol. 303,4 (2012).
55. Maria A. Ermolaeva, Alexandra Segref, Alexander Dakhovnik, Hui-Ling Ou, Jennifer I. Schneider, Olaf Utermohlen, Thorsten Hoppe & Bjorn Schumacher, DNA damage in germ cells induces an innate immune response that triggers systemic stress resistance, *Nature* 501, 416–420 (2013).
56. Hyun Ju Lee, Alireza Noormohammadi, Seda Koyuncu, Giuseppe Calculli, Milos S. Simic, Marija Herholz, Aleksandra Trifunovic, David Vilchez, Prostaglandin signals from adult germline stem cells delay somatic ageing of *Caenorhabditis elegans*, *Nat Metab* 1, 790–810 (2019).
57. D. Updike, S. Strome, P granule assembly and function in *Caenorhabditis elegans* germ cells. *J Androl* 31, 53-60 (2010).
58. Geraldine Seydoux, The P Granules of *C. elegans*: A Genetic Model for the Study of RNA–Protein Condensates, *J Mol Bio* 430, 4702-4010 (2018).
59. V. Verdile, E. De Paola, M. P. Paronetto, Aberrant Phase Transitions: Side Effects and Novel Therapeutic Strategies in Human Disease. *Front Genet* 10, 173 (2019).

- 
60. I, Shim YH, Kirchner J, Kaminker J, Wood WB, Strome S. PGL-1, a predicted RNA-binding component of germ granules, is essential for fertility in *C. elegans*. *Cell* 94, 635–645 (1998)
61. D.L. Updike, A.K. Knutson, T.A. Egelhofer, A.C. Campbell, S. Strome, Germ-granule components prevent somatic development in the *C. elegans* germline, *Curr. Biol.* 24 970–975 (2014).
62. A.K. Knutson, T. Egelhofer, A. Rechtsteiner, S. Strome, Germ granules prevent accumulation of somatic transcripts in the adult *Caenorhabditis elegans* germline, *Genetics* 206 163–178 (2017).
63. A.C. Billi, S.E. Fischer, J.K. Kim, Endogenous RNAi pathways in *C. elegans*, *WormBook* 1–49 (2014).
64. U. Sheth, J. Pitt, S. Dennis, J.R. Priess, Perinuclear P granules are the principal sites of mRNA export in adult *C. elegans* germ cells, *Development* 137, 1305–1314 (2010).
65. I. Kawasaki *et al.*, The PGL family proteins associate with germ granules and function redundantly in *Caenorhabditis elegans* germline development. *Genetics* 167, 645-661 (2004).
66. Strome S, Lehmann R. Germ versus soma decisions: lessons from flies and worms. *Science* 316, 392–393 (2007).
67. S. Strome, W.B. Wood, Generation of asymmetry and segregation of germ-line granules in early *C. elegans* embryos, *Cell* 35, 15–25 (1983).
68. Marnik EA, Updike DL. Membraneless organelles: P granules in *Caenorhabditis elegans*. *Traffic*. 20, 373–379 (2019)
69. Uversky VN, Kuznetsova IM, Turoverov KK, Zaslavsky B. Intrinsically disordered proteins as crucial constituents of cellular aqueous two phase systems and coacervates. *FEBS Lett.*, 589, 15-22 (2015).

- 
70. Toettcher JE, Shin Y, Pannucci N, Berry J, Brangwynne CP, Haataja MP. Spatiotemporal control of intracellular phase transitions using light-activated optoDroplets. *Cell*. 168, 159-171 (2016).
71. Lin Y, Protter DSW, Rosen MK, Parker R. Formation and maturation of phase-separated liquid droplets by RNA-binding proteins. *Mol Cell*. 2, 208-19 (2015).
72. Spike C, Meyer N, Racen E, Orsborn A, Kirchner J, Kuznicki K, Yee C, Bennett K, Strome S. Genetic analysis of the *Caenorhabditis elegans* GLH family of P-granule proteins. *Genetics* 178, 1973–1987 (2008a).
73. Pitt JN, Schisa JA, Priess JR. P granules in the germ cells of *Caenorhabditis elegans* adults are associated with clusters of nuclear pores and contain RNA. *Dev Biol* 219, 315–333 (2000).
74. Schisa JA, Pitt JN, Priess JR. Analysis of RNA associated with P granules in germ cells of *C. elegans* adults. *Development* 128, 1287–1298 (2001).
75. Kawasaki I, Shim YH, Kirchner J, Kaminker J, Wood WB, Strome S. PGL-1, a predicted RNA-binding component of germ granules, is essential for fertility in *C. elegans*. *Cell* 94, 635–645 (1998)
76. M. Hanazawa, M. Yonetani, A. Sugimoto, PGL proteins self associate and bind RNPs to mediate germ granule assembly in *C. elegans*. *J Cell Biol* 192, 929-937 (2011).
77. Romero P., Obradovic Z., Li, X. Garner, E. C. Brown C. J., and Dunker A. K., Sequence complexity of disordered protein. *Proteins* 42, 38–48 (2001).
78. A. P. Mahowald, Polar granules of *Drosophila*. II. Ultrastructural changes during early embryogenesis. *J Exp Zool* **167**, 237-261 (1968).
79. J. T. Wang, G. Seydoux, P granules. *Curr Biol* 24, R637-R638 (2014).

- 
80. E. Voronina, A. Paix, G. Seydoux, The P granule component PGL-1 promotes the localization and silencing activity of the PUF protein FBF-2 in germline stem cells, *Development* 139, 3732-3740 (2012).
81. A. Hubstenberger, S. L. Noble, C. Cameron, T. C. Evans, Translation repressors, an RNA helicase, and developmental cues control RNP phase transitions during early development. *Dev Cell* 27, 161-173 (2013).
82. Shin, Y., and Brangwynne, C. P., Liquid phase condensation in cell physiology and disease. *Science* 357:eaaf4382. (2017).
83. King OD, Gitler AD, Shorter J. The tip of the iceberg: RNA-binding proteins with prion-like domains in neurodegenerative disease. *Brain Res.* 1462, 61–80 (2012).
84. A. Arnold *et al.*, Functional characterization of *C. elegans* Y-box-binding proteins reveals tissue-specific functions and a critical role in the formation of polysomes. *Nucleic Acids Res* 42, 13353-13369 (2014).
85. Sommerville, J., Activities of cold-shock domain proteins in translation control. *Bioessays* 21, 319–325 (1999).
86. Horn, G., Hofweber, R., Kremer, W. and Kalbitzer, H.R., Structure and function of bacterial cold shock proteins. *Cell Mol Life Sci*, 64, 1457-1470 (2007).
87. Arcus, V., OB-fold domains: a snapshot of the evolution of sequence, structure and function. *Curr Opin Struct Biol*, 12, 794-801 (2002).
88. Mihailovich, M., Militti, C., Gabaldon, T. and Gebauer, F., Eukaryotic cold shock domain proteins: highly versatile regulators of gene expression. *Bioessays* 32, 109-118 (2010).
89. Lyabin, D.N., Eliseeva, I.A. and Ovchinnikov, L.P., YB-1 protein: functions and regulation. *Wiley Interdiscip Rev RNA* 5, 95-110 (2014).

- 
90. Skabkin, M.A., Kiselyova, O.I., Chernov, K.G., Sorokin, A.V., Dubrovin, E.V., Yaminsky, I.V., Vasiliev, V.D. and Ovchinnikov, L.P. Structural organization of mRNA complexes with major core mRNP protein YB-1. *Nucleic Acids Res.* 32, 5621-5635 (2004).
91. Bounedjah O, Desforges B, Wu TD, Pioche-Durieu C, Marco S, Hamon L, Curmi PA, Guerquin-Kern JL, Piétrement O, Pastré D., Free mRNA in excess upon polysome dissociation is a scaffold for protein multimerization to form stress granules. *Nucleic Acids Research* 42, 8678-8691 (2014).
92. T. Tanaka, S. Ohashi, S. Kobayashi, Roles of YB-1 under arsenite-induced stress: translational activation of HSP70 mRNA and control of the number of stress granules. *Biochim Biophys Acta* 1840, 985-992 (2014).
93. Eliseeva, I.A., Kim, E.R., Guryanov, S.G., Ovchinnikov, L.P. and Lyabin, D.N. Y-box-binding protein 1 (YB-1) and its functions. *Biochemistry (Moscow)* 76, 1402–1433 (2011).
94. Mansfield, J.H., Wilhelm, J.E. and Hazelrigg, T. Ypsilon Schachtel, a *Drosophila* Y-box protein, acts antagonistically to Orbin the oskar mRNA localization and translation pathway. *Development* 129, 197–209 (2002).
95. Bouvet, P. and Wolffe, A.P. A role for transcription and FRGY2 in masking maternal mRNA within *Xenopus* oocytes. *Cell* 77, 931–941 (1994).
96. Yang, J., Medvedev, S., Yu, J., Schultz, R.M. and Hecht, N.B. Deletion of the DNA/RNA-binding protein MSY2 leads to post-meiotic arrest. *Mol. Cell Endocrinol.* 250, 20–24 (2006).
- 97 Kumari, P., Gilligan, P.C., Lim, S., Tran, L.D., Winkler, S., Philp, R. and Sampath, K. An essential role for maternal control of Nodal signaling. *Elife*, 2, e00683 (2013).
98. Skabkin, M.A., Kiselyova, O.I., Chernov, K.G., Sorokin, A.V., Dubrovin, E.V., Yaminsky, I.V., Vasiliev, V.D. and Ovchinnikov, L.P., Structural organization of mRNA complexes with major core mRNP protein YB-1. *Nucleic Acids Res.*, 32, 5621–5635 (2004).

- 
99. Sanae Abrakhi, Dmitry A. Kretov, Bénédicte Desforges, Ioana Dobra, Ahmed Bouhss, David Pastré, and Loic Hamon, Nanoscale Analysis Reveals the Maturation of Neurodegeneration-Associated Protein Aggregates: Grown in mRNA Granules then Released by Stress Granule Proteins, *AscNano* 11(7), 7189-7200 (2017).
100. H. R. Brignull, F. E. Moore, S. J. Tang, R. I. Morimoto, Polyglutamine proteins at the pathogenic threshold display neuron-specific aggregation in a pan-neuronal *Caenorhabditis elegans* model. *J Neurosci* 26, 7597-7606 (2006)
101. A. Noormohammadi *et al.*, Somatic increase of CCT8 mimics proteostasis of human pluripotent stem cells and extends *C. elegans* lifespan. *Nat Commun* 7, 13649 (2016).
102. A. Calixto, D. Chelur, I. Topalidou, X. Chen, M. Chalfie, Enhanced neuronal RNAi in *C. elegans* using SID-1. *Nat Methods* 7, 554-559 (2010).
103. C. Benedetti, C. M. Haynes, Y. Yang, H. P. Harding, D. Ron, Ubiquitin-like protein 5 positively regulates chaperone gene expression in the mitochondrial unfolded protein response. *Genetics* 174, 229-239 (2006).
104. T. Yoneda *et al.*, Compartment-specific perturbation of protein handling activates genes encoding mitochondrial chaperones. *Journal of Cell Science* 117, 4055-4066 (2004).
105. M. Calfon *et al.*, IRE1 couples endoplasmic reticulum load to secretory capacity by processing the XBP-1 mRNA (vol 415, pg 92, 2002). *Nature* 420, 202-202 (2002).
106. C. D. Link, J. R. Cypser, C. J. Johnson, T. E. Johnson, Direct observation of stress response in *Caenorhabditis elegans* using a reporter transgene. *Cell Stress Chaperon* 4, 235-242 (1999).
107. Q. Zhang *et al.*, The Mitochondrial Unfolded Protein Response Is Mediated Cell-Non-autonomously by Retromer-Dependent Wnt Signaling. *Cell* 174, 870-883 e817 (2018).

- 
108. D. Y. M. Coudreuse, G. Roel, M. C. Betist, O. Destree, H. C. Korswagen, Wnt gradient formation requires retromer function in Wnt-producing cells. *Science* 312, 921-924 (2006).
109. S. Tam, R. Geller, C. Spiess, J. Frydman, The chaperonin TRiC controls polyglutamine aggregation and toxicity through subunit-specific interactions. *Nat Cell Biol* 8, 1155-1162 (2006).
110. F. Hu, F. Liu, Mitochondrial stress: A bridge between mitochondrial dysfunction and metabolic diseases? *Cellular Signalling* 23, 1528-1533 (2011).
111. D. Senft, Z. A. Ronai, UPR, autophagy, and mitochondria crosstalk underlies the ER stress response. *Trends in Biochemical Sciences* 40, 141-148 (2015).
112. Civelek, M., Flory, S., Meloh, H. et al. The polyphenol quercetin protects from glucotoxicity depending on the aggresome in *Caenorhabditis elegans*. *Eur J Nutr* 59, 485–491 (2020)
113. Chen, Yanfang et al. “Approaches for Studying Autophagy in *Caenorhabditis elegans*.” *Cells* 3, 27-30 (2017).
114. R. San Gil, D. Cox, L. McAlary, T. Berg, A. K. Walker, J. J. Yerbury, L. Ooi, H. Ecroyd, Neurodegenerative disease-associated protein aggregates are poor inducers of the heat shock response in neuronal-like cells, *Journal of Cell Science*, jcs.243709 (2020).
115. Artal-Sanz M, Tavernarakis N. Prohibitin couples diapause signalling to mitochondrial metabolism during ageing in *C. elegans*. *Nature* 461, 793–797 (2009).
116. J. Kirstein-Miles, R. I. Morimoto, *Caenorhabditis Elegans* as a Model System to Study Intercompartmental Proteostasis: Interrelation of Mitochondrial Function, Longevity, and Neurodegenerative Diseases. *Dev Dynam* 239, 1529-1538 (2010).

- 
117. Wallace DC. A mitochondrial paradigm of metabolic and degenerative diseases, aging, and cancer: a dawn for evolutionary medicine. *Annu Rev Genet.* 39, 359–407 (2005).
118. Jenkins BG, Koroshetz WJ, Beal MF, Rosen BR. Evidence for impairment of energy metabolism in vivo in Huntington's disease using localized <sup>1</sup>H NMR spectroscopy. *Neurology* 43, 2689–2695 (1993).
119. Mochel F, Durant B, Durr A, Schiffmann R. Altered dopamine and serotonin metabolism in motorically asymptomatic R6/2 mice. *PLoS ONE* 6:e18336 (2011)
120. Mann VM, Cooper JM, Javoy-Agid F, Agid Y, Jenner P, Schapira AH. Mitochondrial function and parental sex effect in Huntington's disease. *Lancet.*; 336:749 (1990).
121. Panov AV, Gutekunst CA, Leavitt BR, Hayden MR, Burke JR, Strittmatter WJ, Greenamyre JT. Early mitochondrial calcium defects in Huntington's disease are a direct effect of polyglutamines. *Nat Neurosci.* 5, 731–736 (2002).
122. Laura C. Greaves, John C. Mathers, Robert W. Taylor, and Douglass M. Turnbull, Modelling mitochondrial DNA mutations in bacterial cytochrome c oxidase: Link to colon cancer? *PNAS*, 106 (22) E57 (2009).
123. Nollen EA, Garcia SM, van Haaften G, Kim S, Chavez A, Morimoto RI, Plasterk RH. Genome-wide RNA interference screen identifies previously undescribed regulators of polyglutamine aggregation. *Proc Natl Acad Sci USA* 101, 6403–6408 (2004).
124. Yaxin Liua, Xiaowen Wanga, Liam P. Coynea, Yuan Yanga, Yue Qib, Frank A. Middletonc, Xin Jie Chen, Mitochondrial carrier protein overloading and misfolding induce aggregates and proteostatic adaptations in the cytosol, *Molecular Biology of the Cell*, 30(11), 1272-1284 (2019).

- 
125. François Gonzalvez, Marilena D'Aurelio, Marie Boutant, Aoula Moustapha, Jean-Philippe Puech, Thomas Landes, Laeticia Arnauné-Pelloquin, Guillaume Vial, Nellie Taleux, Christian Slomianny, Ronald J. Wanders, Riekelt H. Houtkooper, Pascale Bellenger, Ian Max Møller, Eyal Gottlieb, Frederic M. Vaz, Giovanni Manfredi, Patrice X. Petit, Barth syndrome: Cellular compensation of mitochondrial dysfunction and apoptosis inhibition due to changes in cardiolipin remodeling linked to tafazzin (TAZ) gene mutation, *Biochimica et Biophysica Acta (BBA) - Molecular Basis of Disease*, Volume 1832, Issue 8, (2013).
126. Houtkooper RH, Mouchiroud L, Ryu D, N, Katsyuba E, Knott G, Williams RW, Auwerx J. Mitonuclear protein imbalance as a conserved longevity mechanism. *Nature* 497, 451–457 (2013).
127. Wang, S., and Bellen, H.J., The retromer complex in development and disease. *Development* 142, 2392–2396 (2015).
128. Inestrosa, N.C., and Arenas, E., Emerging roles of Wnts in the adult nervous system. *Nat. Rev. Neurosci.* 11, 77–86 (2010).
129. Hult S, et al. Mutant huntingtin causes metabolic imbalance by disruption of hypothalamic neurocircuits. *Cell Metab* 13, 428–439 (2011).
130. van Oosten-Hawle, P., Porter, R.S. and Morimoto, R.I., Regulation of organismal proteostasis by transcellular chaperone signaling. *Cell* 153, 1366–1378 (2013).

---

## ACKNOWLEDGEMENTS

I would like to express my deep gratitude to my supervisor Dr. David Vilchez for giving me the opportunity to work on this project and for constantly supporting me during the last years. His guidance helped me in all the time of research and writing of this thesis. I could not have accomplished this work without his help.

I would like to thank my parents and my sister for their immense love and support.

I would like to acknowledge all the members, current and past, of Vilchez lab who represented more than colleagues but real friends. Thank you for your scientific help and for all the fun we had together.

Phd is hard time and I wouldn't have survived without my friends. All laughs and talks we shared together helped me to overcome all obstacles and challenges I encountered.

I thank the Cologne Graduate School of Ageing for giving me the opportunity to join this unique graduate program, which provided me many opportunities for my personal development. I would like to thank especially Jenny and Daniela, who gave me a huge help when I move to Germany.

I would like to thank my thesis committee members Dr. Nirmal Robinson and Prof. Guenter Schwarz for their feedbacks and help.

Finally, I would like to acknowledge Prof. Aleksandra Trifunovic and Prof. Jans Riemer for being part of my PhD defense committee and for giving me the opportunity to defend my work.

## Erklärung zur Dissertation

gemäß der Promotionsordnung vom 12. März 2020

„Hiermit versichere ich an Eides statt, dass ich die vorliegende Dissertation selbstständig und ohne die Benutzung anderer als der angegebenen Hilfsmittel und Literatur angefertigt habe. Alle Stellen, die wörtlich oder sinngemäß aus veröffentlichten und nicht veröffentlichten Werken dem Wortlaut oder dem Sinn nach entnommen wurden, sind als solche kenntlich gemacht. Ich versichere an Eides statt, dass diese Dissertation noch keiner anderen Fakultät oder Universität zur Prüfung vorgelegen hat; dass sie - abgesehen von unten angegebenen Teilpublikationen und eingebundenen Artikeln und Manuskripten - noch nicht veröffentlicht worden ist sowie, dass ich eine Veröffentlichung der Dissertation vor Abschluss der Promotion nicht ohne Genehmigung des Promotionsausschusses vornehmen werde. Die Bestimmungen dieser Ordnung sind mir bekannt. Darüber hinaus erkläre ich hiermit, dass ich die Ordnung zur Sicherung guter wissenschaftlicher Praxis und zum Umgang mit wissenschaftlichem Fehlverhalten der Universität zu Köln gelesen und sie bei der Durchführung der Dissertation zugrundeliegenden Arbeiten und der schriftlich verfassten Dissertation beachtet habe und verpflichte mich hiermit, die dort genannten Vorgaben bei allen wissenschaftlichen Tätigkeiten zu beachten und umzusetzen. Ich versichere, dass die eingereichte elektronische Fassung der eingereichten Druckfassung vollständig entspricht.“

Teilpublikationen:



19.12.2020,

Giuseppe Calculli,

Datum,

Name

und

Unterschrift

